

CHARACTERIZING THE ENVIRONMENTAL FATE OF AQUATIC HERBICIDES
BY CONNECTING QUANTIFICATION IN LAKES TO LABORATORY STUDIES

by

Sydney R. Van Frost

A thesis submitted in partial fulfillment of

the requirements for the degree of

Master of Science

(Civil and Environmental Engineering)

at the

UNIVERSITY OF WISCONSIN-MADISON

2023

Abstract

Aquatic herbicides are a class of organic compounds that are used in surface water bodies to manage the persistence of invasive and nuisance aquatic plants. Understanding their degradation and transformation pathways are critical for managing herbicide effectiveness and target species resistance. This study examines the fate and transport of two aquatic herbicides, fluridone and florpyrauxifen-benzyl (**FPB**). A field campaign was conducted during the summer of 2022 to collect concentrations of the herbicides and their degradation products over time in three study lakes in Wisconsin. These field studies were followed by supplemental laboratory experiments to further analyze the dominant environmental transformation pathways for each herbicide. Photolysis, sorption, biodegradation, and hydrolysis can all be quantified separately under isolated conditions in the lab. Combined, the conclusions from these experiments along with mass balance modeling can illustrate which processes dictate the persistence of the herbicides in aquatic environments. Hydrolysis experiments show that FPB is transformed into its primary degradation product, florpyrauxifen, through base-promoted hydrolysis. Florpyrauxifen is then degraded microbially as determined by microcosm batch reactors. Photolysis experiments show that FPB, florpyrauxifen, and fluridone all undergo direct photodegradation and that indirect photodegradation is negligible. Fluridone differs from FPB in that it is very resistant to both abiotic and biotic processes, which is reflected by its longer half-life observed in lakes. Overall, a deeper understanding of aquatic herbicide behavior will allow resource managers to develop better application strategies, as well as have broader implications for further understanding processes that impact organic compounds in freshwater systems.

Acknowledgements

I would first like to thank my wonderful co-advisors, Dr. Christy Remucal and Dr. Trina McMahon. I came into this program with very little research experience due to the COVID-19 pandemic, but you helped shape me into the scientist I am today. I am wholeheartedly grateful for your constructive feedback, critical guidance, and unwavering support during my time at UW-Madison. From balancing administrative to mentoring to familial responsibilities, the amount of enthusiasm and commitment you put into your work is something I will always admire.

I would also like to thank the third member of my committee, Dr. Haoran Wei, for their role in helping me earn my M.S. degree. I am grateful to have had the opportunity to take one of your courses where I was able to develop integral knowledge related to my research. I am very appreciative of your time and commitment to my learning and growth as a graduate student.

A resounding thank you to Dr. Amber White, the person I truly would not have completed this thesis without. You took me under your wing as a wide-eyed undergraduate student and taught me the fundamentals to being a researcher which included everything from filtering water to handling boat trailer mishaps. I am incredibly inspired by your work ethic and ability to accomplish great things. Everyone talked about how once you graduated there would be some big shoes to fill, and they weren't kidding. Your mentorship and guidance were pivotal in my development as a graduate student and I will be forever grateful.

None of the work described in this thesis would be nearly as complete without the extraordinary help of Josie Jauquet. You were always willing to step up to the plate with everything from long field days to extensive sample processing in the lab. Wherever your career takes you, just know that they will be extremely lucky to have you.

To the members of the Remucal Lab, thank you! Your dedication to your research has helped me, taught me, and inspired me immensely. I cannot imagine having worked side-by-side with anyone else. Whenever I needed help, there was never any hesitation and your assistance/knowledge was invaluable. I will forever cherish our terrace outings, conference room lunches and potlucks, and many other social events. I am very excited to see what all of your futures hold.

The projects included in this thesis have been funded by several sources which require acknowledgement. I am very thankful for the resources and opportunities made possible by the Midwest Aquatic Plant Management Society, specifically Eddie Heath for your dedication to the development and success of students, as well as the Wisconsin Department of Natural Resources and the UW-Madison Center for Limnology Anna Grant Birge Award.

The quality of data presented in this thesis would not have been possible without the immeasurable assistance of James Lazarcik. Even though I was very intimidated by you at first (and maybe a little still), I know it was all for the best and you helped mold me into the researcher I am today. Your knowledge and contributions to the successful research that comes out of Water Science cannot be overstated and I feel incredibly lucky to have worked with you.

To Ansel, you have truly been there for me through thick and thin and there are no words to describe my gratitude for you. After even the longest and most exhausting days at the lab you never failed to make me smile. From listening to all my practice presentations to picking me up from lab on rainy days, your unending support means the world. I cannot wait to continue this adventure of life with you by my side and I am very excited to see what Alaska has in store for us.

Finally, I would like to thank my parents, who are nothing less than amazing. You have never dissuaded me from pursuing my dreams and I do not know where I would be without your unconditional love and support. You have allowed me to achieve above and beyond what I ever thought I was capable of, but you also taught me to be content with my best effort. Thank you for being the best role models a daughter could ask for.

To everyone who has loved and supported me along the way: thank you.

Table of Contents

Abstract	ii
Acknowledgements	iii
Table of Contents	vi
List of Figures	ix
List of Tables	xiii
Chapter 1. Introduction	1
Florpyrauxifen-benzyl usage and transformation processes.	2
Fluridone usage and transformation processes.....	5
Research needs.	6
References	9
Chapter 2. Quantifying the role of simultaneous transformation pathways in the fate of the novel aquatic herbicide florpyrauxifen-benzyl	13
Prologue.	13
Abstract	14
Introduction	15
Materials and Methods	17
Chemicals.	17
FPB sample preservation and processing.	17
Field sampling.	17
Analytical methods.	19
Hydrolysis.....	19
Sorption.	19
Microcosm incubations.....	20
Photodegradation.	20
Sediment and plant extractions.....	21
Results and Discussion.....	21
FPB degradation and florpyrauxifen formation in lakes.	21
Hydrolysis.....	24
Sorption.	26

Microcosm incubations.....	26
Photochemical degradation.....	29
Identification of primary loss pathways.	31
Plant uptake and transformation of FPB.....	33
Environmental Implications.	34
Acknowledgements.	35
References	35
Chapter 3. Evaluating persistence and transformation of aquatic herbicide fluridone in field and laboratory experiments.....	41
Prologue.	41
Abstract	42
Introduction	43
Materials and Methods	46
Chemicals.	46
Field sampling.	47
Photochemical irradiations.	47
Sorption.	49
Microcosm incubations.....	49
Sediment extractions.....	50
Analytical methods.....	50
Results and Discussion.....	51
Photodegradation of fluridone in lake water.	51
Sorption.	53
Microcosm incubations.....	55
Fluridone behavior in lakes.	56
Conclusions.	58
Acknowledgements.	59
References	59
Chapter 4. Conclusions	64
FPB summary and future research needs.	65
Fluridone summary and future research needs.....	66

References	67
Appendix A. Supplementary Material for Chapter 2.....	70
Section A.1. Materials and chemical structures	70
Section A.2. Field sampling methods.....	72
Section A.3. Analytical methods.....	74
Section A.4. Hydrolysis experiments.....	77
Section A.5. Sorption experiments.....	79
Section A.6. Microcosm incubations	82
Section A.7. Photochemical irradiations and modeling	84
Irradiation experiments.....	84
Quantum yield calculations.	84
In-lake photodegradation modeling.....	85
Section A.8. Sediment and plant extractions.....	90
Section A.9. Treatment data.....	93
Section A.10. Material balance calculations	98
FPB recovery in lakes.....	98
Material balance using product yields from field data.	99
Material balance based on measured kinetics under laboratory conditions.	100
References	101
Appendix B. Supplementary Material for Chapter 3	104
Section B.1. Summary of previous fluridone studies.....	104
Section B.2. Field sampling methods.....	105
Section B.3. Photochemical irradiations	106
Section B.4. Sorption experiments.....	109
Section B.5. Microcosm incubations.....	110
Section B.6. Sediment extractions.....	111
Section B.7. Analytical methods.....	112
References	114

List of Figures

- Figure 1.1. Chemical structures of (a) FPB and its five potential degradation products: (b) florpyrauxifen, (c) dechloro-FPB, (d) dechloro-florpyrauxifen, (e) hydroxy-FPB, and (f) hydroxy-florpyrauxifen. 5
- Figure 1.2. Chemical structures of (a) fluridone and a biodegradation product (b) 3-trifluoromethyl benzoic acid. 6
- Figure 2.1. Concentrations of (a) FPB and (b) florpyrauxifen in the treatment zone of all studied lakes. Data for all sampling points and maps of each lake are provided in Figures A.15 – A.19. (c) Epilimnion concentrations of FPB and its degradation products in the treatment area of Kettle Moraine Lake. (d) Contribution of photodegradation (Photo.), biodegradation (Bio.), hydrolysis (Hydro.), and sorption (Sorp.) in the field and lab data based on material balance calculations outlined in Section A.10. Biodegradation and sorption were quantified separately with the field data which is indicated by the blue and black bar (blue represents contribution of biodegradation while black indicates sorption). The rate loss in the sediment-water microcosms is due to biodegradation and sorption, therefore the lab data combines these two processes. 22
- Figure 2.2. (a) Loss of FPB and formation of florpyrauxifen during hydrolysis at pH 8. (b) Hydrolysis rates of FPB as a function of pH. Kettle Moraine Lake sediment sorption isotherms for (c) FPB and (d) florpyrauxifen. The slope of the isotherm is equivalent to the sediment sorption partitioning coefficient (K_d) in $L\ kg^{-1}$. Loss of (e) FPB and (f) florpyrauxifen and formation of photoproducts during irradiation with 311 nm light in ultrapure water (pH 7). Error bars represent the standard deviation of samples taken from triplicate reactors. Error bars in panels (b), (e), and (f) are smaller than the data point symbols. 25
- Figure 2.3. Kettle Moraine Lake microcosms incubated with (a-c) FPB and (d-f) florpyrauxifen. (a, d) Abiotic controls contained 0.2 μm filter sterilized water only. (b, e) Sediment-water microcosms contained 0.2 μm filter sterilized water with sediment. (c, f) Water-only microcosms contained unfiltered lake water only. Error bars in each figure are smaller than the data point symbols. 27
- Figure 2.4. Proposed FPB degradation mechanism in aquatic environments. Product identified in each reaction by number as follows: 1- field campaign; 2- photodegradation experiments; 3- FPB incubated-microcosms; 4- florpyrauxifen-incubated microcosm, and 5- hydrolysis experiment. Red boxes represent changed functional group after reaction. 33
- Figure 3.1. Chemical structures of (a) fluridone and a biodegradation product (b) 3-trifluoromethyl benzoic acid. 44
- Figure 3.2. (a) Photochemical irradiation of fluridone at 311 nm in ultrapure water (direct control) and five different lake waters. Natural log of the ratio of [fluridone] at time t to initial [fluridone]. (b) Rate constants measured during 311 nm irradiation experiment corrected for

light screening in the lake waters compared to the direct control. Error bars represent standard deviation of triplicate samples. (c) Representation of half-life variability under different conditions where A = 311 nm irradiation in the lab, B = lab conditions corrected for light screening, C = noontime solar irradiance, D = noontime irradiance with diurnal cycling, E = average solar irradiance, and F = average irradiance integrated over 1 m. It is important to note that the y-axis is a natural log scale. 52

Figure 3.3. (a) Hooker Lake sediment sorption isotherm for fluridone. The slope of the isotherm is equivalent to the sediment sorption partitioning coefficient (K_d) in $L\ kg^{-1}$. (b) [Fluridone] in microcosms incubated with relevant environmental inocula from Hooker Lake at 3 μM . (c) Sediment extraction data from Hooker Lake water-sediment microcosms. Mass balance represents percent of fluridone sorbed to sediment. Concentration represents μmol of fluridone per kg of dried sediment. (d) [Fluridone], [3-trifluoromethyl benzoic acid], and area of an unknown product detected in the water-sediment microcosms only. Error bars represent standard deviation of triplicate samples. 54

Figure 3.4. (a) All sample sites on Hooker Lake. Map made using ArcGIS. (b) [Fluridone] in each sample site during treatment. Dashed line is expected lake-wide [fluridone] concentration. 57

Figure A.1. Map of lakes sampled during 2021 and 2022 field campaigns. Map made using Leaflet package in RStudio. 73

Figure A.2. FPB and florpyrauxifen concentrations in hydrolysis experiments in buffered ultrapure water at (a) pH 10, (b) pH 9, (c) pH 8, (d) pH 7, (e) pH 6, (f) pH 5, and (g) pH 4, as well as in unbuffered water from (h) Muskellunge (pH 7.15), (i) Silver (pH 7.22), and (j) South Twin (pH 8.62) lakes. Error bars represent the standard deviation of triplicate reactors. 77

Figure A.3. Absorbance data for florpyrauxifen from pH 2.5-4 at 239 nm. An acid dissociation constant (pK_a) of 3.18 was determined by measuring pH at different wavelengths and using least squares regression. 78

Figure A.4. Sorption kinetics of FPB interaction with lake sediment and control of FPB without sediment over time. FPB with sediment shows equilibrium is reached by 8 hours of sediment interaction. FPB control without sediment shows little to no loss occurs through volatilization, photodegradation, or sorption to the glass bottles. 79

Figure A.5. Lilly Lake sediment sorption isotherms for (a) FPB and (b) florpyrauxifen. The slope of the isotherm is equivalent to the sediment sorption partitioning coefficient (K_d) in $L\ kg^{-1}$. Error bars represent the standard deviation of triplicate reactors. 80

Figure A.6. Lilly Lake microcosms incubated with (a-c) FPB and (d-f) florpyrauxifen. Reactors contained (a, d) 0.2 μm filter sterilized water only (abiotic controls), (b, e) 0.2 μm filter sterilized water with sediment, and (c, f) unfiltered lake water only. Error bars represent the standard deviation of samples from triplicate microcosms. Error bars in each figure are smaller than the data point symbols. 82

- Figure A.7. Pseudo-first-order microcosm kinetics for FPB in (a) Kettle Moraine Lake and (b) Lilly Lake, as well as florpyrauxifen incubations in (c) Kettle Moraine Lake and (d) Lilly Lake. “Abiotic control” is 0.2 μm filter sterilized water only, “sediment-water” is 0.2 μm filter sterilized water with sediment, and “water only” is unfiltered lake water. Error bars represent the standard deviation of triplicate reactors. 83
- Figure A.8. Molar absorptivity (ϵ) of FPB and florpyrauxifen overlapping with 311 nm intensity of Rayonet bulbs used in photochemistry experiments..... 84
- Figure A.9. (a) Irradiance data for the global horizontal irradiance spectra of each study lake generated using SMARTS. (b) Hourly irradiance at Kettle Moraine Lake during the day of treatment from 7 am to 7 pm..... 86
- Figure A.10. First-order kinetics of photodegradation of (a) FPB and (b) florpyrauxifen at 311 nm in buffered ultrapure water (direct control) and filtered lake water (Kettle Moraine and Lily) alongside dark controls. Error bars represent the standard deviation of triplicate reactors. 89
- Figure A.11. Solution determination for sediment and plant extractions. All solution recoveries were comparable; therefore 90% ACN was chosen due to being a previously established method..... 90
- Figure A.12. FPB and florpyrauxifen concentrations in nearshore sediment from (a) Kettle Moraine Lake and (b) Lilly Lake. Concentration represents nmol per kg of dried sediment. ^{13}C -FPB and ^{13}C -florpyrauxifen concentrations were used to correct for extraction efficiency... 90
- Figure A.13. Sediment extraction data from Kettle Moraine Lake microcosms incubated with (a) FPB and (b) florpyrauxifen and Lilly Lake microcosms incubated with (c) FPB and (d) florpyrauxifen. Concentration represents nmol per kg of dried sediment. ^{13}C -FPB and ^{13}C -florpyrauxifen concentrations were used to correct for extraction efficiency. 91
- Figure A.14. Plant extraction data from (a) Kettle Moraine Lake and (b) Lilly Lake. Concentration represents nmol per kg of dried plant material. ^{13}C -FPB and ^{13}C -florpyrauxifen concentrations were used to correct for extraction efficiency. 92
- Figure A.15. (a) All sites on Kettle Moraine Lake. Concentrations of (b) FPB, florpyrauxifen, hydroxy-florpyrauxifen, hydroxy-FPB, and dechloro-FPB in site KM1. Concentrations of (c) FPB, (d) florpyrauxifen, (e) hydroxy-florpyrauxifen, (f) hydroxy-FPB, and (g) dechloro-FPB in all sites. Dashed line in panel (c) is the potential lake-wide FPB concentration of 1.28 nM. 93
- Figure A.16. (a) All sites on Muskellunge Lake. (b) Lake-wide average concentrations of FPB and florpyrauxifen. Concentrations of (c) FPB and (d) florpyrauxifen in all sites. Dashed line in panel (b) is potential lake-wide FPB concentration of 0.48 nM. Error bars in (b) represent standard deviation of three samples (one from each site) at each time point. 94

- Figure A.17. (a) All sites on Silver Lake. (b) Lake-wide average concentrations of FPB and florpyrauxifen. Concentrations of (c) FPB and (d) florpyrauxifen in all sites. Dashed line panels (b) and (c) is potential lake wide concentration of 0.36 nM. Error bars in (b) represent standard deviation of three samples (one from each site) at each time point. 95
- Figure A.18. (a) All sites on South Twin Lake. (b) Lake-wide average concentrations of FPB and florpyrauxifen. Concentrations of (c) FPB and (d) florpyrauxifen in all sites. Dashed line in panels (b) and (c) is potential lake wide concentration of 0.93 nM. Error bars in (b) represent standard deviation of three samples (one from each site) at each time point. 96
- Figure A.19. (a) All sites on Lilly Lake. (b) Lake-wide average concentrations of FPB, florpyrauxifen, and hydroxy-florpyrauxifen. Concentrations of (c) FPB, (d) florpyrauxifen, and (e) hydroxy-florpyrauxifen in all sites. Dashed line in panels (b) and (c) is potential lake wide concentration of 2.16 nM. Error bars in (b) represent standard deviation of three samples (one from each site) at each time point. 97
- Figure A.20. Modeling results of first-order kinetics compared with measured epilimnion concentrations of FPB in Kettle Moraine Lake. 101
- Figure B.1. Molar absorptivity (ϵ) fluridone and the irradiance of the 311 nm bulbs used in photochemistry experiments (second y-axis). 106
- Figure B.2. Average of the hourly irradiance at Hooker Lake during the day of treatment from 6 am to 6 pm. Global horizontal irradiance spectra at each time was generated using SMARTS. 107
- Figure B.3. Sorption kinetics of fluridone interaction with lake sediment along with controls of fluridone without sediment and the lake sediment with no fluridone. Fluridone with sediment shows equilibrium is reached by 6 hours of sediment interaction. Fluridone control without sediment shows little to no loss occurs through volatilization, photodegradation, or sorption to the glass bottles. The sediment control shows no signs of preexisting fluridone that would skew the measured concentrations. Error bars represent the standard deviation of triplicate reactors. 109
- Figure B.4. Pseudo-first-order microcosm kinetics for fluridone. Error bars represent the standard deviation of triplicate reactors. 110
- Figure B.5. [Fluridone] in original microcosms incubated with relevant environmental inocula from Hooker Lake at 3 μ M. 110
- Figure B.6. Percent recovery of fluridone from sediment samples using a 50:50 methanol:water extraction solution. Error bars represent the standard deviation of triplicate reactors. 111

List of Tables

Table 2.1. Summary of sampled lakes including waterbody identification code (WBIC), herbicide application area, treatment date, target concentration, and treatment history. Trophic status is designated as eutrophic (E), mesotrophic (M), or oligotrophic (O). Target FPB concentration is from treatment permit application. When not stated on permit application, target concentration was calculated from lake/bay volume and amount of herbicide applied as listed on treatment record.....	18
Table A.1. Chemical structures, formulas, and molecular weight of florpyrauxifen-benzyl and five degradation products.....	71
Table A.2. Precursor and product ion information for FPB, internal standards, and degradation products.....	75
Table A.3. Gradient chromatography details for LC-MS/MS analytical method of FPB, internal standard, and degradation products.....	75
Table A.4. Method information for quantification of 2-nitrobenzaldehyde via high pressure liquid chromatography.....	76
Table A.6. Sediment sorption parameters for FPB and florpyrauxifen. K_d is the sediment-specific partitioning coefficient in $L\ kg^{-1}$ and f_{oc} is the fraction of organic content in each sediment.....	81
Table A.7. SMARTS modeling input parameters for the in-lake photolysis degradation of FPB.....	87
Table A.8. Half-lives of FPB in field study and laboratory experiments.....	99
Table B.1. Summary of literature reports of field, photodegradation, biodegradation, and sorption studies of fluridone.....	104
Table B.2. Location, pH, dissolved organic carbon, $E_2:E_3$ (absorbance at 250 nm divided by absorbance at 365 nm), and $SUVA_{254}$ (specific UV absorbance at 254 nm) for all lakes visited during field sampling.....	105
Table B.3. SMARTS modeling input parameters for the in-lake photolysis degradation of fluridone in Hooker Lake on the day of treatment.....	108
Table B.4. Time segments for gradient method used to analyze fluridone and 3-trifluoromethyl benzoic acid on HPLC.....	112
Table B.5. Instrument parameters for detection of fluridone, 3-trifluoromethyl benzoic acid, and 2-nitrobenzaldehyde in water.....	113
Table B.6. Time segments for gradient method used to analyze fluridone on LC-MS/MS.....	114

Chapter 1. Introduction

Invasive aquatic plant species are ubiquitous throughout the state of Wisconsin and their presence has led to an increasing need for control. Invasive plants are particularly destructive to native plant communities,^{1,2} threaten the integrity of aquatic ecosystems,³ and impede recreational use of water bodies.⁴ These invasive plants are also notorious in an economic sense in addition to their negative ecological effects.⁵⁻⁷ Spending on aquatic plant management in Wisconsin alone totals approximately \$9.3 million a year,⁸ and lakefront property values on invaded lakes have lowered by 13-19%.⁹ Groups involved in the management of invasive and nuisance aquatic plants range from homeowners to local and state governments, indicating a widespread need for the development and optimization of strategic invasive aquatic plant control.⁹

Of particular prevalence in Wisconsin is the invasive Eurasian watermilfoil (*Myriophyllum spicatum*, **EWM**) as well as its hybridization with native watermilfoil, or hybrid watermilfoil (*Myriophyllum spicatum* × *Myriophyllum sibiricum*, **HWM**). EWM has been found in 911 lakes and rivers throughout Wisconsin,¹⁰ while HWM populations have been confirmed in ~170 lakes in Wisconsin.^{11,12} EWM and HWM are known to cause recreational nuisances and significantly decrease native biodiversity.^{8,13} While there are other methods for controlling invasive and nuisance aquatic plants such as physical control (e.g., mechanical harvesting), and biological control (e.g., weevil release), chemical control is often preferred due to its selectivity and greater efficacy with long-term control.¹³⁻¹⁵

Herbicide application is conducted with either whole-lake or spot treatments in order to reach a specific concentration and exposure time (**CET**) throughout the water body in its entirety or in the area of interest.^{16,17} However, an understanding of herbicide degradation in the aquatic environment is critical to discern if the exposure time is sufficient for invasive species eradication or if the treatment will fail, necessitating extra costly treatments. Additionally, increased herbicide application can cause further harm to native vegetation along with target species resistance. For example, there have been observations of EWM and HWM genotypes developing reduced susceptibility to aquatic herbicides.^{18,19} To best combat this issue, application managers will alternate between multiple aquatic herbicides with different modes of action. Therefore, application managers as well as agrochemical companies have great interest in developing herbicides with new modes of action and understanding which environmental characteristics control their degradation. The extent of this thesis involves the study of two commonly used aquatic herbicides: florpyrauxifen-benzyl (**FPB**) and fluridone.

Florpyrauxifen-benzyl usage and transformation processes. FPB (trade name: ProcellaCOR) is an emerging aquatic herbicide that is effective at targeting EWM and HWM.¹⁷ It operates as a synthetic auxin (i.e., a growth hormone) which causes excessive plant growth that cannot be supported and leads to frail plant tissue. FPB has established CET requirements ranging from 12-24 hours, indicating it reacts with the target species relatively quickly.²⁰ This, in addition to its strong ability to combat EWM and HWM, makes it a more efficient and favorable herbicide compared to previously established auxin-mimic herbicides such as 2,4-

dichlorophenoxyacetic acid (**2,4-D**), which has shown to have unreliable efficacy towards HWM^{15,17,20} and requires a longer CET of 24-72 hours at higher concentrations.^{21,22}

Recent data collected from lakes in Wisconsin treated with FPB have shown dramatic differences in EWM and HWM control, with southern lakes experiencing significantly less control. This observation could be due to aquatic environmental chemical differences such as higher pH and proximity to more urban areas. At a neutral pH, the half-life of FPB due to strictly hydrolysis has been reported to be 111 days,²³ but this half-life decreases at a pH above 9.²⁴ In surface waters, FPB can degrade by aqueous photolysis, with reported half-lives of 0.07-2 days.^{23,25} Photolysis can be either a direct or indirect process depending on the quantity and quality of dissolved organic matter (**DOM**) in the lake environment. During indirect photolysis, sunlight reacts with DOM to produce reactive intermediates (**PPRI**), such as hydroxyl radical (**•OH**), singlet oxygen (**¹O₂**), and triplet state DOM (**³DOM**), that could potentially break down FPB.²⁶ Another factor contributing to the relatively short half-life of FPB is that it is a highly sorptive substance, with its organic soil adsorption coefficient (**K_{oc}**) ranging from around 22,000 ± 44,000 L kg⁻¹.²³

The major degradation product of FPB is florpyrauxifen, which is commonly referred to as the acid form of FPB.²³ Florpyrauxifen is considerably more persistent than FPB itself; FPB has a half-life of around 4-8.4 days in aerobic environments and 2-2.7 days under anaerobic conditions,^{23,27} while florpyrauxifen has a half-life ranging from 6.3-21 days.^{17,20,23} Florpyrauxifen is herbicidal to a lesser extent than FPB, however its persistence may have unintended consequences for non-target species in lakes.^{28,29} Not only is florpyrauxifen more

persistent, but the majority of FPB will transform into this degradation product. One study found that under experimental conditions, 44-59% of FPB applied to water samples converted to its acid form only one day after treatment (**DAT**), and nearly all the herbicide converted to florpyrauxifen 7-14 DAT.^{24,29} Virtually no additional information is available on the fate and transport of florpyrauxifen, despite its expected formation following FPB application to surface waters and observed ability to act as a less effective herbicide.

FPB is known to have several other potential degradation products that could form in aquatic environments.^{28,30,31} In addition to florpyrauxifen, dechloro-FPB and dechloro-florpyrauxifen are expected to form mainly through photodegradation, while hydroxy-FPB and hydroxy-florpyrauxifen are expected to be produced predominantly through biodegradation (**Figure 1.1**).^{25,30} Identifying specific degradation products in the field can provide insight into which transformation pathways are degrading FPB in the water. Given that FPB is a very attractive aquatic herbicide in terms of effectiveness for combatting EWM/HWM and shorter required exposure for the majority of aquatic environments, knowledge on the fate and transport of the parent compound in addition to the potential degradation products is critical for optimizing its use.

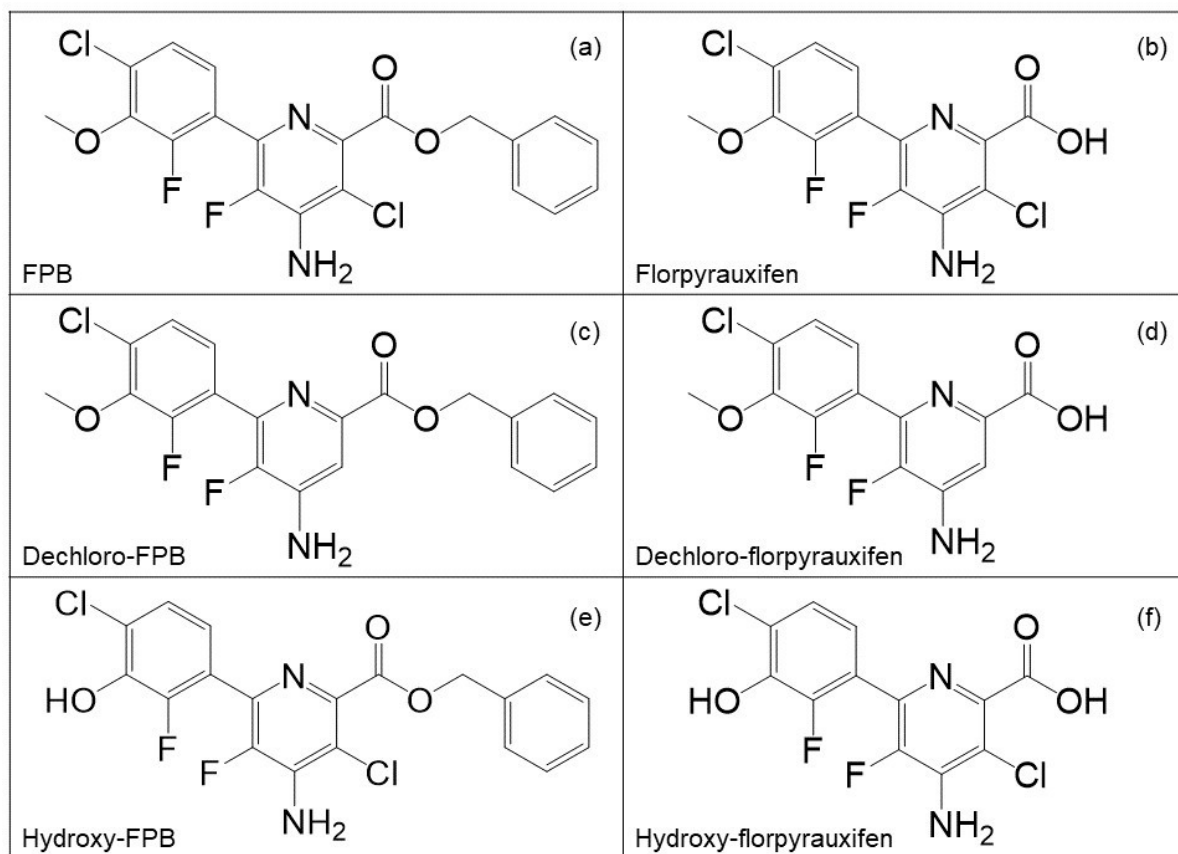


Figure 1.1. Chemical structures of (a) FPB and its five potential degradation products: (b) florpyrauxifen, (c) dechloro-FPB, (d) dechloro-florpyrauxifen, (e) hydroxy-FPB, and (f) hydroxy-florpyrauxifen.

Fluridone usage and transformation processes. Fluridone is an aquatic herbicide that is known to control invasive hydrilla (*Hydrilla verticillate*), but is also effective at treating EWM and HWM (**Figure 1.2a**).^{32,33} Fluridone acts as a photobleaching agent by inhibiting the production of pigments that protect chlorophyll from breaking down in the sun, thus preventing the plant's ability to photosynthesize.^{34,35} For this reason, fluridone is only effective while the plants are actively growing.³² Fluridone is applied at relatively low concentrations (6-36 nM), but requires a significantly long CET (over 100 days) as the plants will easily be able to resume

growth if fluridone is removed from the water.³⁶ As a result, fluridone treatments often require multiple applications in order to maintain an effective concentration.^{9,37}

The reported half-life of fluridone in aquatic environments ranges from 4 to 97 days depending on various water conditions.³² Photolysis is proposed as a major degradation pathway of fluridone, with half-lives of 28 hours and 12 days in ultrapure water and lake water, respectively.³⁸⁻⁴⁰ Microbial degradation is relatively slow with half-lives reported from 44 days to 192 days.^{41,42} However, it is still an important transformation pathway of fluridone, with 3-trifluoromethyl benzoic acid being a biodegradation product detected in the field (**Figure 1.2b**).³² Fluridone is also able to adsorb to sediments with K_{oc} values ranging from 270 to 6400 $L\ kg^{-1}$.⁴³⁻⁴⁵ Because of this, fluridone has been detected in sediments for up to a year post-treatment, indicating its affinity to sediments is an important factor in fluridone persistence.^{46,47}

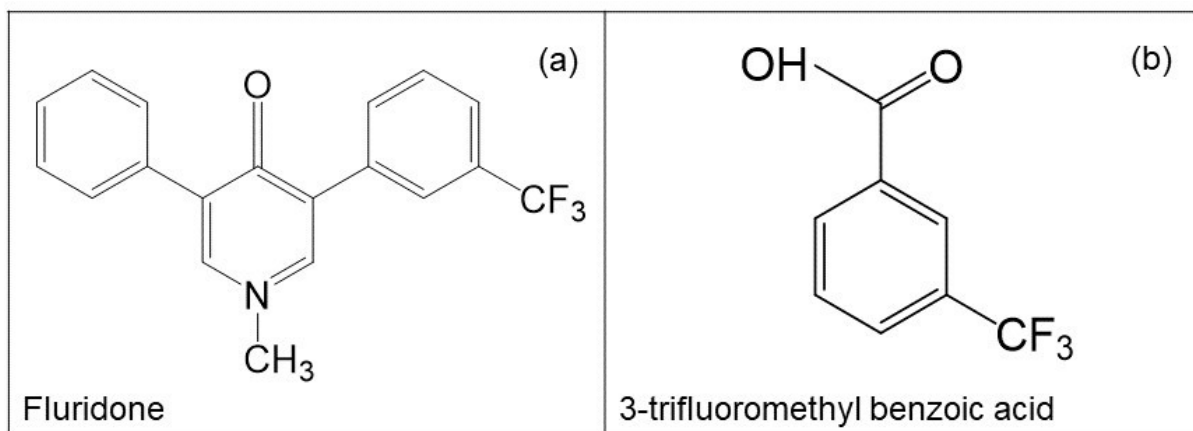


Figure 1.2. Chemical structures of (a) fluridone and a biodegradation product (b) 3-trifluoromethyl benzoic acid.

Research needs. While there are many laboratory studies conducted on aquatic herbicides and their behavior under various conditions, little research has been conducted that directly connect these laboratory studies to herbicide behavior in the field. Environmental half-

lives are predicted based off these experiments. However, due to the isolated nature of laboratory experiments, these assessments often fall short of accurately predicting the fate of these aquatic herbicides. There are several processes in the natural environment such as sediment/suspended solids interaction, advective transport, sunlight, and chemical conditions that are difficult to replicate in a controlled experiment. There is also a lack of comprehensive environmental fate studies with organic compounds due to the technical and logistical challenges involved with conducting field investigations and tracking the compound from its initial introduction into the aquatic system of study. Aquatic herbicides represent a unique opportunity to study organic chemical fate under field conditions because herbicides are intentionally added at known times and locations, typically at concentrations that are readily detectable.

Not only is there a need for research that investigates the link between laboratory tests and environmental fate, but there are also critical knowledge gaps with FPB and fluridone specifically. Fluridone is expected to be mainly influenced by photodegradation, but there are no studies on the specific interaction of fluridone with PPRIs in lake water to determine if its susceptible to indirect photodegradation. Furthermore, little is known about the transformation of FPB to florpyrauxifen despite the persistence of this degradation product in lake waters long after application.

In Chapter 2, we investigate the fate of FPB and its known transformation products in water, sediment, and plants in five lakes throughout Wisconsin. We also conduct parallel laboratory experiments to quantify rates and mechanisms of hydrolysis, sorption,

biodegradation, and photodegradation. Two different material balance approaches are used to quantify the relative importance of each pathway under field conditions.

In Chapter 3, we study the susceptibility of fluridone to direct and indirect photodegradation, sorption, and biodegradation in water only or water-sediment suspensions through tandem laboratory experiments. We also elucidate degradation product formation by isolating each transformation pathway. These results are compared to fluridone behavior quantified during a field treatment in Wisconsin as well as existing literature related to fluridone fate in lakes.

This research is unique in the sense that the field studies were conducted in conjunction with application managers and consultants to capture a holistic picture of aquatic herbicide degradation from beginning to end. The behavior of the herbicides in the field and the transformation products that formed were then compared to laboratory experiments that further substantiated the major degradation pathways of the herbicide. This allows resource managers to further discern how quickly the herbicide will degrade and to what extent the chemical will persist in various environments, as well as provide a fundamental understanding for linking the behavior of organic compounds in laboratory studies to their fate in freshwater environments.

References

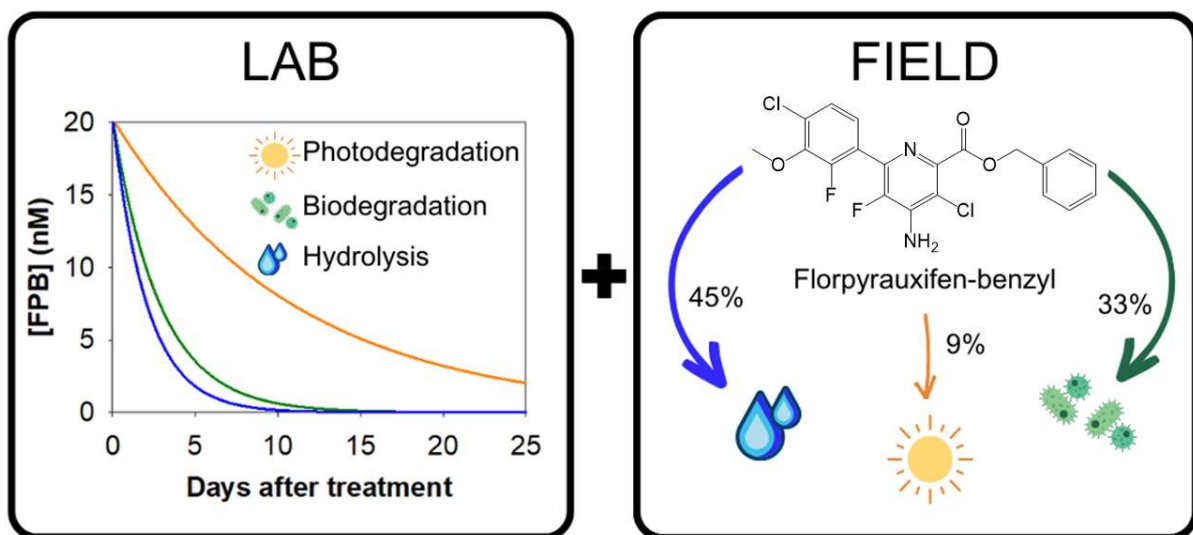
1. Boylen, C. W.; Eichler, L. W.; Madsen, J. D. Loss of native aquatic plant species in a community dominated by Eurasian watermilfoil. *Hydrobiologia* **1999**, *415*, 207–211.
2. Madsen, J. D.; Sutherland, J. W.; Bloomfield, J. A.; Eichler, L. W.; Boylen, C. W. The decline of native vegetation under dense Eurasian watermilfoil canopies. *J. Aquat. Plant Manage.* **1991**, *29*, 94–99.
3. Schleppebach, B. T.; Matzke, G.; Shaw, S. L.; Sass, G. G. Fish and zooplankton community responses to the cessation of long-term invasive Eurasian watermilfoil (*Myriophyllum spicatum*) chemical treatments in a north-temperate, USA lake. *Fishes* **2022**, *7* (4), 165.
4. Smith, C. S.; Barko, J. W. Ecology of Eurasian watermilfoil. *J. Aquat. Plant Manage.* **1990**, *28*, 55–64.
5. Horsch, E. J.; Lewis, D. J. The effects of aquatic invasive species on property values: Evidence from a quasi-experiment. *Land Economics* **2009**, *85* (3), 391–409.
6. Olden, J. D.; Tamayo, M. Incentivizing the public to support invasive species management: Eurasian milfoil reduces lakefront property values. *PLoS ONE* **2014**, *9* (10), e110458.
7. Lovell, S. J.; Stone, S. F.; Fernandez, L. The economic impacts of aquatic invasive species: A review of the literature. *Agric. Res. Econ. Rev.* **2006**, *35* (1), 195–208.
8. Mikulyuk, A., Kujawa, E., Nault, M. E., Van Egeren, S., Wagner, K. I., Barton, M., Hauxwell, J., & Vander Zanden, M. J. Is the cure worse than the disease? Comparing the ecological effects of an invasive aquatic plant and the herbicide treatments used to control it. *Facets* **2020**, *5* (1), 353–366.
9. Blanke, C.; Mikulyuk, A.; Nault, M.; Provost, S.; Schaal, C.; Van Egeren, S.; Williams, M.; Mednick, A. Strategic Analysis of Aquatic Plant Management in Wisconsin https://dnr.wisconsin.gov/sites/default/files/topic/Aid/grants/surfacewater/APMSA_Final_2019-06-14.pdf (accessed April 2023).
10. Wisconsin Department of Natural Resources. Wisconsin Eurasian watermilfoil locations <https://dnr.wi.gov/lakes/invasives/AISLists.aspx?species=EWM&location=ANY> (accessed April 2023).
11. Moody, M.L.; D.H. Les. Geographic distribution and genotypic composition of invasive hybrid watermilfoil (*Myriophyllum spicatum* x *M. sibiricum*) populations in North America. *Biol. Invasions* **2007**, *9*, 559-570.
12. Zuelling, M. P.; Thum, R. A. Multiple introductions of invasive Eurasian watermilfoil and recurrent hybridization with native northern watermilfoil in North America. *J. Aquat. Plant Manage.* **2012**, *50*, 1-19.
13. Kujawa, E. R.; Frater, P.; Mikulyuk, A.; Barton, M.; Nault, M. E.; Van Egeren, S.; Hauxwell, J. Lessons from a decade of lake management: Effects of herbicides on Eurasian watermilfoil and native plant communities. *Ecosphere* **2017**, *8* (4), e01718.

14. Nault, M. E.; Barton, M.; Hauxwell, J.; Heath, E.; Hoyman, T.; Mikulyuk, A.; Netherland, M. D.; Provost, S.; Skogerboe, J.; Van Egeren, S. Evaluation of large-scale low-concentration 2,4-D treatments for Eurasian and hybrid watermilfoil control across multiple Wisconsin lakes. *Lake Reservoir Manage.* **2018**, *34* (2), 115–129.
15. Nault, M. E.; Netherland, M. D.; Mikulyuk, A.; Skogerboe, J. G.; Asplund, T.; Hauxwell, J.; Toshner, P. Efficacy, selectivity, and herbicide concentrations following a whole-lake 2,4-D application targeting Eurasian watermilfoil in two adjacent northern Wisconsin lakes. *Lake Reservoir Manage.* **2014**, *30* (1), 1–10.
16. Richardson, R. J. Aquatic Plant Management and The Impact of Emerging Herbicide Resistance Issues. *Weed Technol.* **2008**, *22* (1), 8–15.
17. Mudge, C. R., Sartain, B. T., Sperry, B. P., Getsinger, K. D. (2021). Efficacy of Florpyrauxifen-benzyl for Eurasian Watermilfoil Control and Nontarget Illinois Pondweed, Elodea, and Coontail Response <https://erdc-library.erd.dren.mil/jspui/bitstream/11681/42063/1/ERDC-TN%20APCRP-CC-24.pdf> (accessed April 2023).
18. Larue, E. A.; Zuellig, M. P.; Netherland, M. D.; Heilman, M. A.; Thum, R. A. Hybrid watermilfoil lineages are more invasive and less sensitive to a commonly used herbicide than their exotic parent (Eurasian watermilfoil). *Evol. Appl.* **2013**, *6* (3), 462–471.
19. Berger, S. T.; Netherland, M. D.; MacDonald, G. E. Laboratory documentation of multiple-herbicide tolerance to fluridone, norflurazon, and topamazone in a hybrid watermilfoil (*Myriophyllum spicatum* × *M. sibiricum*) population. *Weed Sci.* **2015**, *63* (1), 235–241.
20. Wisconsin Department of Natural Resources Florpyrauxifen-benzyl Chemical Fact Sheet <https://dnr.wi.gov/water/wsSWIMSDocument.ashx?documentSeqNo=164039981> (accessed April 2023).
21. Green, W. R.; Westerdahl, H. E. Response of Eurasian Watermilfoil to 2,4-D Concentrations and Exposure Times. *J. Aquat. Plant Manage.* **1990**, *28*, 27–32.
22. Nault, M.; Mikulyuk, A.; Hauxwell, J.; Skogerboe, J.; Asplund, T.; Barton, M.; Wagner, K.; Hoyman, T.; Heath, E. Herbicide Treatments in Wisconsin Lakes https://files.dnr.state.mn.us/eco/invasives/Herbicide_Treatments_in_WI.pdf (accessed April 2023).
23. Review of Florpyrauxifen-benzyl for Application to Massachusetts Lakes and Ponds, <https://www.mass.gov/doc/florpyrauxifen-benzyl/download> (accessed April 2023).
24. Heilman, M.A., M.D. Netherland, R.J. Richardson, E.J. Haug, J.P. Beets, B.E. Willis. PROCELLACOR™ - A novel herbicide technology for selective management of aquatic invasive plants <https://apirs.plants.ifas.ufl.edu/site/assets/files/380553/380553.pdf> (accessed April 2023).
25. U.S. EPA. Independent Laboratory Validation of a Dow AgroSciences Method for the Determination of XDE-848 Benzyl Ester and Three Metabolites (X11438848, X12300837 and X11966341) in Soil. <https://www.epa.gov/sites/default/files/2017->

- 09/documents/ilv_-_florpyrauxifen-benzyl_degradates_in_soil_-_mrid_49677776.pdf (accessed April 2023).
26. McConville, M. B.; Mezyk, S. P.; Remucal, C. K. Indirect photodegradation of the lampricides TFM and niclosamide. *Environ. Sci.: Processes Impacts* **2017**, *19* (8), 1028–1039.
 27. Washington State Department of Ecology (WSDE). Final Supplemental Environmental Impact Statement for State of Washington Aquatic Plant and Algae Management. <https://fortress.wa.gov/ecy/publications/documents/1710020.pdf> (accessed April 2023).
 28. Arena, M.; Auteri, D.; Barmaz, S.; Brancato, A.; Brocca, D.; Bura, L.; Carrasco Cabrera, L.; Chaideftou, E.; Chiusolo, A.; Civitella, C.; Court Marques, D.; Crivellente, F.; Ctverackova, L.; de Lentdecker, C.; Egsmose, M.; Erdos, Z.; Fait, G.; Ferreira, L.; Goumenou, M.; Greco, L.; Ippolito, A.; Istace, F.; Jarrah, S.; Kardassi, D.; Leuschner, R.; Lostia, A.; Lythgo, C.; Magrans, J. O.; Medina, P.; Mineo, D.; Miron, I.; Molnar, T.; Padovani, L.; Parra Morte, J. M.; Pedersen, R.; Reich, H.; Sacchi, A.; Santos, M.; Serafimova, R.; Sharp, R.; Stanek, A.; Streissl, F.; Sturma, J.; Szentes, C.; Tarazona, J.; Terron, A.; Theobald, A.; Vagenende, B.; van Dijk, J.; Villamar-Bouza, L. Peer review of the pesticide risk assessment of the active substance florpyrauxifen (variant assessed florpyrauxifen-benzyl). *EFSA J.* **2018**, *16* (8), 5378.
 29. Netherland, M. D.; Richardson, R. J. Evaluating sensitivity of five aquatic plants to a novel arylpicolinate herbicide utilizing an organization for economic cooperation and development protocol. *Weed Sci.* **2016**, *64* (1), 181–190.
 30. U.S. EPA. Independent Laboratory Validation of a Dow AgroSciences Method for the Determination of XDE-848 Benzyl Ester and Five Metabolites (X11438848, X12300837, X11966341, X12131932 and X12393505) in Water https://www.epa.gov/sites/production/files/2017-09/documents/ilv_-_florpyrauxifen-benzyl_degradates_in_water_-_mrid_49677802.pdf (accessed April 2023).
 31. U.S. EPA. Final Registration Decision on the New Active Ingredient Florpyrauxifen-benzyl <https://www.regulations.gov/document/EPA-HQ-OPP-2016-0560-0065> (accessed April 2023).
 32. Wisconsin Department of Natural Resources Fluridone Chemical Fact Sheet, <https://dnr.wi.gov/lakes/plants/factsheets/FluridoneFactsheet.pdf>, (accessed April 2023).
 33. Jeremy, S. G.; Poovey, A. G.; Netherland, M. D. Efficacy of Fluridone on Eurasian and Hybrid Watermilfoil. *J. Aquat. Plant Manage.* **2007**, *45*, 116–118.
 34. Arnold, W. R. Fluridone: A new aquatic herbicide. *J. Aquat. Plant Manage.* **1979**, *17*, 30–33.
 35. Bartels, P. G.; Watson, C. W. Inhibition of carotenoid synthesis by fluridone and norflurazon. *Weed Sci.* **1978**, *26* (2), 198–203.
 36. Netherland, M. D.; Getsinger, K. D.; Turner, E. G. Fluridone concentration and exposure time requirements for control of Eurasian watermilfoil and hydrilla. *J. Aquat. Plant Manage.* **1993**, *31*, 189–194.

37. West, S. D.; Burger, R. O.; Poole, G. M.; Mowrey, D. H. Bioconcentration and field dissipation of the aquatic herbicide fluridone and its degradation products in aquatic environments. *J. Agric. Food Chem.* **1983**, *31* (3), 579–585.
38. Macdonald, G. E.; Haller, W. T.; Shilling, D. G. UV-b filtration to reduce photolysis of fluridone in experimental tanks. *J. Aquat. Plant Manage.* **1996**, *34* (2), 78–80.
39. Saunders, D. G.; Mosier, J. W. Photolysis of the aquatic herbicide fluridone in aqueous solution. *J. Agric. Food Chem.* **1983**, *31* (2), 237–241.
40. Mossler, M. A.; Shilling, D. G.; Haller, W. T. Photolytic degradation of fluridone. *J. Aquat. Plant Manage.* **1989**, *27*, 69–73.
41. Mossler, M. A.; Shilling, D. G.; Albrecht, S. L.; Haller, W. T. Microbial degradation of fluridone. *J. Aquat. Plant Manage.* **1991**, *29*, 77–80.
42. Howard, P.H. Handbook of Environmental Fate and Exposure Data for Organic Chemicals, Lewis Publishers, Chelsea, MI, **1991**.
43. Weber, J.; P. Shea; S. Weed. Fluridone retention and release in soils. *Soil Sci. Soc. Am. J.* **1986**, *50* (3), 582-588.
44. Reinert, K.H. Reactions and Movements of Organic Chemicals in Soils, Soil Science Society of American and American Society of Agronomy, Madison, WI, **1989**.
45. Hornsby, A. G.; Wauchope, R. D.; Herner, A. E. Pesticide Properties in the Environment, Springer-Verlag, New York, **1996**.
46. Muir, D.; Grift, N. P.; Blouw, A. P.; Lockhart, W. L. Persistence of fluridone in small ponds. *J. Environ. Qual.* **1980**, *9* (1), 151–156.
47. Muir, D. C. G.; Grift, N. P. Fate of fluridone in sediment and water in laboratory and field experiments. *J. Agric. Food Chem.* **1982**, *30* (2), 238–244.

Chapter 2. Quantifying the role of simultaneous transformation pathways in the fate of the novel aquatic herbicide florpyrauxifen-benzyl



Prologue. Chapter 2 is a collaboration between Sydney Van Frost, Amber White, Josie Jauquet, Angela Magness, Katherine McMahon, and Christy Remucal. This is a draft manuscript that will be submitted for publication. S.V. and A.W. collected the samples, analyzed the samples, and wrote the manuscript. J.J. and A.M. assisted with field work and laboratory experiments. K.M. and C.R. were the principal investigators.

Abstract

Predicting the fate of organic compounds in the environment is difficult due to the inability of laboratory studies to replicate field conditions. We used the aquatic herbicide florpyrauxifen-benzyl (FPB) as a tool to investigate the contribution of multiple transformation pathways to FPB fate in lakes for the first time. FPB persisted in five Wisconsin lakes for 5-7 days with an in-lake half-life less than 2 days. FPB formed four transformation products over the same timescale, with the bioactive product florpyrauxifen persisting up to 30 days post-treatment. Parallel laboratory experiments showed FPB is degraded to florpyrauxifen via base-promoted hydrolysis. Hydroxy-FPB and hydroxy-florpyrauxifen were determined to be biodegradation products, while dechloro-FPB was identified as a photoproduct. Material balance calculations using both laboratory rates and field product concentrations demonstrate that hydrolysis, biodegradation, sorption, and photodegradation occur on similar timescales. Furthermore, the combined results demonstrate that abiotic and plant-catalyzed hydrolysis of FPB to florpyrauxifen, followed by biodegradation of florpyrauxifen to hydroxy-florpyrauxifen, is the dominant transformation pathway in lakes. This study demonstrates how combined field and laboratory studies can be used to elucidate the role of simultaneous and interacting pathways in the fate of organic compounds in aquatic environments.

Introduction

Organic contaminant accumulation in aquatic environments poses a risk to environmental health and ecosystem services.^{1,2} The mixture of organic chemicals found in freshwaters includes intentionally released compounds (e.g., pesticides), unintentionally released compounds (e.g., pharmaceuticals in wastewater effluent), and biotic and abiotic transformation products of these compounds. Additionally, transformation products may retain or increase persistence or toxicity once in the ecosystem such that transformation of the parent compound does not always lead to a reduction of environmental impacts.³⁻⁶

Laboratory studies used to investigate transformation of pesticides and other polar organic compounds for regulatory risk assessment often fall short of accurately replicating environmental conditions.⁷⁻¹¹ For example, photodegradation studies do not require modeling for all compounds under *in situ* conditions or quantification of indirect photodegradation rates, which can be an important transformation pathway.¹²⁻¹⁴ Similarly, biodegradation experiments oversimplify sediment-water dynamics and do not replicate ambient nutrients, oxygen, and light that microbial populations experience in aquatic environments.¹⁵⁻²⁰ In addition, regulatory studies typically do not consider transformation products, which may retain bioactivity.³⁻⁶ Thus, the emphasis of regulatory studies on active ingredients under highly idealized conditions may inadequately describe the complete fate of applied pesticide solutions at an ecosystem scale.

Florpyrauxifen-benzyl (FPB) is an auxin mimic herbicide registered in 2017 for use in aquatic environments.²¹ Commonly used to combat hydrilla, Eurasian watermilfoil, and other

broadleaf plants, FPB was developed to address increasing tolerance to other herbicides,²² such as 2,4-dichlorophenoxyacetic acid (2,4-D), an auxin mimic targeting different binding sites than FPB,^{23–26} and fluridone, a photobleaching agent.^{27–29} FPB is an active ingredient in at least seven commercial formulations which contain 1.3 – 26.2% FPB.^{30–36}

FPB is understudied in laboratory and field settings with most existing information in US Environmental Protection Agency registration reports, product labels, and safety data sheets. Laboratory data suggest transformation of FPB via multiple pathways, including photodegradation, biodegradation, and hydrolysis.^{21–22,37,38} However, it is unknown which mechanisms are dominant as these isolated laboratory experiments are not directly applicable to aquatic environments where FPB may undergo multiple transformation processes simultaneously. Five degradation products of FPB have been identified in laboratory studies: florpyrauxifen, hydroxy-FPB, hydroxy-florpyrauxifen, dechloro-FPB, and dechloro-florpyrauxifen (**Table A.1**).^{21,39,40} It is possible that different transformation pathways form unique products, which would allow for determination of primary transformation mechanisms based on product formation; however, this hypothesis has not been evaluated for FPB. Finally, the lack of field data quantifying transformation of FPB confounds decision-making by resource managers.⁴¹ Field studies need to be conducted in tandem with laboratory studies to understand how each pathway contributes to the fate of FPB under environmental conditions and to identify transformation products of concern.

The goal of this study is to use the aquatic herbicide FPB as a tool to study competing pesticide transformation mechanisms in aquatic environments through combined laboratory and field studies. Intentional FPB application allows for controlled tracking of its fate in study

lakes, providing a holistic view of its behavior under environmental conditions. Parallel laboratory studies allow for the isolation of transformation pathways to determine individual transformation rates and product formation mechanisms. The synthesis of both laboratory and field measurements was used to determine the contribution of multiple simultaneous transformation and loss pathways to FPB fate in lakes for the first time. This study provides insight to the complete transformation of end-use FPB formulations from the active ingredient to its transformation products, along with an understanding for how this methodology can be applied to predict the behavior of other organic compounds in aquatic environments.

Materials and Methods

Chemicals. Chemicals were used as received and are described in **Section A.1**. All in-lake FPB treatments used ProcellaCOR EC, which consists of 2.7% FPB and 97.3% inactive ingredients (2.1% ethylhexanol, 0.9% methanol, 94.3% unknown).^{34,37}

FPB sample preservation and processing. Water samples for FPB analysis were preserved with methanol (50:50 methanol:water ratio) and 0.1% formic acid prior to syringe filtering through a 0.22 μm PES filter. A ^{13}C -labeled FPB internal standard was added at 2.2 nM (field campaign) or 11 nM (hydrolysis, microcosm, and sediment/plant extraction experiments), as well as 14 nM ^{13}C -florpyrauxifen (sediment/plant extractions) to account for loss during processing and storage. All laboratory experiments were conducted in amber glass bottles to prevent sorption and photodegradation (**Figure A.4**).

Field sampling. Five FPB treatments were studied during the summers of 2021 and 2022 (**Figure A.1**; **Table 2.1**). These treatments applied FPB to areas of high-density Eurasian

watermilfoil but had the potential to mix completely throughout the lake. Waterbodies with potential lake-wide FPB concentrations high enough to detect several orders of magnitude of loss were selected in collaboration with the Wisconsin Department of Natural Resources (WDNR).

Table 2.1. Summary of sampled lakes including waterbody identification code (WBIC), herbicide application area, treatment date, target concentration, and treatment history. Trophic status is designated as eutrophic (E), mesotrophic (M), or oligotrophic (O). Target FPB concentration is from treatment permit application. When not stated on permit application, target concentration was calculated from lake/bay volume and amount of herbicide applied as listed on treatment record.

Lake (WBIC)	Herbicide application area (m ²)	Lake surface area (m ²)	Trophic status	Treatment date	Water temp. (°C)	pH	Target lake wide conc. (nM)/(ppb)
South Twin Lake 31623700	234,718	2,541,000	O	June 9th, 2021	24	8.6	0.93/0.41
Muskellunge Lake 1596600	80,128	1,093,000	E	June 23 rd , 2021	24	7.2	0.48/0.21
Silver Lake 555700	60,703	1,283,000	O-M	June 23 rd , 2021	22	7.2	0.36/0.16
Lilly Lake 740900	42,492	343,983	O	May 23 rd , 2022	17	8.0	2.16/0.95
Kettle Moraine Lake 43900	72,843	845,793	M	June 3 rd , 2022	21	8.8	1.28/0.56

Pretreatment surface water was collected from the epilimnion by grab sampling and pretreatment sediment was collected from a nearshore area by Eckman dredge or hand-coring ≤ 2 hours prior to treatment (**Section A.2**). Pretreatment samples were used for all laboratory experiments. Water samples were collected for FPB and product analysis at one site in the treatment area, one outside of the treatment area (i.e., not intended to be treated), and one site

at the deepest point of each lake. Nearshore sediment samples were collected during each sampling event. Samples were collected immediately after FPB application (<1 hour after application), at 3- to 4-hour intervals for 12 hours after treatment, every 1 to 2 days after treatment for one week after treatment, and weekly thereafter. Samples collected after FPB treatments were preserved as described above and stored at 4 °C in the dark until analysis.

Analytical methods. FPB, florpyrauxifen, ¹³C-FPB, ¹³C-florpyrauxifen, hydroxy-FPB, hydroxy-florpyrauxifen, dechloro-FPB, and dechloro-florpyrauxifen were measured using liquid chromatography-tandem mass spectrometry. 2-Nitrobenzaldehyde was quantified using high-performance liquid chromatography. Ultraviolet-visible light spectra for each lake and compound were collected from 200-800 nm. Method details are provided in **Section A.3**.

Hydrolysis. FPB (45 nM) was added to ultrapure water buffered with 10 mM acetate (pH 4-5), phosphate (pH 6-7), or borate (pH 8-10), as well as water from five study lakes at ambient pH. Triplicate 250 mL glass amber bottles were stored at room temperature (20-25°C) in the dark and sampled regularly, ranging from every three hours for high pH conditions to weekly/biweekly for low pH conditions (**Section A.4**).

Sorption. Pretreatment sediment from two study lakes (Kettle Moraine and Lilly) was dried at 100°C for ≥8 hours. Kettle Moraine sediment (0.5 g) and Lilly Lake sediment (2.0 g) was separately added to buffered ultrapure water (pH 7, 5 mM phosphate buffer, 100 mL) with five varying concentrations of FPB and florpyrauxifen in triplicate (**Section A.5**). Different sediment masses were used because Lilly Lake sediment had a smaller organic content (0.4%) than Kettle Moraine (5%). Samples were shaken in an incubator shaker. Equilibrium concentrations were measured after 8 hours for FPB and 24 hours for florpyrauxifen.

Microcosm incubations. Water and sediment from Kettle Moraine and Lilly Lakes were used for microcosm biodegradation studies of FPB and florpyrauxifen (**Section A.6**). Degradation by the water column microbial community was quantified in triplicate microcosms with unfiltered lake water (3 L), while degradation by the sediment microbial community was quantified in microcosms with filtered lake water (2 L) and sediment (1 kg) at room temperature. Abiotic loss processes were assessed in control microcosms with filtered lake water (2 L). Microcosms were separately incubated with 23 nM (10 ppb) FPB and 29 nM (10 ppb) florpyrauxifen. This FPB concentration was representative of the maximum FPB application concentration in spot treatments.^{21,34,37}

Photodegradation. Photodegradation experiments were conducted in a Rayonet merry-go-round photoreactor with sixteen bulbs that emit light at 311 nm (± 22 nm width at half-max), which is within the solar spectrum and overlaps with the absorbance spectra of FPB and florpyrauxifen (**Figure A.8**).⁴² Irradiation experiments in borosilicate glass tubes were conducted in triplicate using 23 nM FPB and 29 nM florpyrauxifen in buffered (pH 7, 10 mM phosphate) ultrapure water (direct photodegradation) or 3 mg-C L⁻¹ buffered (pH 7, 10 mM phosphate) lake water (indirect photodegradation) alongside dark controls. Light intensity was quantified using 10 μ M 2-nitrobenzaldehyde⁴³ as a chemical actinometer. The direct quantum yield of each compound was calculated relative to the actinometer as described previously.^{7,42,44-45} The calculated quantum yield was combined with solar irradiance modeling using the Simple Model of Atmospheric Transfer of Sunshine (SMARTS)⁴⁶ to calculate FPB half-lives in sunlight (**Section A.7**).

Sediment and plant extractions. Sediment samples collected in the field and microcosm experiments were dried at 100°C for ≥ 8 hours. Plant samples collected in the field were freeze-dried and manually crushed.⁴⁷ Dried sediment and plant samples were extracted with 90% acetonitrile, 9.5% ultrapure water, and 0.5% formic acid (**Figure A.11**).⁴⁷⁻⁴⁹ Samples were shaken for 2 hours before the extraction solution was filtered for analysis (**Section A.8**).

Results and Discussion

FPB degradation and florpiauxifen formation in lakes. FPB was quantified in five Wisconsin lakes following application of commercial formulations (**Table 2.1**; **Figure A.1**). FPB reached up to 32 nM in treatment areas, which was near its solubility of 34 nM.³⁸ FPB was transported by advection from the site of application to the non-treated sites of all lakes except Kettle Moraine within 4-6 hours after treatment and reached a lake-wide homogenous concentration within 12-48 hours (**Figures 2.1a**; **Section A.9**). FPB transport beyond the treatment area showed that FPB did not remain localized to the treatment area, suggesting appropriate dosing measures and considerations of non-target impacts should be made for the whole lake. FPB half-lives were estimated using lake-wide average [FPB] and ranged <1 day to 2 days (**Figure 2.1a**; **Table A.8**). [FPB] was below detection (LOD = 0.07 nM) after 7 days in all lakes.

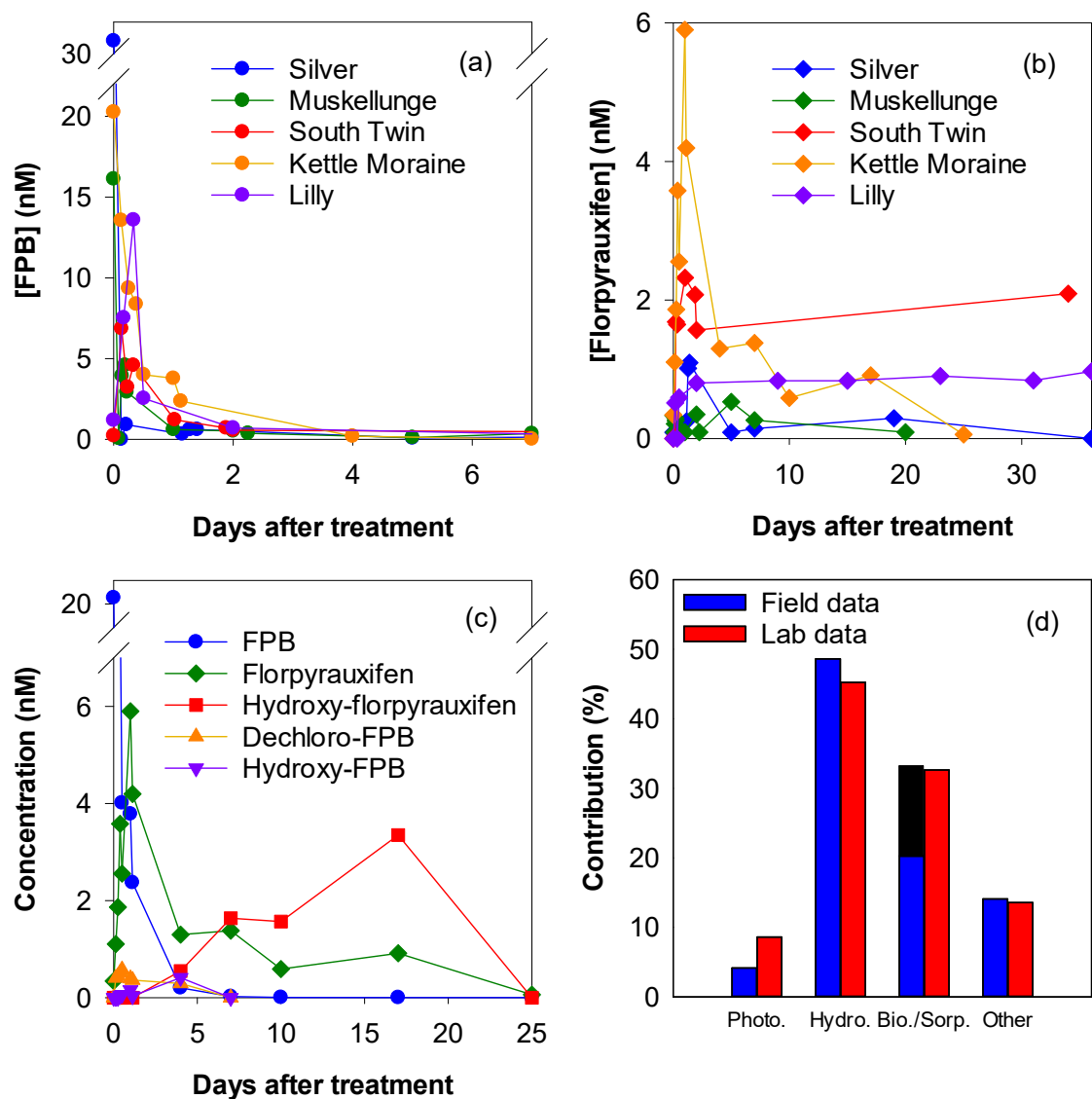


Figure 2.1. Concentrations of (a) FPB and (b) florpyrauxifen in the treatment zone of all studied lakes. Data for all sampling points and maps of each lake are provided in **Figures A.15 – A.19**. (c) Epilimnion concentrations of FPB and its degradation products in the treatment area of Kettle Moraine Lake. (d) Contribution of photodegradation (Photo.), biodegradation (Bio.), hydrolysis (Hydro.), and sorption (Sorp.) in the field and lab data based on material balance calculations outlined in **Section A.10**. Biodegradation and sorption were quantified separately with the field data which is indicated by the blue and black bar (blue represents contribution of biodegradation while black indicates sorption). The rate loss in the sediment-water microcosms is due to biodegradation and sorption, therefore the lab data combines these two processes.

While advective transport was important in initial FPB loss from the treatment area, the degradation product florpyrauxifen appeared nearly immediately after FPB treatment, suggesting transformation occurred on the same timescale as physical transport. Florpyrauxifen concentrations ranged from <0.09 to 3 nM in all lakes and persisted up to 20-30 days in each lake (**Figures 2.1b-2.1c**). While only florpyrauxifen was quantified in the 2021 lakes (Muskellunge, South Twin, and Silver), additional degradation products were measured in Kettle Moraine and Lilly lakes with a more comprehensive LC-MS/MS method (**Section A.3**). Hydroxy-florpyrauxifen was the most dominant product besides florpyrauxifen, with detection starting at days 4 and 7 in Kettle Moraine (**Figure 2.1c**) and Lilly (**Figure A.19**), respectively, and reached concentrations of up to 3.3 and 3.1 nM. Hydroxy-florpyrauxifen was more persistent than FPB and was detected 25 days post-treatment. Two additional products were detected in Kettle Moraine at lower concentrations: dechloro-FPB (up to 0.6 nM) and hydroxy-FPB (0.4 nM).

The magnitude of florpyrauxifen accumulation suggests it is a major environmental degradation product of FPB. FPB recovery was estimated by comparing the observed epilimnion-wide average [FPB] and [florpyrauxifen] at 12-48 hours after treatment with the expected lake-wide FPB concentrations based on the known herbicide application using Equation S8. We calculated a recovery range of 103-160% (**Table A.8**), demonstrating that florpyrauxifen was the dominant transformation product of FPB because its concentration fully accounted for the observed loss of FPB. The overestimation of FPB recovery in some cases was likely due to averaging across the epilimnion while FPB and florpyrauxifen were mixing

throughout the water column. Nevertheless, the dominance of florpyrauxifen as the primary environmental transformation product is critical due to its known herbicidal properties,^{40,50} indicating its formation and persistence in lakes could exert additional, unintended herbicidal activity on the plant population.

FPB and florpyrauxifen were also detected in nearshore sediments collected after the FPB applications. The highest concentrations of FPB and florpyrauxifen, 15 nmol kg⁻¹ and 10 nmol kg⁻¹, respectively, were observed on the day of treatment (**Figure A.12a**). Florpyrauxifen was no longer detected in the sediments after the first day. However, FPB was detected in the sediments up to 50 days after treatment, compared to only 7 days in the water column (**Figure A.12b**). Thus, FPB may undergo enhanced persistence in lake sediments compared to water.

The field data demonstrated that FPB had a short lifetime (~days) in water of the study lakes and was subject to advective transport, sorption, and degradation on similar timescales. However, the field data alone could not be used to identify which transformation mechanisms contributed to FPB loss. Laboratory studies isolating photodegradation, biodegradation, and sorption of both FPB and florpyrauxifen and FPB hydrolysis were used to identify transformation rates and additional products for these reactions in a controlled setting to determine what process(es) were dominant in lakes.

Hydrolysis. FPB is a carboxylic acid ester and is therefore susceptible to hydrolysis.^{51,52} The hydrolysis rate increased with increasing pH, suggesting a base-promoted reaction (**Figures 2.2a-2.2b** and **A.2**). The measured hydrolysis rates at low pH were faster than registration documentation (i.e., 37 days in this study versus 913 days at pH 4; 18 days versus 111 days at pH 7) but were the same at pH 9 (1.3 days).³⁷ Florpyrauxifen was the only

degradation product detected during hydrolysis experiments and accounted for 89% and 99% of added FPB at pH 9 and 10, respectively (**Figure A.2**). Based on these results, FPB hydrolysis could impact the required exposure time of ~ 24 hours in lakes with $\text{pH} > 9$.^{50,53} However, given the pH of Kettle Moraine was ~ 8.5 , other processes beyond hydrolysis were responsible for the increased FPB degradation rate observed in the field and the production of other transformation products.

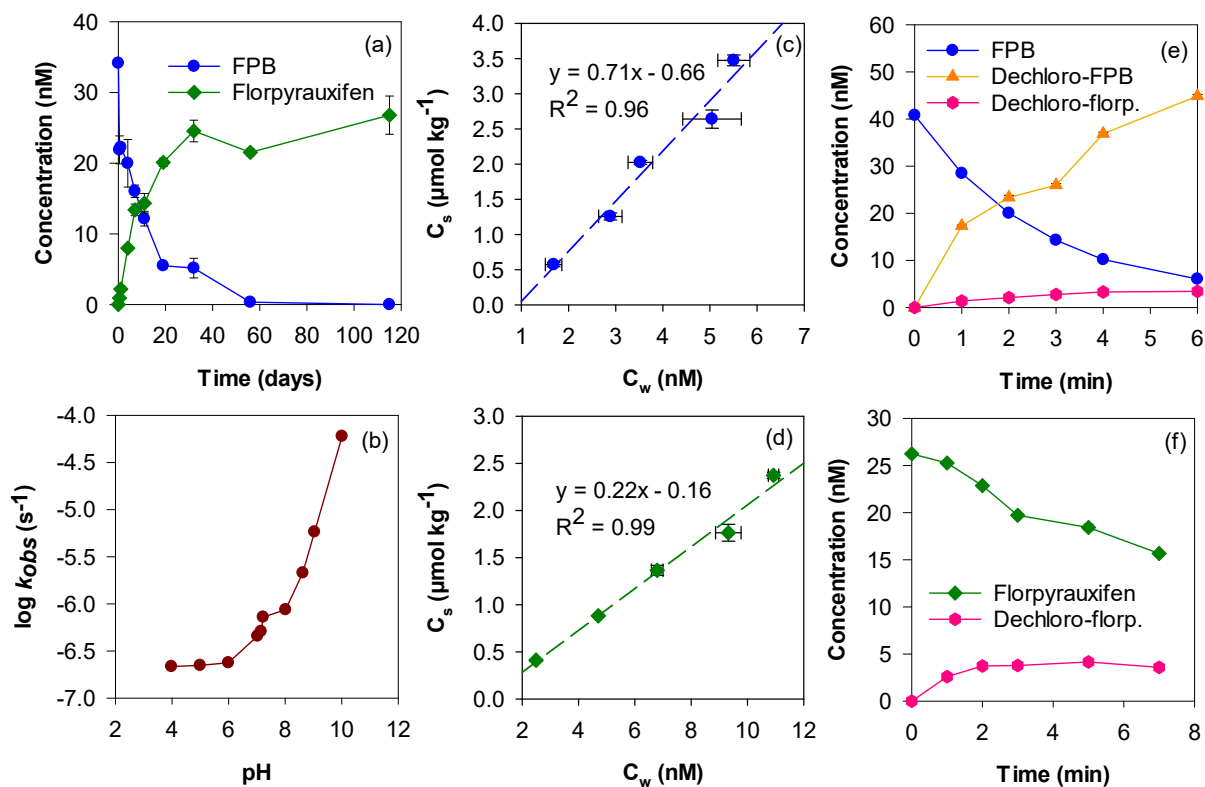


Figure 2.2. (a) Loss of FPB and formation of florpyrauxifen during hydrolysis at pH 8. (b) Hydrolysis rates of FPB as a function of pH. Kettle Moraine Lake sediment sorption isotherms for (c) FPB and (d) florpyrauxifen. The slope of the isotherm is equivalent to the sediment sorption partitioning coefficient (K_d) in L kg^{-1} . Loss of (e) FPB and (f) florpyrauxifen and formation of photoproducts during irradiation with 311 nm light in ultrapure water (pH 7). Error bars represent the standard deviation of samples taken from triplicate reactors. Error bars in panels (b), (e), and (f) are smaller than the data point symbols.

Sorption. Sorption experiments were conducted with Kettle Moraine and Lilly sediments at pH 7.0. Both FPB and florpyrauxifen are deprotonated under these conditions due to their acid dissociation constants of -1.0 and 3.2, respectively (**Figure A.3**).^{22,38,54} Water-sediment partitioning coefficients (K_d) for FPB were $712 \pm 69 \text{ L kg}^{-1}$ and $64 \pm 5 \text{ L kg}^{-1}$ for Kettle Moraine and Lilly, respectively (**Figures 2.2c** and **A.5a**; **Table A.6**). The average organic carbon partitioning coefficient was $10^{4.14} \text{ L kg}^{-1}$ for both lakes, which is comparable to the literature value of $10^{4.53} \text{ L kg}^{-1}$.⁴⁰ Therefore, sorption may be an important FPB removal mechanism in lakes with high sediment-water surface area relative to lake volume and/or suspended solids.

Florpyrauxifen was less sorptive than FPB, as expected given its higher polarity and lower molecular weight. K_d values were $222 \pm 8 \text{ L kg}^{-1}$ and $19 \pm 3 \text{ L kg}^{-1}$ for Kettle Moraine and Lilly sediments, respectively (**Figures 2.2d** and **A.5b**; **Table A.6**). The average K_{oc} value of $10^{3.62} \text{ L kg}^{-1}$ was larger than the reported literature value of $10^{2.3} \text{ L kg}^{-1}$.⁴⁰

Microcosm incubations. FPB loss was observed in microcosm incubations under all control and experimental conditions (**Figures 2.3a-2.3c** and **A.6a-A.6c**). Loss in the microcosms followed pseudo-first-order kinetics with no significant lag time (**Figure A.7**). The FPB half-life of 6.6 days in microcosms with filter-sterilized lake water (**Figures 2.3a** and **A.6a**; **Table A.8**) was similar to the half-lives in unfiltered water (i.e., 7.3 – 8.5 days; **Figures 2.3c** and **A.6c**) and was consistent with the hydrolysis half-life (**Figure A.2**). Florpyrauxifen was the only detected transformation product under these conditions. Therefore, FPB loss in the abiotic controls and water-only microcosms was solely attributable to hydrolysis.

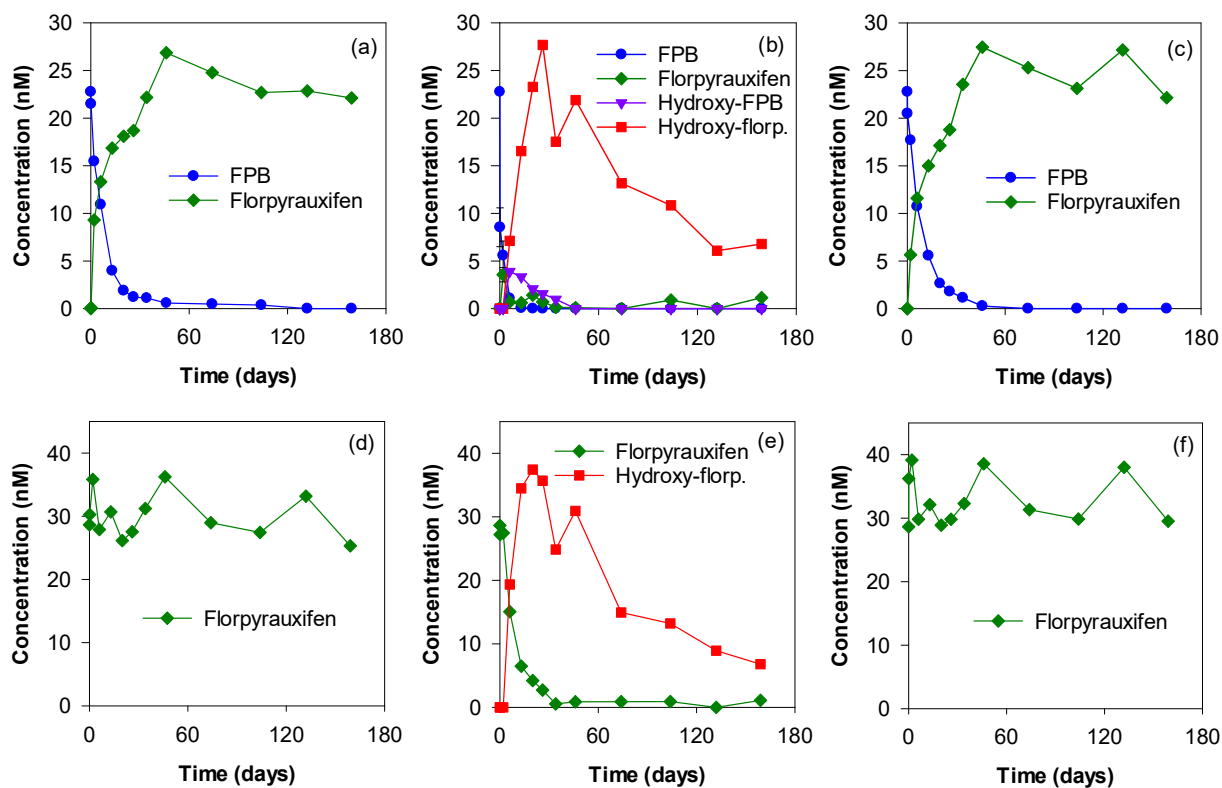


Figure 2.3. Kettle Moraine Lake microcosms incubated with (a-c) FPB and (d-f) florpyrauxifen. (a, d) Abiotic controls contained 0.2 μm filter sterilized water only. (b, e) Sediment-water microcosms contained 0.2 μm filter sterilized water with sediment. (c, f) Water-only microcosms contained unfiltered lake water only. Error bars in each figure are smaller than the data point symbols.

Shorter FPB half-lives of 2.5 and 1.8 days were observed in the sediment-water microcosms with inocula from Lilly and Kettle Moraine, respectively (**Figures 2.3b** and **A.6b**). Sorption of FPB to solids contributed to the decrease in initial [FPB] from 23 nM to 8.5 and 9.9 nM in Lilly and Kettle Moraine, respectively, during the first 24 hours (i.e., over the same timescale as sorption experiments). As observed under field conditions, both FPB and florpyrauxifen were detected over 80 days after treatment in microcosm sediments, compared to up to 34 days in the water (**Figure A.13c-A.13d**). The formation of hydroxy-FPB and hydroxy-florpyrauxifen in addition to florpyrauxifen, as well as more rapid transformation

rates, demonstrated that biodegradation occurred under these conditions. Additional microcosms were incubated with florpyrauxifen to isolate its behavior (**Figures 2.3d-2.3f** and **A.6d-A.6f**). No florpyrauxifen loss was observed in filter-sterilized controls or unfiltered water microcosms. Florpyrauxifen half-lives of 72 and 6.4 days were observed in the Lilly and Kettle Moraine sediment-water microcosms, respectively, along with hydroxy-florpyrauxifen accumulation (**Figures 2.3e** and **A.6**). Therefore, florpyrauxifen loss was attributed primarily to biodegradation under these conditions due to its smaller K_{oc} value (**Table A.6**).

Both FPB and florpyrauxifen degraded fastest in the sediment-water microcosms. Faster degradation of other organic compounds has been observed with sediment inocula^{7,10,19} and this underscores the importance of conducting laboratory experiments with relevant microbial communities and concentrations.^{18,55} Kettle Moraine sediments likely had a higher number of active microbes than Lilly due to their higher organic content.^{48,56,57} This hypothesis was supported by the faster degradation of both FPB and florpyrauxifen, as well as the greater accumulation of hydroxy-florpyrauxifen, in Kettle Moraine compared to Lilly sediment-water microcosms. It also was consistent with the observation of an additional biodegradation product, hydroxy-FPB, solely in the Kettle Moraine microcosms. This product was also observed in Kettle Moraine during the FPB application (**Figure 2.1c**).

Since hydroxy-florpyrauxifen was generated in both FPB and florpyrauxifen sediment-water microcosms, we hypothesized FPB degradation occurred in two major steps in the microcosms and lakes. First, FPB underwent hydrolysis to florpyrauxifen. This intermediate product then underwent biodegradation to hydroxy-florpyrauxifen (**Figure 2.4**). Biodegradation of FPB to hydroxy-FPB was also possible but was a minor pathway. While not

tested, it was likely that hydroxy-FPB underwent hydrolysis to hydroxy-florpyrauxifen based on its chemical structure. While the microcosms provided evidence of sorption, hydrolysis, and biodegradation occurring on similar timescales, they did not explain the formation of dechloro-FPB observed in the field (**Figure 2.1c**).

Photochemical degradation. FPB underwent direct photodegradation under 311 nm irradiation with an observed first-order loss rate constant of $(3.4 \pm 0.1) \times 10^{-3} \text{ s}^{-1}$ ($t_{1/2} = 200$ seconds) (**Figure A.10a**), which corresponded to a quantum yield (Φ) of $(2.5 \pm 0.3) \times 10^{-2}$; this is the first reported quantum yield for this compound. The observed rate constants in the presence of dissolved organic matter (DOM) were almost identical to the direct photodegradation rate constant (average $k = (3.3 \pm 0.1) \times 10^{-3} \text{ s}^{-1}$; corrected for light screening), demonstrating that indirect photodegradation was negligible for FPB under these conditions. Hydrolysis of FPB was also negligible due to the short duration of the experiment (6 minutes).

Modeling of *in situ* depth-integrated photodegradation was conducted with sunlight intensity generated using SMARTS on the day of treatment for each study lake, assuming an average irradiance from 7 am to 7 pm (**Figure A.9; Table A.7**). The estimated photodegradation half-lives of FPB in the top 1 cm of water (near-surface) were 3.8 hours (0.16 days) on average, which was longer than 0.07 days estimated at noon in registration documents.^{37,38,58} However, these were overestimated half-lives since sunlight intensity varies seasonally and photodegradation half-lives increase exponentially with water depth, as the half-life of FPB increased to 8.1 days when integrated over a depth of 1 m.

Direct photodegradation was also dominant for florpyrauxifen compared to indirect photodegradation. The direct first-order loss rate constant for florpyrauxifen was $(1.3 \pm 0.03) \times 10^{-3} \text{ s}^{-1}$ ($t_{1/2} = 550$ seconds; **Figure A.10b**) at 311 nm, which corresponds to a quantum yield (Φ) of $(3.6 \pm 0.5) \times 10^{-3}$. The presence of DOM did not alter the observed photodegradation rate ($t_{1/2} = 550$ seconds), demonstrating that indirect photodegradation was negligible. The slower photodegradation rates and smaller quantum yield of florpyrauxifen compared to FPB indicated florpyrauxifen was less susceptible to photolysis. This was corroborated by photochemical modeling calculations using sunlight intensity from SMARTS, where the estimated half-life of florpyrauxifen on average in the study lakes was 68 days in the top 1 cm of water assuming average sunlight irradiance from 7 am to 7 pm.

Irradiation of FPB produced dechloro-FPB and dechloro-florpyrauxifen (**Figure 2.2e** and **Figure 2.4**), which is consistent with the European Food Safety review document.⁴⁰ Dechloro-FPB was the dominant photodegradation product based on its larger accumulation compared to dechloro-florpyrauxifen. Irradiation of florpyrauxifen only produced dechloro-florpyrauxifen (**Figure 2.2f**). Due to its low abundance in both experiments, dechloro-florpyrauxifen would most likely not accumulate in aquatic environments. This product was not detected in any of the lake samples (**Figure 2.1c**).

The production of dechloro-FPB during the Kettle Moraine treatment provided direct evidence of FPB photodegradation under field conditions for the first time. While this photodegradation product was only detected in Kettle Moraine, this could be due to the lack of complete mixing throughout the lake, which resulted in a higher epilimnetic FPB concentration remaining in the treatment area.

Identification of primary loss pathways. Material balance calculations were carried out to determine the relative importance of each transformation pathway in Kettle Moraine because this treatment had the most degradation products detected (**Section A.10**). We separately evaluated field and laboratory data to assess whether isolated laboratory measurements could be used to predict the role of multiple processes that occurred at similar timescales in the field. First, the concentration of each degradation product was divided by the sum of all detected products in Kettle Moraine at the time of mixing (24 hours after treatment, **Equation A9**) to estimate the contribution of each pathway to FPB transformation. This calculation was performed on a molar basis and assumed a 1:1 mole ratio of FPB loss to product formation based on compound structures. We assumed that dechloro-FPB was produced through photodegradation, hydroxy-florpyrauxifen and hydroxy-FPB were produced through biodegradation, and florpyrauxifen was produced through hydrolysis based on laboratory experiments.

A second material balance calculation was conducted using pseudo-first-order kinetics from laboratory experiments where contributions of each pathway were calculated by dividing their respective pseudo-first-order rate constants by the observed rate loss of FPB in the field (**Equation A11; Figure A.20**). The rate loss of biodegradation observed in the FPB microcosms was an overestimation due to sorption contribution, while sorption was calculated separately with the field data (**Section A.10**). Therefore, the biodegradation rate loss observed in the lab would be equivalent to the combination of sorption and biodegradation in the field.

While the two material balance approaches relied on separate data sets (i.e., measurement of transformation products in the field versus isolated laboratory experiments),

they yielded very similar results. In both cases, hydrolysis was the largest contributor to FPB loss (45 – 49%), followed by biodegradation/sorption (33%), and photodegradation (4.1 – 8.6%) (**Figure 2.1d**). Importantly, these calculations demonstrated that all considered processes occurred simultaneously and must therefore all be considered when assessing the fate of FPB. The dominance of hydrolysis emphasized that florpyrauxifen, which is still herbicidal,^{40,50} was the primary environmental degradation product. Overall, both material balances confirm the dominant transformation pathway to be FPB hydrolysis to florpyrauxifen followed by biodegradation, which primarily forms hydroxy-florpyrauxifen based on field and microcosm observations (**Figure 2.4**). However, both methods had an average of 14% FPB loss unaccounted for, indicating other pathways contributed to the fate of FPB. Part of this loss was likely attributable to physical transport from the lake, which was not measured in this study. In addition, we hypothesized that plant interactions could also influence FPB transformation due to the rapid formation of florpyrauxifen.

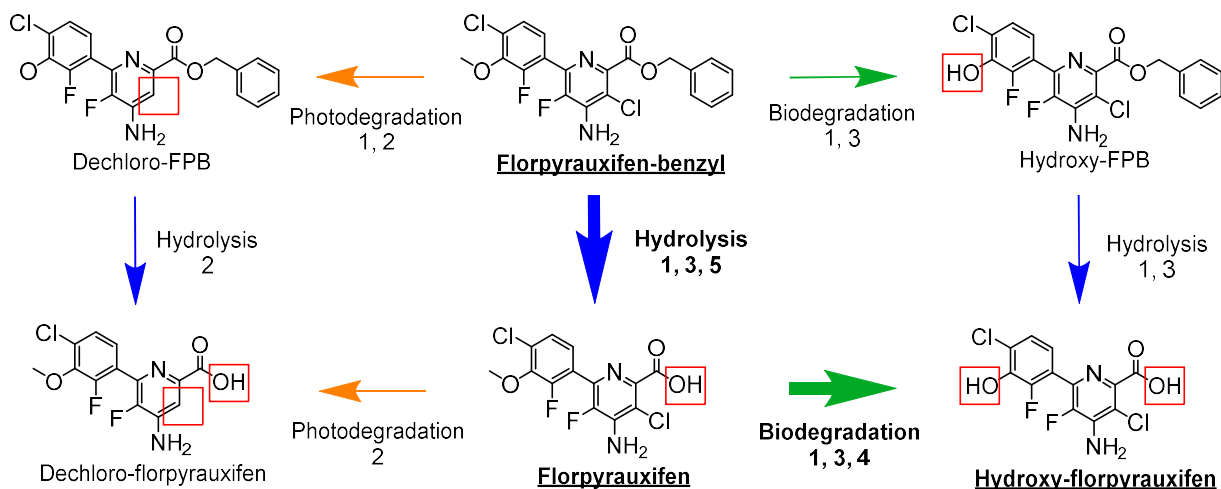


Figure 2.4. Proposed FPB degradation mechanism in aquatic environments. Product identified in each reaction by number as follows: 1- field campaign; 2- photodegradation experiments; 3- FPB incubated-microcosms; 4- florpyrauxifen-incubated microcosm, and 5- hydrolysis experiment. Red boxes represent changed functional group after reaction. The dominant transformation pathway as determined through the material balances is highlighted in bold.

Plant uptake and transformation of FPB. While florpyrauxifen identification in lakes demonstrated that hydrolysis is an important transformation pathway, florpyrauxifen accumulated more rapidly in lakes (~1 day) than predicted based on hydrolysis experiments ($t_{1/2}$ ~6-8 days; **Table A.8**). This discrepancy in florpyrauxifen generation suggests the hydrolysis of FPB can be catalyzed through a mechanism not captured in the microcosms.⁵² For example, hydrolysis via aquatic plants is part of the uptake and toxicity mechanism described for both FPB and the predecessor to FPB, halauxifen-methyl, which suggests the rapid hydrolysis in lakes could potentially be due to FPB uptake and florpyrauxifen release by the targeted plant community.^{22,48,59}

Plant extractions were conducted to assess whether plant uptake catalyzed florpyrauxifen production. Both FPB and florpyrauxifen accumulated considerably in plants collected during and after FPB treatment, with highest concentrations occurring the day after

treatment at $10^{3.8}$ nmol kg⁻¹ and $10^{4.1}$ nmol kg⁻¹, respectively (**Figure A.14**). Florpyrauxifen quickly decreased until it was no longer detected after 26 days. FPB also rapidly decreased but was detected almost 40 days after treatment. While plant uptake was not included in the material balance calculations because the plant density was unknown, these findings indicate that plant biomass provided an important pathway for FPB transformation to florpyrauxifen, thereby influencing the persistence of FPB.

Environmental Implications. We combined field and laboratory studies to investigate the fate of an herbicide added to aquatic environments for the control of nuisance plants. This herbicide represented a unique opportunity to investigate the contribution of multiple interacting mechanisms on herbicide fate, which is typically not possible for most organic contaminants that are added unintentionally to the environment. Our study combined kinetics and product tracking to determine the mechanisms responsible for degradation of FPB and to quantify their relative importance.

Our study demonstrated the limitations of laboratory experiments in predicting the environmental fate of polar organic compounds. For example, isolating different transformation pathways in laboratory experiments missed combinations of transformation pathways that occurred in the environment, such as the proposed plant-catalyzed florpyrauxifen hydrolysis and subsequent microbial degradation to hydroxy-florpyrauxifen. Furthermore, laboratory experiments overpredicted FPB photodegradation when environmental factors (e.g., water depth) were not considered.

Regulatory studies emphasizing the active ingredient of an intentionally applied chemical mixture may overlook potentially bioactive degradation products. Florpyrauxifen,

the major product, is bioactive and much more persistent than FPB.^{40,50} While our study focused on the chemical fate of these compounds, additional studies are needed to understand how the concentration and persistence of these compounds can impact aquatic or plant life. Additionally, more research is needed on the effects of compound mixtures, such as combination herbicide treatments using triclopyr and FPB. As such, the current approach to regulatory studies relying on active ingredients alone should be revisited from a holistic environmental fate perspective.

Acknowledgements. The authors would like to thank Onterra, LLC., Lilly Lake Resort, Tiki Beach Resort on Kettle Moraine Lake, Camp Birch Knoll, and the homeowners and lake associations of all five study lakes for their assistance sampling. The Wisconsin Department of Natural Resources provided logistical and technical support during treatments, especially Michelle Nault, Scott Van Egeren, and Ty Krajewski. Field equipment was provided by the University of Wisconsin-Madison Center for Limnology and Trout Lake Station. Funding was provided by the Wisconsin Department of Natural Resources, National Science Foundation Graduate Research Fellowship Program, Midwest Aquatic Plant Management Society, Anna Grant Birge Memorial Award, and the United States Air Force.

References

1. Schwarzenbach, R. P.; Escher, B. I.; Fenner, K.; Hofstetter, T. B.; Johnson, C. A.; von Gunten, U.; Wehrli, B. The challenge of micropollutants in aquatic systems. *Science* **2006**, *313* (5790), 1072–1077.
2. Yang, Y.; Zhang, X.; Jiang, J.; Han, J.; Li, W.; Li, X.; Yee Leung, K. M.; Snyder, S. A.; Alvarez, P. J. J. Which micropollutants in water environments deserve more attention globally? *Environ. Sci. Technol.* **2022**, *56* (1), 13–29.
3. Sinclair, C. J.; Boxall, A. B. A. Assessing the ecotoxicity of pesticide transformation products. *Environ. Sci. Technol.* **2003**, *37* (20), 4617–4625.

4. Tian, Z.; Zhao, H.; Peter, K. T.; Gonzalez, M.; Wetzel, J.; Wu, C.; Hu, X.; Prat, J.; Mudrock, E.; Hettinger, R.; Cortina, A. E.; Biswas, R. G.; Vinicius, F.; Kock, C.; Soong, R.; Jenne, A.; Du, B.; Hou, F.; He, H.; Lundeen, R.; Gilbreath, A.; Sutton, R.; Scholz, N. L.; Davis, J. W.; Dodd, M. C.; Simpson, A.; McIntyre, J. K.; Kolodziej, E. P. A ubiquitous tire rubber-derived chemical induces acute mortality in coho salmon. *Science* **2021**, *371* (6525), 185–189.
5. Cwiertny, D. M.; Snyder, S. A.; Schlenk, D.; Kolodziej, E. P. Environmental designer drugs: When transformation may not eliminate risk. *Environ. Sci. Technol.* **2014**, *48* (20), 11737–11745.
6. Puhlmann, N.; Olsson, O.; Kümmerer, K. Transformation products of sulfonamides in aquatic systems: Lessons learned from available environmental fate and behaviour data. *Sci. Total Environ.* **2022**, *830*, 154744.
7. White, A. M.; Nault, M. E.; McMahon, K. D.; Remucal, C. K. Synthesizing laboratory and field experiments to quantify dominant transformation mechanisms of 2,4-dichlorophenoxyacetic acid (2,4-D) in aquatic environments. *Environ. Sci. Technol.* **2022**, *56* (15), 10838–10848.
8. Honti, M.; Fenner, K. Deriving persistence indicators from regulatory water-sediment studies - Opportunities and limitations in OECD 308 data. *Environ. Sci. Technol.* **2015**, *49* (10), 5879–5886.
9. Fenner, K.; Canonica, S.; Wackett, L. P.; Elsner, M. Evaluating pesticide degradation in the environment: blind spots and emerging opportunities. *Science* **2013**, *341* (6147), 752–758.
10. Zhi, H.; Miannecki, A. L.; Kolpin, D. W.; Klaper, R. D.; Iwanowicz, L. R.; LeFevre, G. H. Tandem field and laboratory approaches to quantify attenuation mechanisms of pharmaceutical and pharmaceutical transformation products in a wastewater effluent-dominated stream. *Water Res.* **2021**, *203*, 117537.
11. Escher, B. I.; Fenner, K. Recent advances in environmental risk assessment of transformation products. *Environ. Sci. Technol.* **2011**, *45* (9), 3835–3847.
12. McConville, M. B.; Mezyk, S. P.; Remucal, C. K. Indirect photodegradation of the lampricides TFM and niclosamide. *Environ. Sci.: Processes Impacts* **2017**, *19*, 1028–1039.
13. McConville, M. B.; Cohen, N. M.; Nowicki, S. M.; Lantz, S. R.; Hixson, J. L.; Ward, A. S.; Remucal, C. K. A field analysis of lampricide photodegradation in great lakes tributaries. *Environ. Sci.: Processes Impacts* **2017**, *19*, 891–900.
14. Remucal, C. K. The role of indirect photochemical degradation in the environmental fate of pesticides: a review. *Environ. Sci.: Processes Impacts* **2014**, *16*, 628–653.
15. Honti, M.; Hahn, S.; Hennecke, D.; Junker, T.; Shrestha, P.; Fenner, K. Bridging across OECD308 and 309 data in search of a robust biotransformation indicator. *Environ. Sci. Technol.* **2016**, *50* (13), 6865–6872.
16. Li, J.; Shimizu, K.; Sakharkar, M. K.; Utsumi, M.; Zhang, Z.; Sugiura, N. Comparative study for the effects of variable nutrient conditions on the biodegradation of microcystin-LR and concurrent dynamics in microcystin-degrading gene abundance. *Bioresour. Technol.* **2011**, *102* (20), 9509–9517.

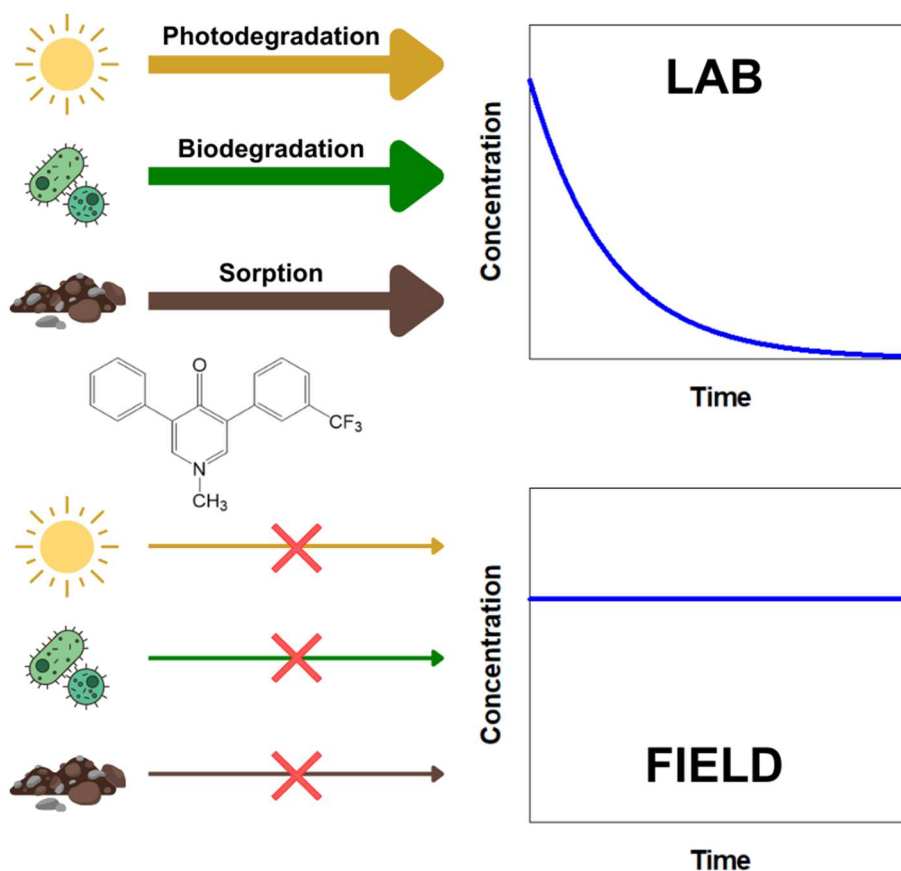
17. Trigo, A.; Valencia, A.; Cases, I. Systemic approaches to biodegradation. *FEMS Microbiol. Rev.* **2009**, *33* (1), 98–108.
18. Thouand, G.; Durand, M. J.; Maul, A.; Gancet, C.; Blok, H. New concepts in the evaluation of biodegradation/persistence of chemical substances using a microbial inoculum. *Front. Microbiol.* **2011**, *2* (164), 1-6.
19. Seller, C.; Honti, M.; Singer, H.; Fenner, K. Biotransformation of chemicals in water-sediment suspensions: influencing factors and implications for persistence assessment. *Environ. Sci. Technol. Lett.* **2020**, *7* (11), 854–860.
20. Shrestha, P.; Junker, T.; Fenner, K.; Hahn, S.; Honti, M.; Bakkour, R.; Diaz, C.; Hennecke, D. Simulation studies to explore biodegradation in water-sediment systems: from OECD 308 to OECD 309. *Environ. Sci. Technol.* **2016**, *50* (13), 6856–6864.
21. U.S. EPA. Final Registration Decision on the New Active Ingredient Florpyrauxifen-benzyl <https://www.regulations.gov/document/EPA-HQ-OPP-2016-0560-0065> (accessed April 2023).
22. Epp, J. B.; Alexander, A. L.; Balko, T. W.; Buysse, A. M.; Brewster, W. K.; Bryan, K.; Daeuble, J. F.; Fields, S. C.; Gast, R. E.; Green, R. A.; Irvine, N. M.; Lo, W. C.; Lowe, C. T.; Renga, J. M.; Richburg, J. S.; Ruiz, J. M.; Satchivi, N. M.; Schmitzer, P. R.; Siddall, T. L.; Webster, J. D.; Weimer, M. R.; Whiteker, G. T.; Yerkes, C. N. The discovery of arylexTM active and rinskorTM active: two novel auxin herbicides. *Bioorg. Med. Chem.* **2016**, *24* (3), 362–371.
23. Busi, R.; Goggin, D. E.; Heap, I. M.; Horak, M. J.; Jugulam, M.; Masters, R. A.; Napier, R. M.; Riar, D. S.; Satchivi, N. M.; Torra, J.; Westra, P.; Wright, T. R. Weed resistance to synthetic auxin herbicides. *Pest Manage. Sci.* **2018**, *74* (10), 2265–2276.
24. Richardson, R. J. Aquatic plant management and the impact of emerging herbicide resistance issues. *Weed Technol.* **2008**, *22* (1), 8–15.
25. Moody, M. L.; Les, D. H. Evidence of hybridity in invasive watermilfoil (*Myriophyllum*) populations. *Proc. Natl. Acad. Sci. U.S.A.* **2002**, *99* (23), 14867–14871.
26. Larue, E. A.; Zuellig, M. P.; Netherland, M. D.; Heilman, M. A.; Thum, R. A. Hybrid watermilfoil lineages are more invasive and less sensitive to a commonly used herbicide than their exotic parent (Eurasian watermilfoil). *Evol. Appl.* **2013**, *6* (3), 462–471.
27. Berger, S. T.; Netherland, M. D.; MacDonald, G. E. Laboratory documentation of multiple-herbicide tolerance to fluridone, norflurazon, and topiramazone in a hybrid watermilfoil (*Myriophyllum spicatum* × *M. sibiricum*) population. *Weed Sci.* **2015**, *63* (1), 235–241.
28. Netherland, M. D.; Jones, D. Fluridone-resistant hydrilla (*hydrilla verticillate*) is still dominant in the Kissimmee Chain of Lakes, FL. *Invasive Plant Sci. Manage.* **2015**, *8* (2), 212–218.
29. Mallory-Smith, C. A.; Retzinger Jr., E. J. Revised classification of herbicides by site of action for weed resistance management strategies. *Weed Technol.* **2003**, *17* (3), 605–619.

30. SePRO. ProcellaCOR SC label https://sepro.com/Documents/ProcellaCOR_SC--Label.pdf (accessed April 2023).
31. Corteva Agriscience. TerraVue specimen label <https://www.corteva.us/products-and-solutions/land-management/terravue.html> (accessed April 2023).
32. Corteva Agriscience. Agixa Rinskor active label <https://www.corteva.com.au/products-and-solutions/crop-protection/agixa-rinskor-active.html> (accessed April 2023).
33. Corteva Agriscience. Ubeniq® Rinskor® active <https://www.corteva.com.au/products-and-solutions/crop-protection/ubeniq-rinskor-active.html> (accessed April 2023).
34. SePRO. ProcellaCOR EC https://sepro.com/Documents/ProcellaCOR_EC--Label.pdf (accessed April 2023).
35. Corteva Agriscience. Loyant label <https://www.corteva.us/products-and-solutions/crop-protection/loyant.html> (accessed April 2023).
36. Corteva Agriscience. Novixid label https://s3-us-west-1.amazonaws.com/agrian-cg-fs1-production/pdfs/Novixid1d_with_Rinskor_active_Label.pdf (accessed April 2023).
37. SePRO. ProcellaCOR EC SDS https://sepro.com/Documents/ProcellaCOR_EC--SDS.pdf (accessed April 2023).
38. Corteva Agriscience. Rinskor Active Technical Bulletin https://www.corteva.com/content/dam/dpagco/corteva/global/corporate/general/files/active-ingredients/DF_Rinskor-TechBulletin_12-14-18.pdf (accessed April 2023).
39. U.S. EPA. Independent Laboratory Validation of a Dow AgroSciences Method for the Determination of XDE-848 Benzyl Ester and Five Metabolites (X11438848, X12300837, X11966341, X12131932 and X12393505) in Water https://www.epa.gov/sites/production/files/2017-09/documents/ilv_-_florpyrauxifen-benzyl_degradates_in_water_-_mrid_49677802.pdf (accessed April 2023).
40. Arena, M.; Auteri, D.; Barmaz, S.; Brancato, A.; Brocca, D.; Bura, L.; Carrasco Cabrera, L.; Chaideftou, E.; Chiusolo, A.; Civitella, C.; Court Marques, D.; Crivellente, F.; Ctverackova, L.; de Lentdecker, C.; Egsmose, M.; Erdos, Z.; Fait, G.; Ferreira, L.; Goumenou, M.; Greco, L.; Ippolito, A.; Istace, F.; Jarrah, S.; Kardassi, D.; Leuschner, R.; Lostia, A.; Lythgo, C.; Magrans, J. O.; Medina, P.; Mineo, D.; Miron, I.; Molnar, T.; Padovani, L.; Parra Morte, J. M.; Pedersen, R.; Reich, H.; Sacchi, A.; Santos, M.; Serafimova, R.; Sharp, R.; Stanek, A.; Streissl, F.; Sturma, J.; Szentes, C.; Tarazona, J.; Terron, A.; Theobald, A.; Vagenende, B.; van Dijk, J.; Villamar-Bouza, L. Peer review of the pesticide risk assessment of the active substance florpyrauxifen (variant assessed florpyrauxifen-benzyl). *EFSA J.* **2018**, *16* (8), 5378.
41. Northeast Aquatic Research. Tuxedo Lake, Wee Wah, and Little Wee Wah Aquatic Plant Sampling Report http://www.tpfyi.com/docs/NEAR_Aquatic_Plant_SamplingReport_1-24-2020.pdf (accessed April 2023).
42. Bulman, D. M.; P. Mezyk, S.; K. Remucal, C. The impact of pH and irradiation wavelength on the production of reactive oxidants during chlorine photolysis. *Environ. Sci. Technol.* **2019**, *53* (8), 4450–4459.

43. Galbavy, E. S.; Ram, K.; Anastasio, C. 2-nitrobenzaldehyde as a chemical actinometer for solution and ice photochemistry. *J. Photochem. Photobiol., A* **2010**, *209* (2–3), 186–192.
44. Berg, S. M.; Whiting, Q. T.; Herrli, J. A.; Winkels, R.; Wammer, K. H.; Remucal, C. K. The role of dissolved organic matter composition in determining photochemical reactivity at the molecular level. *Environ. Sci. Technol.* **2019**, *53* (20), 11725–11734.
45. McConville, M. B.; Hubert, T. D.; Remucal, C. K. Direct photolysis rates and transformation pathways of the lampricides TFM and niclosamide in simulated sunlight. *Environ. Sci. Technol.* **2016**, *50* (18), 9998–10006.
46. Gueymard, C. A. Interdisciplinary applications of a versatile spectral solar irradiance model: A review. *Energy* **2005**, *30* (9), 1551–1576.
47. Stiegler, A. N.; Cecchetti, A. R.; Sedlak, D. L. Plant uptake of trace organic contaminants in effluent-dominated streams: An overlooked terrestrial exposure pathway. *Environ. Sci. Technol. Lett.* **2022**, *9* (11), 929–936.
48. Miller, M. R.; Norsworthy, J. K. Influence of soil moisture on absorption, translocation, and metabolism of florypyrauxifen-benzyl. *Weed Sci.* **2018**, *66* (4), 418–423.
49. U.S. EPA. Independent Laboratory Validation of a Dow AgroSciences Method for the Determination of XDE-848 Benzyl Ester and Three Metabolites (X11438848, X12300837 and X11966341) in Soil. https://www.epa.gov/sites/default/files/2017-09/documents/ilv_-_florpyrauxifen-benzyl_degradates_in_soil_-_mrid_49677776.pdf (accessed April 2023).
50. Netherland, M. D.; Richardson, R. J. Evaluating sensitivity of five aquatic plants to a novel arylpicolinate herbicide utilizing an organization for economic cooperation and development protocol. *Weed Sci.* **2016**, *64* (1), 181–190.
51. Schwarzenbach, R. P.; Gschwend, P. M.; Imboden, D. M. *Environmental Organic Chemistry, 3rd edition*, Wiley-Interscience, New Jersey, 2017.
52. Haag, W. R.; Mill, T. Effect of a subsurface sediment on hydrolysis of haloalkanes and epoxides. *Environ. Sci. Technol.* **1988**, *22* (6), 658–663.
53. Blanke, C.; Mikulyuk, A.; Nault, M.; Provost, S.; Schaal, C.; Van Egeren, S.; Williams, M.; Mednick, A. Strategic Analysis of Aquatic Plant Management in Wisconsin https://dnr.wisconsin.gov/sites/default/files/topic/Aid/grants/surfacewater/APMSA_Final_2019-06-14.pdf (accessed April 2023).
54. Chemical Book. Florpyrauxifen-Benzyl https://www.chemicalbook.com/ChemicalProductProperty_EN_CB03352607.htm (accessed April 2023).
55. Kowalczyk, A.; Martin, T. J.; Price, O. R.; Snape, J. R.; Van Egmond, R. A.; Finnegan, C. J.; Schäfer, H.; Davenport, R. J.; Bending, G. D. Refinement of biodegradation tests methodologies and the proposed utility of new microbial ecology techniques. *Ecotoxicol. Environ. Saf.* **2015**, *111*, 9–22.
56. Wu, X.; Wu, L.; Liu, Y.; Zhang, P.; Li, Q.; Zhou, J.; Hess, N. J.; Hazen, T. C.; Yang, W.; Chakraborty, R. Microbial interactions with dissolved organic matter drive carbon dynamics and community succession. *Front. Microbiol.* **2018**, *9* (1234), 1–12.

57. Kanazawa, S.; Filip, Z. Distribution of microorganisms, total biomass, and enzyme activities in different particles of brown soil. *Microb. Ecol.* **1986**, *12*, 205–215.
58. DOW AgroSciences. Rinskor Active Technical Bulletin http://storage.dow.com.edgesuite.net/dowagro/rinskor/Rinskor_Tech_Bulletin.pdf (accessed April 2023).
59. Deboer, G. J.; Satchivi, N. Comparison of translocation properties of insecticides versus herbicides that leads to efficacious control of pests as specifically illustrated by IsoclastTM active, a new insecticide, and ArylexTM active, a new herbicide. *ACS Symp. Ser.* **2014**, *4*, 75-93.

Chapter 3. Evaluating persistence and transformation of aquatic herbicide fluridone in field and laboratory experiments



Prologue. Chapter 3 is a collaboration between Sydney Van Frost, Amber White, Josie Jauquet, Angela Magness, Katherine McMahon, and Christy Remucal. This is a draft manuscript that will be submitted for publication. S.V. collected the samples, analyzed the samples, and wrote the manuscript. A.W., J.J., and A.M. assisted with field work and laboratory experiments. K.M. and C.R. were the principal investigators.

Abstract

Fluridone is an aquatic herbicide commonly used to treat invasive plant species such as Eurasian watermilfoil, hydrilla, and curly-leaf pondweed. However, required exposures times are very long, often exceeding 100 days. Thus, understanding the mechanisms responsible for degrading fluridone in lakes is critical for supporting effective herbicide treatments and minimizing non-target impacts. We used a combination of laboratory and field studies to quantify the photodegradation of fluridone as well as sorption and microbial degradation in water and sediment microcosms. Irradiation studies found fluridone is susceptible to direct photodegradation with negligible indirect photodegradation. Modeling with natural sunlight intensities corrected for diurnal variability predicted in-lake photodegradation half-lives to be 13 days integrated over a depth of 10 cm of water and 120 days over a depth of 1 meter. Biodegradation only occurred in the sediment microcosms with an observed half-life of 57 days. Lastly, sorption to solids was quantified with a K_{oc} value of $340 \pm 28 \text{ L kg}^{-1}$ and accounted for 39% of fluridone loss in the microcosm experiments. Combined, these results demonstrate the importance of all three transformation pathways on fluridone fate. However, laboratory studies oversimplify herbicide behavior due to their inability to replicate field conditions. Fluridone was measured over a 60-day period in a lake following commercial application and little loss was observed during this time. This indicates that fluridone is very persistent in water and does not experience analogous susceptibility to these degradation mechanisms under environmentally relevant conditions.

Introduction

Chemical control of invasive aquatic plants through herbicide application is becoming increasingly popular due to their efficiency of use and ability to be selective towards invasive species.¹⁻⁵ To achieve an effective application, herbicides need to attain a sufficient concentration and exposure time with the target plants, which is often successfully realized through whole-lake exposures compared to spot treatments.⁶⁻⁸ However, the unique environmental characteristics of each water body results in variable degradation rates of these herbicides. This may cause treatment failure, which can lead to additional applications and subsequently higher costs. Additionally, extensive herbicide application with similar modes of action have shown to induce herbicide tolerance and resistance, which has been observed more frequently over time.⁹⁻¹² Not only does extensive herbicide use impact efficacy of herbicidal control on nuisance plant populations, but increased herbicide application can also cause unintended harm to native plant communities.¹³ Therefore, understanding the transformation pathways and environmental characteristics that influence herbicide degradation is crucial to developing responsible herbicide application strategies that simultaneously prevent the rise of herbicide resistance and protect native plant populations.

Fluridone (**Figure 3.1a**) is a commonly used aquatic herbicide used to control invasive hydrilla (*Hydrilla verticillata*), curly-leaf pondweed (*Potamogeton crispus*), as well as Eurasian watermilfoil (EWM; *Myriophyllum spicatum*) and its hybridization with native watermilfoil (hybrid watermilfoil; HWM; *Myriophyllum spicatum* × *Myriophyllum sibiricum*).^{1,14-20} Fluridone prevents the synthesis of biomolecules that protect the plant from

photobleaching, thus inhibiting the ability of the plant to photosynthesize.^{21,22} For this reason, fluridone is only effective if applied while the plants are actively growing. Its unique mode of action makes it a popular alternative to auxin-mimic herbicides such as 2,4-dichlorophenoxyacetic acid (2,4-D), for treating 2,4-D-tolerant HWM.^{11,23} Fluridone is typically applied at a low concentration (6-26 nM) for a longer exposure time of 45-100 days,¹⁶⁻¹⁸ compared to 2,4-D (24-72 hours)^{24,25} or floryprauxifen-benzyl (12-24 hours).²⁶ This exposure time threshold often requires multiple applications to maintain an effective concentration.^{18,27-29} However, preliminary studies have begun documenting fluridone resistance by HWM⁹ and Hydrilla,³⁰ while others have shown evidence of sublethal effects on fish populations,³¹ underscoring the importance of responsible herbicide applications.

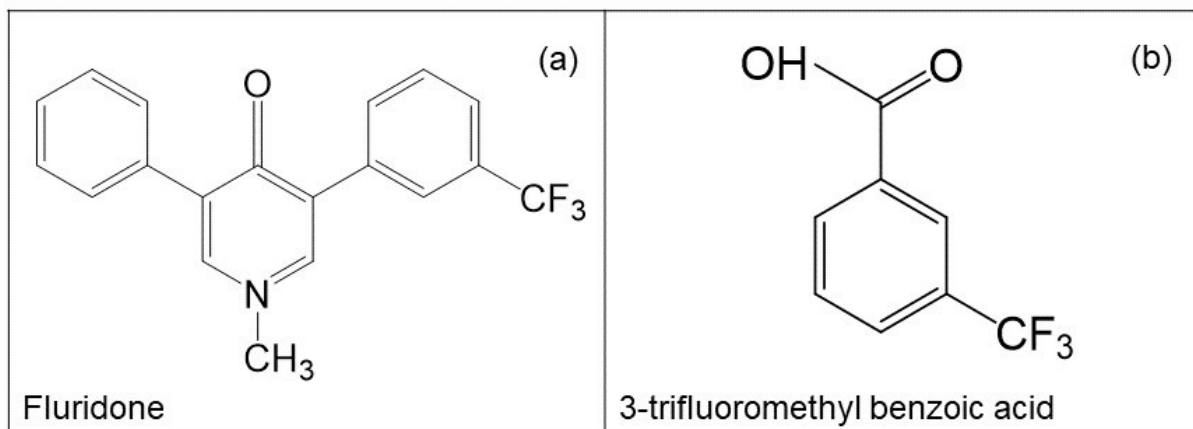


Figure 3.1. Chemical structures of (a) fluridone and (b) a biodegradation product 3-trifluoromethyl benzoic acid.

In aquatic environments, fluridone is expected to be predominantly influenced by photodegradation, with reported half-lives due to photolysis of 15 hours to 12 days in ultrapure and lake water, respectively (**Table B.1**).³²⁻³⁴ Limited studies have investigated fluridone degradation in lake water, but all have demonstrated the ability of fluridone to photolyze.

While outside the scope of this study, fluridone is known to photolyze into *n*-methylformamide, benzaldehydes, and benzoic acids.^{28,33} However, no study has focused on the susceptibility of fluridone through dissolved organic matter (DOM) mediated indirect photodegradation.^{33,34} During indirect photodegradation, the interaction between DOM and light generates photochemically produced reactive intermediates (PPRI) that can increase the rate of photodegradation; this process can be important for many polar organic contaminants, including some pesticides.³⁵⁻³⁷ Thus, a thorough investigation into potential of indirect photodegradation of fluridone is critical to understanding its environmental fate in lakes.

Laboratory studies also indicate that biodegradation can be an important loss pathway of fluridone under some conditions, with reported half-lives of 50 days to 12 months (**Table B.1**).^{38,39} Although these biodegradation half-lives are longer than the reported photolysis half-lives, biodegradation may still be an important transformation pathway of fluridone. For example, the biodegradation product 3-trifluoromethyl benzoic acid has been detected under field conditions in a small eutrophic pond and persisted up to 30 days post-application (**Figure 3.1b**).¹⁴

While laboratory studies suggest that photo- and biodegradation contribute to fluridone degradation on the order of hours to weeks, measurements of fluridone in lakes indicate that the compound can be highly persistent. Persistence of fluridone has been observed in field studies, with reported half-lives in the range of hours to hundreds of days,^{29,40} with some instances detecting fluridone in the water column for more than a year post-treatment (**Table B.1**).¹⁸ Additionally, fluridone has a capacity to sorb to sediments with a pKa of 12.3, indicating the compound will be protonated in natural environments which allows for stronger

sorption to organic carbon compared to its neutral form.⁴¹ It has been found to persist for up to a year following initial treatment, suggesting sediments are a possible host for unreacted fluridone that can undergo future resuspension or uptake by plants.^{29,42-43} The long persistence of fluridone under field conditions indicates a need for additional investigation into the specific degradation pathways of fluridone that can reduce this level of persistence.

The considerable exposure time requirement for efficacy of fluridone in lakes requires a mechanistic understanding of the environmental transformation processes that degrade fluridone in order to develop more effective herbicide application strategies and reduce negative impacts on ecosystems. Laboratory experiments allow for the isolation of various degradation pathways to determine their respective effects on the target compound as well as elucidate transformation product formation, but they lack a direct translation to field conditions where there are competing transformation mechanisms and many environmental factors that do not have influence in a controlled experiment. Conducting laboratory experiments in tandem with field studies will provide a holistic understanding of fluridone fate in aquatic environments. This study provides a first insight into the simultaneous effects of photodegradation, sorption to sediments, and biodegradation in both lab and field conditions. The findings of this study will be used to improve fluridone treatment success and minimize potential effects to non-target communities.

Materials and Methods

Chemicals. All chemicals were used as received. Fluridone (99.5%) was purchased from ChemService, Inc. Dibasic potassium phosphate (ACS, 98%), monobasic potassium

phosphate (ReagentPlus(R)), 3-trifluoromethyl benzoic acid (99%) were purchased from Sigma Aldrich. Acetonitrile (HPLC grade) and formic acid (ACS, 88%) were purchased from Fisher Chemical. 2-Nitrobenzaldehyde (99%) was purchased from Acros Organics. Ultrapure water (18.2 M Ω cm) for all analyses and photochemical irradiations was obtained from a Milli-Q water purification system. Calibration solutions for the pH meter were obtained from Aqua Solutions.

Field sampling. Hooker Lake in Kenosha County, Wisconsin, USA (44.56°N, 88.10°W) underwent a fluridone treatment in May 2022 which served as the focus of our field campaign (**Figure 3.4a, Table B.2**). This treatment applied a pellet formulation of fluridone across the lake to target hybrid watermilfoil and curly-leaf pondweed. Pretreatment surface water was collected from the epilimnion by grab sampling while pretreatment sediment was collected from a nearshore area by Eckman dredge or hand-coring ≤ 2 hours prior to treatment and stored at 4°C until processing. Water samples were collected every 1-2 weeks until 60 days post-treatment. Samples collected during the treatment were stored on ice and in the dark until processing (**Section B.2**).

Photochemical irradiations. Photodegradation experiments were conducted in a Rayonet merry-go-round photoreactor equipped with sixteen bulbs that emit light at 311 nm (± 22 nm width at half-max). This wavelength range is within the solar irradiance spectrum and overlaps with the absorbance spectrum of fluridone (**Figure B.1**).⁴⁴ Irradiation experiments were conducted in triplicate in borosilicate glass tubes using 20 μ M (6.6 ppm) fluridone in 10 mM pH 7 buffered ultrapure water to measure direct photodegradation. Identical solutions were held in the dark to serve as dark controls. Indirect photodegradation was measured in lake

water diluted to 3 mg-C L⁻¹ from four lakes and undiluted water from Hooker Lake (**Table B.2**). Light intensity was quantified using 2-nitrobenzaldehyde⁴⁵ as a chemical actinometer. The fluridone concentration used in irradiations was higher than typical fluridone applications but was selected to enable detection over several orders of magnitude of loss.

The direct quantum yield of fluridone was calculated relative to the actinometer as described previously^{44,46-48} using Equation 3.1:

$$\Phi_{fluridone} = \frac{k_{screened,direct,fluridone}}{k_{direct,act}} \times \frac{k_{abs,act}}{k_{abs,fluridone}} \times \Phi_{act} \quad \text{Eq. 3.1}$$

where $k_{screened,direct,fluridone}$ is the direct photodegradation rate constant for the direct control corrected for light screening (s⁻¹), $k_{direct,act}$ is the photodegradation rate constant of the actinometer (s⁻¹), $k_{abs,act}$ (s⁻¹) is the rate of light absorbance of the actinometer, $k_{abs,fluridone}$ (s⁻¹) is the rate of light absorption for fluridone, and $\Phi_{act} = 0.41$ for 2-nitrobenzaldehyde (**Section B.3**).⁴⁵

The calculated quantum yield was combined with solar irradiance modeling using the Simple Model of Atmospheric Transfer of Sunshine (SMARTS)⁴⁹ to calculate fluridone half-life in sunlight in lakes using Equation 3.2:

$$k_{photodegradation} = k_{abs,sun} \times \Phi_{fluridone} \quad \text{Eq. 3.2}$$

where $k_{abs,sun}$ is a light absorbance rate constant calculated for the horizontal global irradiance spectrum for Kenosha County, Wisconsin, USA on May 12, 2022, which was the location and date of our treatment of study, averaged over the time span of 6 am to 6 pm (**Figure B.2**). A depth-integrated photodegradation^{36,47} rate was calculated as described previously. We

calculated the photodegradation rate in 1 cm intervals through a 1-meter-deep water column (i.e., at 1 cm, 2 cm, 3 cm ... 100 cm) and averaged the rates throughout the water column.

Sorption. Pretreatment sediment from Hooker Lake was dried at 100°C for ≥ 8 hours (**Section B.2**). Dried sediment (1 g) was added to buffered ultrapure water (pH 7, 5 mM phosphate buffer, 100 mL) with five varying concentrations of fluridone over the range of 1-20 μM in triplicate to create an isotherm. Samples were shaken in an incubator shaker and equilibrium aqueous concentrations (C_w) were measured after seven hours (**Figure B.3**). The concentration remaining in the sediment at equilibrium was calculated based on Equation 3.3:

$$C_s = \frac{V (C_0 - C_w)}{M} \quad \text{Eq. 3.3}$$

where V is the volume of the solution, C_0 is the initial spiked concentration of fluridone, and M is the mass of lake sediment used.⁵⁰

The organic content of the sediment was measured through a loss-on-ignition method by combusting the dried sediment at 550°C for 4 hours.⁵¹ The organic content was used to calculate the organic carbon partitioning coefficient (K_{oc}) of fluridone using Equation 3.4:

$$K_{oc} = \frac{K_d}{f_{oc}} \quad \text{Eq. 3.4}$$

where K_d is the sediment-specific sorption partitioning coefficient which is equivalent to the slope of the sorption isotherm and f_{oc} is the fraction of organic content.⁵⁰

Microcosm incubations. Pretreatment water and sediment was collected from Hooker Lake for microcosm biodegradation studies of fluridone. Degradation by the water column microbial community was quantified in triplicate microcosms with unfiltered lake water (3 L), while degradation by the sediment microbial community was quantified in microcosms with

0.2 μm filtered lake water (2 L) and sediment (0.5 kg) at room temperature. Abiotic loss processes were assessed in control microcosms with 0.2 μm filtered lake water (2 L). Microcosms were incubated with 3 μM (1 ppm) fluridone and incubated for 204 days. Water and sediment samples were collected bi-weekly during the first three months and then monthly thereafter. Water samples were filtered through a 0.45 μm nylon filter and stored in a 4°C fridge prior to analysis. Sediment samples were collected using a serological pipette and stored in a 2.5 mL PCR tube in a -20°C freezer until analysis.

Sediment extractions. Fluridone extractions from sediment samples were conducted using 100 mg of microcosm sediment dried at 100°C for at least 8 hours. An extraction solution of 50:50 methanol:water consistently achieved an average of (103 ± 9) % recovery over a [fluridone] range of 1 to 20 μM (**Figure B.5**). This suggested the extraction protocol was reliable for microcosm sediment quantification. Dried samples were placed in falcon tubes with 7 mL of a 50:50 methanol:water extraction solution, shaken in an incubator shaker for 2 hours, centrifuged, and syringe filtered (0.45 μm) into clean 2 mL glass amber vial for analysis.

Analytical methods. Fluridone from laboratory experiments, 3-trifluoromethyl benzoic acid, and 2-nitrobenzaldehyde were analyzed via high performance liquid chromatography (HPLC).³¹ Fluridone analyzed through HPLC had a limit of detection (LOD) of 0.6 μM . Fluridone in the field samples was quantified using an Agilent Triple Quad 6460 liquid chromatograph-tandem mass spectrometer (LC-MS/MS) using positive mode electrospray ionization which had an LOD of 2.6 nM. Ultraviolet-visible light spectra for each lake and compound were collected from 200-800 nm. Method details are provided in **Section B.7**.

Results and Discussion

Photodegradation of fluridone in lake water. Fluridone underwent rapid photodegradation under laboratory conditions. Irradiation of fluridone at 311 nm (**Figure 3.2**) followed first-order loss with a direct photodegradation rate constant in buffered ultrapure water (k_{direct}) of $(4.1 \pm 0.5) \times 10^{-4} \text{ s}^{-1}$ ($t_{1/2} = 28$ minutes). The measured direct photodegradation rate constant corresponded to a quantum yield (Φ), or reaction efficiency, of $(3.8 \pm 0.6) \times 10^{-4}$. This was larger than previous measurements of quantum yield of $(2.7 - 6.7) \times 10^{-5}$ in ultrapure water.³³ However, this could be due to several differences in experimental methods, with their study involving a pH range of 3-9 with various buffers, oxygen-containing and nitrogen-purged water, as well as the use of fluorescent sunlamps with black lights as the light source.

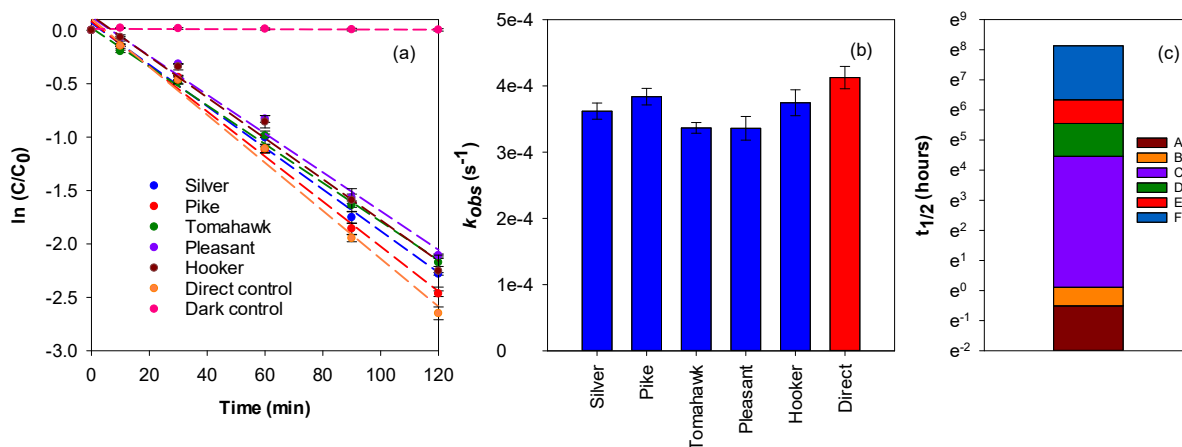


Figure 3.2. (a) Photochemical irradiation of fluridone at 311 nm in ultrapure water (direct control) and five different lake waters. Natural log of the ratio of [fluridone] at time t to initial [fluridone]. (b) Rate constants measured during 311 nm irradiation experiment corrected for light screening in the lake waters compared to the direct control. Error bars represent standard deviation of triplicate samples. (c) Representation of half-life variability under different conditions where A = 311 nm irradiation in the lab, B = lab conditions corrected for light screening, C = noontime solar irradiance, D = noontime irradiance with diurnal cycling, E = average solar irradiance, and F = average irradiance integrated over 1 m. It is important to note that the y-axis is a natural log scale.

Irradiation of fluridone in lake water also followed first order loss (**Figure 3.2a**). k_{obs} in lake water was similar to the direct photodegradation rate constant when corrected for light screening (**Figure 3.2b**), with an average rate constant across all irradiated samples of $(3.6 \pm 0.2) \times 10^{-4} \text{ s}^{-1}$. The similarity of rate constants across all irradiated samples demonstrated that indirect photodegradation of fluridone is negligible under these conditions. Previous literature has described similar photodegradation rates between ultrapure water and one natural water sample in sunlight,^{33,52} but our study confirms the dominance of direct photodegradation by testing several different natural waters with varied DOC concentrations and DOM compositions (**Table B.2**).

In situ photodegradation modeling was conducted using the calculated quantum yield and an average sunlight intensity in Kenosha County, WI on May 12th, 2022 (i.e., the location of Hooker Lake on the day of treatment), assuming an average irradiance from 6 am to 6 pm which was the range of sunlight exposure (**Figure B.2**). This estimated an aquatic photodegradation half-life of 13 days when integrated through the top 10 cm of water. Previous studies report an environmental photodegradation half-life of 7 to 12 days in mesocosm³² and glass bottle³³ experiments, respectively, which is consistent with our modeled half-life of 13 days. However, the half-life increased steeply to 120 days when integrated over a depth of 1 m, indicating that these are overestimated half-lives given fluridone, especially the granular formulation, most likely mixes throughout the entire water column. Variability in half-life is also introduced through changes in solar irradiance, with the half-life decreasing to 65 days when assuming noontime irradiance over a depth of 1 m. This wide range of half-lives indicates how fluridone susceptibility to photodegradation is highly variable due to frequent temporal and spatial differences that occur in the natural environment (**Figure 3.2c**).

Sorption. Sediment-water partitioning of fluridone was measured over a concentration range of 1-20 μM after seven hours to establish a sorption isotherm (**Figures 3.3a** and **B.3**). The slope of this isotherm is equivalent to the sediment-water partitioning coefficient (K_d) specific to Hooker Lake sediment which was found to be $12 \pm 0.97 \text{ L kg}^{-1}$. Given the organic carbon fraction of Hooker Lake sediment was measured to be $(3.5 \pm 0.08) \%$, we calculated a K_{oc} value of $340 \pm 28 \text{ L kg}^{-1}$. This was slightly lower than the literature values of 350 - 2462 L kg^{-1} , although these measurements were made using field sediments in experimental ponds

rather than lakes, which could introduce uncharacterized variability from other transformation reactions, temperature changes, pH and soil differences, and water mixing compared to our measurements.^{39,53} Thus, fluridone is moderately sorptive and partitioning to sediment may influence its fate and persistence in the environment.

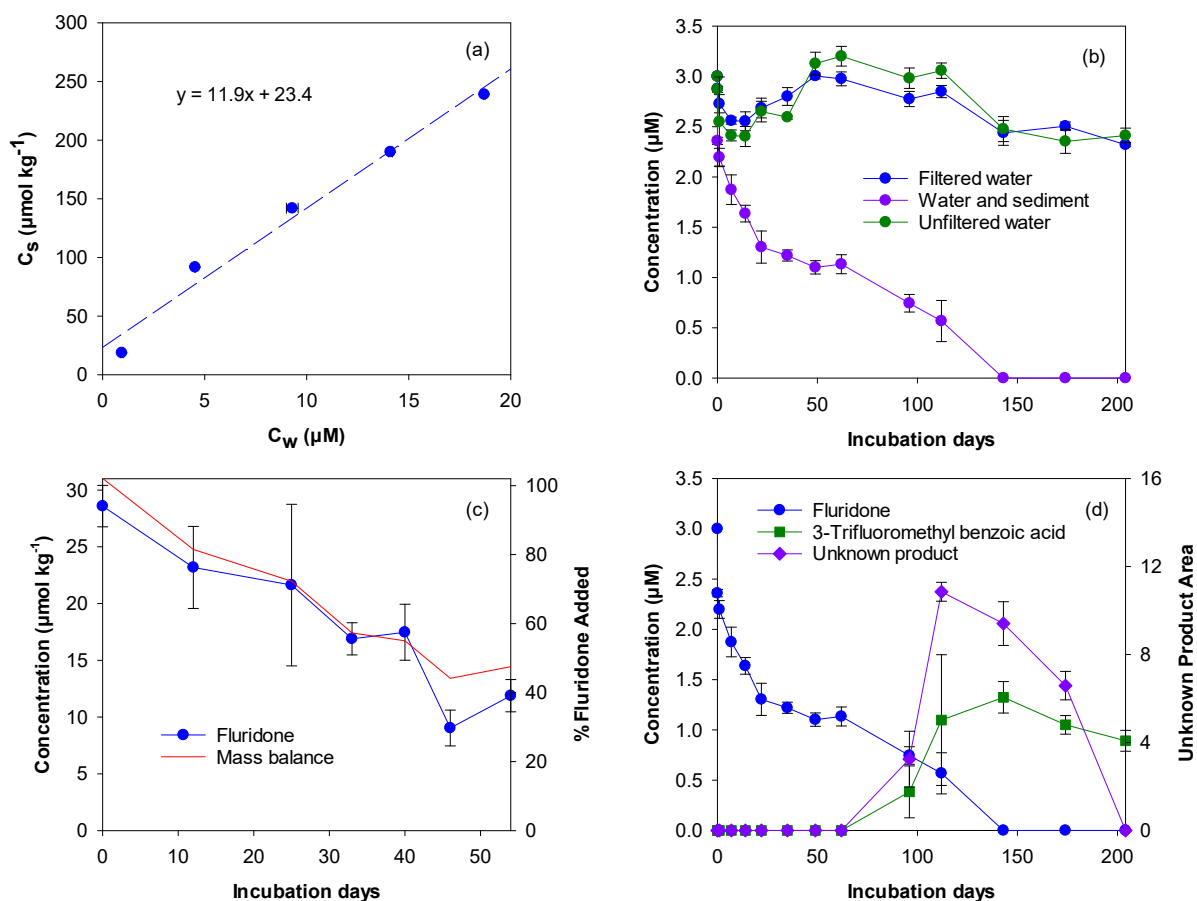


Figure 3.3. (a) Hooker Lake sediment sorption isotherm for fluridone. The slope of the isotherm is equivalent to the sediment sorption partitioning coefficient (K_d) in L kg^{-1} . (b) [Fluridone] in microcosms incubated with relevant environmental inocula from Hooker Lake at $3 \mu\text{M}$. (c) Sediment extraction data from Hooker Lake water-sediment microcosms. Mass balance represents percent of fluridone sorbed to sediment. Concentration represents μmol of fluridone per kg of dried sediment. (d) [Fluridone], [3-trifluoromethyl benzoic acid], and area of an unknown product detected in the water-sediment microcosms only. Error bars represent standard deviation of triplicate samples.

Microcosm incubations. Fluridone experienced virtually no loss throughout the duration of the experiment in the abiotic control (filtered water) as well as the unfiltered water only microcosms (**Figure 3.3b**). This signified that fluridone is very stable in water and its susceptibility to microbes throughout the water column is negligible. However, fluridone underwent pseudo-first-order kinetics in the sediment-water microcosms (**Figure B.4**) with an observed half-life of 57 days and it was no longer detected in the sediment microcosms past day 143. This was comparable to literature values and indicates that fluridone is not easily biodegraded in the environment.^{29,38}

Given that sorption is expected to be a sink for fluridone in sediment-water environments, extractions were carried out on microcosm sediment samples to quantify the amount of sorption to solids. Fluridone concentration in the sediment was greatest initially with a concentration of $29 \mu\text{mol kg}^{-1}$, which steadily decreased over time (**Figure 3.3c**). Overall, sediment microcosm extractions found an average fluridone concentration of $(18 \pm 6.2) \mu\text{mol kg}^{-1}$ across seven samples collected over the first 60 days, which accounted for $(15 \pm 5.1) \%$ of the initial fluridone added. This average sorption percentage was consistent with previous studies reporting 10-27% of added fluridone partitioning to the solid phase.^{52,54,55} Mass balance calculations found that sorption accounted for all of the fluridone loss initially, but this decreased immediately, with sorption only accounting for 48% of the added fluridone by day 54. This indicated that subsequent fluridone loss was explained by a mechanism other than sorption, such as biodegradation.

Fluridone experiences a steady pseudo-first-order rate loss before day 60, which is followed by an increased rate loss until it was no longer present. This increased fluridone loss

directly correlates with product formation, as 3-trifluoromethyl benzoic acid and an unidentified product were both detected by HPLC after day 60 (**Figure 3.3d**). 3-Trifluoromethyl benzoic acid accumulated to a peak concentration of 1.3 μM and remained relatively stable. Both compounds were present in the microcosms for over 100 days, indicating they could be persistent compounds under environmental conditions. However, sorption only accounted for all fluridone loss during the first time point, therefore any loss after time zero and before our observed product formation was also due to biodegradation. Additional products could have been formed that were not detected in our HPLC methods, such as fluridone-acid (1,4-dihydro-1-methyl-4-oxo-5-[3-(trifluoromethyl)phenyl]-3-pyridinecarboxylic acid), 4-hydroxyfluridone, or the 2-hydroxy derivative that have been detected in other fluridone-sediment experiments.^{39,56} The degradation of fluridone only in the sediment microcosms is consistent with several other polar organic compounds, likely due to a higher concentration of microbes or additional nutrients in the sediments.^{48,57-61} The extended lag period and then onset of faster degradation is also common for persistent polar organic compounds.^{62,63} Ultimately, the microcosm incubations showed that sorption and biodegradation both have the potential to be key sources of fluridone loss in the environment.

Fluridone behavior in lakes. Fluridone was quantified following a commercial application of the pellet formulation in Hooker Lake for up to 60 days after treatment. The herbicide formulation was applied lake-wide, therefore we sampled from three sites that included two opposing shorelines and one central site to characterize the lake as a whole (**Figure 3.4a**). Samples from each of the three sites reached a peak concentration ranging from 18-20 nM and by day 60 the concentration of each site was 10 nM, which was equivalent to

the expected lake-wide concentration (**Figure 3.4b**). While these concentrations were consistent with the typical exposure time requirement of 45-100 days, two additional treatments were conducted shortly after our sampling period.¹⁶⁻¹⁸

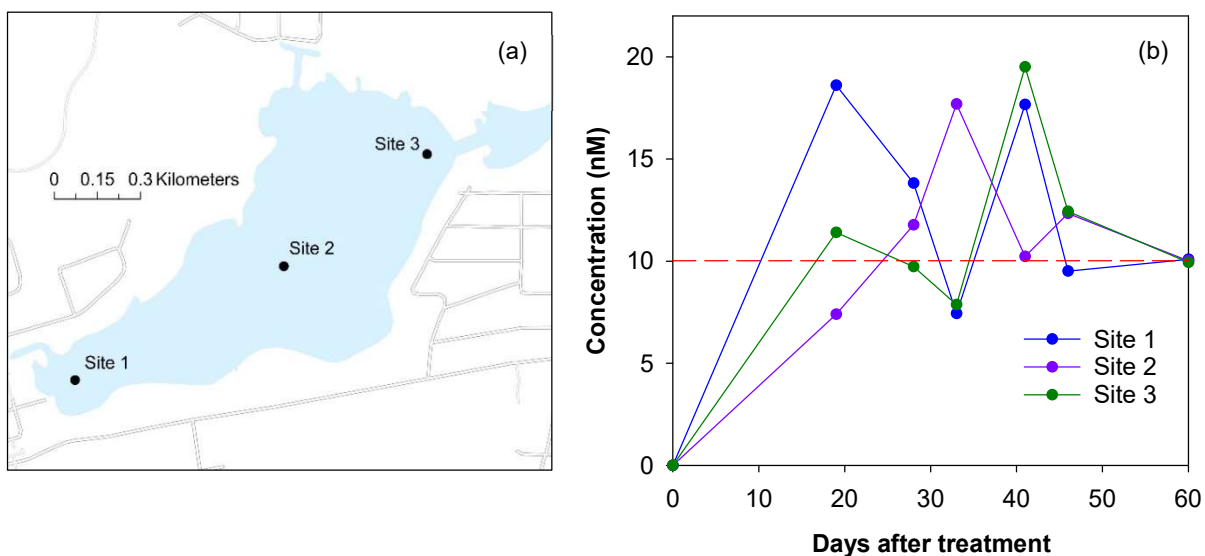


Figure 3.4. (a) All sample sites on Hooker Lake. Map made using ArcGIS. (b) [Fluridone] in each sample site during treatment. Dashed line is expected lake-wide [fluridone] concentration.

Fluridone concentrations appeared to remain steady throughout the sampling period, indicating that it is very stable under environmental conditions. Based on our laboratory experiments, photodegradation would appear to be an important loss mechanism in the epilimnion, but there was no evidence of this occurring. Similarly, our biodegradation measured half-life of 57 days was not consistent with the field concentrations as no significant loss was observed by day 60 in the lake. Interestingly, there were several outlets in this lake for potential fluridone removal through physical transport, but this was not observed either. This indicates that fluridone is much less susceptible to degradation mechanisms under

environmentally relevant conditions where natural processes have less influence compared to controlled experiments. The type of fluridone formulation also influences behavior and persistence in the water column, for the solid form acts as a slow release of fluridone into the water, causing a delayed susceptibility to degradation compared to the liquid form.⁶⁴ Previous studies have shown that the pellet formulation of fluridone reaches peak concentration 1-3 weeks after treatment, with the rate of release being strongly dependent on the sediment type (sand, clay, organic).^{3,5,42} This is consistent with our field data as Hooker Lake has a relatively higher organic content, therefore it would be expected for fluridone to experience a slower release rate and the target concentration is reached by day 20. Given fluridone was still present at 10 nM throughout the lake by day 60 and there was a notable discrepancy between the field data and our laboratory observations, more research is needed into understanding the duration of complete fluridone degradation in the lake and which transformation mechanisms are dominant.

Conclusions. Our work quantified the photodegradation, biodegradation, and sorption of fluridone in laboratory experiments in addition to quantification under environmental conditions in the field. Our results found fluridone is susceptible to all three transformation pathways, although the water depth, water clarity, and sediment composition of a treated water body will be critical for determining which degradation process is dominant. Additionally, the importance of photodegradation in shallow waters and sediment sorption suggests physical lake parameters such as sediment surface area and composition, average depth, or surface area to volume ratios may be important in understanding the in-lake degradation mechanisms of fluridone.

Fluridone was ultimately more persistent under *in situ* conditions, as fluridone concentration remained consistent up to day 60 in Hooker Lake which is longer than each of the half-lives observed in all laboratory experiments. This does not consider additional potential loss processes such as plant uptake⁶⁵ and discharge from lakes.⁴⁸ The difference in conclusions based off fluridone behavior in the lab compared to the field indicates that laboratory experiments cannot fully describe how compounds will actually persist in the natural environment. Due to these discrepancies, fluridone fate and transport in aquatic environments should continue to be evaluated holistically through the combination of both field and laboratory studies.

Acknowledgements. This work was funded by the Midwest Aquatic Plant Management Society Robert L. Johnson Memorial Grant (S.V.F. and A.M.W.), Anna Grant Birge Memorial Award (S.V.F., A.M.W., and A.M.M.) and a National Science Foundation Graduate Research Fellowship.

References

1. Slade, J. G.; Poovey, A. G.; Netherland, M. D. Efficacy of fluridone on Eurasian and hybrid watermilfoil. *J. Aquat. Plant Manage.* **2007**, *45* (2), 116–118.
2. Bartels, P. G.; Watson, C. W. Inhibition of carotenoid synthesis by fluridone and norflurazon. *Weed Sci.* **1978**, *26* (2), 198–203.
3. Koschnick, T. J.; Haller, W. T.; Vandiver, V. V.; Santra, U. Efficacy and residue comparisons between two slow-release formulations of fluridone. *J. Aquat. Plant Manage.* **2003**, *41*, 25-27.
4. Peterson, M. A.; McMaster, S. A.; Riechers, D. E.; Skelton, J.; Stahlman, P. W. 2,4-d past, present, and future: a review. *Weed Technol.* **2016**, *30* (2), 303–345.
5. Netherland, M. D.; Sisneros, D.; Fox, A. M.; Haller, W. T. Field Evaluation of Low-Dose Metering and Polymer Endothall Applications and Comparison of Fluridone Degradation from Liquid and Slow Release-Pellet Applications. <https://erdc-library.erd.dren.mil/jspui/bitstream/11681/6301/1/8745.pdf> (accessed April 2023).

6. Wagner, K. I.; Hauxwell, J.; Rasmussen, P. W.; Koshere, F.; Toshner, P.; Aron, K.; Helsel, D. R.; Toshner, S.; Provost, S.; Gansberg, M.; Masterson, J.; Warwick, S. Whole-lake herbicide treatments for Eurasian watermilfoil in four Wisconsin lakes: Effects on vegetation and water clarity. *Lake Reservoir Manage.* **2007**, *23* (1), 83–94.
7. Nault, M. E.; Netherland, M. D.; Mikulyuk, A.; Skogerboe, J. G.; Asplund, T.; Hauxwell, J.; Toshner, P. Efficacy, selectivity, and herbicide concentrations following a whole-lake 2,4-D application targeting Eurasian watermilfoil in two adjacent northern Wisconsin lakes. *Lake Reservoir Manage.* **2014**, *30* (1), 1–10.
8. Getsinger, K. D.; Madsen, J. D.; Koschnick, T. J.; Netherland, M. D. Whole Lake fluridone treatments for selective control of Eurasian watermilfoil: I. Application strategy and herbicide residues. *Lake Reservoir Manage.* **2002**, *18* (3), 181–190.
9. Berger, S. T.; Netherland, M. D.; MacDonald, G. E. Laboratory documentation of multiple-herbicide tolerance to fluridone, norflurazon, and topiramazone in a hybrid watermilfoil (*Myriophyllum spicatum* × *M. sibiricum*) population. *Weed Sci.* **2015**, *63* (1), 235–241.
10. Mallory-Smith, C. A.; Retzinger Jr., E. J. Revised classification of herbicides by site of action for weed resistance management strategies. *Weed Technol.* **2003**, *17* (3), 605–619.
11. Nault, M. E.; Barton, M.; Hauxwell, J.; Heath, E.; Hoyman, T.; Mikulyuk, A.; Netherland, M. D.; Provost, S.; Skogerboe, J.; Van Egeren, S. Evaluation of large-scale low-concentration 2,4-D treatments for eurasian and hybrid watermilfoil control across multiple Wisconsin lakes. *Lake Reservoir Manage.* **2018**, *34* (2), 115–129.
12. Richardson, R. J. Aquatic plant management and the impact of emerging herbicide resistance issues. *Weed Technol.* **2008**, *22* (1), 8–15.
13. Mikulyuk, A.; Kujawa, E.; Nault, M. E.; Van Egeren, S.; Wagner, K. I.; Barton, M.; Hauxwell, J.; Vander Zanden, M. J. Is the cure worse than the disease? comparing the ecological effects of an invasive aquatic plant and the herbicide treatments used to control it. *Facets* **2020**, *5* (1), 353–366.
14. Wisconsin Department of Natural Resources. Fluridone Chemical Fact Sheet <https://dnr.wi.gov/lakes/plants/factsheets/FluridoneFactsheet.pdf> (accessed April 2023).
15. Jeremy, S. G.; Poovey, A. G.; Netherland, M. D. Efficacy of Fluridone on Eurasian and Hybrid Watermilfoil. *J. Aquat. Plant Manage.* **2007**, *45*, 116–118.
16. Netherland, M. D.; Getsinger, K. D.; Skogerboe, J. D. Mesocosm evaluation of the species-selective potential of fluridone. *J. Aquat. Plant Manage.* **1997**, *35* (2), 41–50.
17. Netherland, M. D.; Getsinger, K. D.; Turner, E. G. Fluridone concentration and exposure time requirements for control of Eurasian watermillfoil and hydrilla. *J. Aquat. Plant Manage.* **1993**, *31*, 189–194.
18. Onterra. Silver Lake Management Plan https://www.townshipofmarion.com/wp-content/uploads/2018/01/SilverWaushara_HWMmonitorReport2017_v1-1.pdf (accessed April 2023).

19. Valley, R. D.; Crowell, W.; Welling, C. H.; Proulx, N. Effects of a low-dose fluridone treatment on submersed aquatic vegetation in a eutrophic Minnesota lake dominated by Eurasian watermilfoil and coontail. *J. Aquat. Plant Manage.* **2006**, *44*, 19–25.
20. Madsen, J. D.; Getsinger, K. D.; Stewart, R. M.; Owens, C. S. Whole Lake fluridone treatments for selective control of Eurasian watermilfoil: II. Impacts on submersed plant communities. *Lake Reservoir Manage.* **2002**, *18* (3), 191–200.
21. Arnold, W. R. Fluridone: A new aquatic herbicide. *J. Aquat. Plant Manage.* **1979**, *17*, 30–33.
22. Bartels, P. G.; Watson, C. W. Inhibition of carotenoid synthesis by fluridone and norflurazon. *Weed Sci.* **1978**, *26* (2), 198–203.
23. Larue, E. A.; Zuellig, M. P.; Netherland, M. D.; Heilman, M. A.; Thum, R. A. Hybrid watermilfoil lineages are more invasive and less sensitive to a commonly used herbicide than their exotic parent (Eurasian watermilfoil). *Evol. Appl.* **2013**, *6* (3), 462–471.
24. Green, W. R.; Westerdahl, H. E. Response of Eurasian watermilfoil to 2,4-D concentrations and exposure times. *J. Aquat. Plant Manage.* **1990**, *28*, 27–32.
25. Nault, M.; Mikulyuk, A.; Hauxwell, J.; Skogerboe, J.; Asplund, T.; Barton, M.; Wagner, K.; Hoyman, T.; Heath, E. Herbicide Treatments in Wisconsin Lakes. *Lakeline* **2012**, 21–26.
26. Wisconsin Department of Natural Resources. Florpyrauxifen-benzyl Chemical Fact Sheet
<https://dnr.wi.gov/water/wsSWIMSDocument.ashx?documentSeqNo=164039981>
(accessed April 2023).
27. Blanke, C.; Mikulyuk, A.; Nault, M.; Provost, S.; Schaal, C.; Van Egeren, S.; Williams, M.; Mednick, A. Strategic Analysis of Aquatic Plant Management in Wisconsin
https://dnr.wi.gov/topic/EIA/documents/APMSA/APMSA_Final_2019-06-14.pdf
(accessed 2023-03-15).
28. Osborne, J. A.; West, S. D.; Cooper, Raymond, B.; Schmitz, D. C.; Cooper B., R.; Schmitz, D. C. Fluridone and n-methylformaide residue determination in ponds. *J. Aquat. Plant Manage.* **1989**, *27*, 74–78.
29. West, S. D.; Burger, R. O.; Poole, G. M.; Mowrey, D. H. Bioconcentration and field dissipation of the aquatic herbicide fluridone and its degradation products in aquatic environments. *J. Agric. Food Chem.* **1983**, *31* (3), 579–585.
30. Netherland, M. D.; Jones, D. Fluridone-resistant hydrilla (*Hydrilla verticillata*) is still dominant in the Kissimmee Chain of Lakes, FL. *Invasive Plant Sci. Manage.* **2015**, *8* (2), 212–218.
31. Cozzola, A. J.; Dehnert, G. K.; White, A. M.; Karasov, W. H. Effects of subchronic exposure to environmentally relevant concentrations of a commercial fluridone formulation on fathead minnows (*Pimephales promelas*). *Aquat. Toxicol.* **2022**, *244*, 106098.
32. Macdonald, G. E.; Haller, W. T.; Shilling, D. G. UV-B filtration to reduce photolysis of fluridone in experimental tanks. *J. Aquat. Plant Manage.* **1996**, *34* (2), 78–80.

33. Saunders, D. G.; Mosier, J. W. Photolysis of the aquatic herbicide fluridone in aqueous solution. *J. Agric. Food Chem.* **1983**, *31* (2), 237–241.
34. Mossler, M. A.; Shilling, D. G.; Haller, W. T. Photolytic degradation of fluridone. *J. Aquat. Plant Manage.* **1989**, *27*, 69–73.
35. Remucal, C. K. The role of indirect photochemical degradation in the environmental fate of pesticides: a review. *Environ. Sci.: Processes Impacts* **2014**, *16* (4), 628–653.
36. McConville, M. B.; Mezyk, S. P.; Remucal, C. K. Indirect photodegradation of the lampricides tfm and niclosamide. *Environ. Sci.: Processes Impacts* **2017**, *19* (8), 1028–1039.
37. Maizel, A. C.; Li, J.; Remucal, C. K. Relationships between dissolved organic matter composition and photochemistry in lakes of diverse trophic status. *Environ. Sci. Technol.* **2017**, *51* (17), 9624–9632.
38. Mossler, M. A.; Shilling, D. G.; Albrecht, S. L.; Haller, W. T. Microbial degradation of fluridone. *J. Aquat. Plant Manage.* **1991**, *29*, 77–80.
39. Muir, D. C. G.; Grift, N. P. Fate of fluridone in sediment and water in laboratory and field experiments. *J. Agric. Food Chem.* **1982**, *30* (2), 238–244.
40. Wickham, P.; Pandey, P.; Harter, T.; Sandovol-Solis, S. UV light and temperature induced fluridone degradation in water and sediment and potential transport into aquifer. *Environ. Pollut.* **2020**, *265*, 114750.
41. Tomlin, C. *The e-Pesticides Manual*, British Crop Protection Council, Surrey, **2004**.
42. Mossler, M. A.; Shilling, D. G.; Milgram, K. E.; Haller, W. T. Interaction of formulation and soil components on the aqueous concentration of fluridone. *J. Aquat. Plant Manage.* **1993**, *31*, 257–260.
43. Muir, D.; Grift, N. P.; Blouw, A. P.; Lockhart, W. L. Persistence of fluridone in small ponds. *J. Environ. Qual.* **1980**, *9* (1), 151–156.
44. Bulman, D. M.; P. Mezyk, S.; K. Remucal, C. The impact of pH and irradiation wavelength on the production of reactive oxidants during chlorine photolysis. *Environ. Sci. Technol.* **2019**, *53* (8), 4450–4459.
45. Galbavy, E. S.; Ram, K.; Anastasio, C. 2-Nitrobenzaldehyde as a chemical actinometer for solution and ice photochemistry. *J. Photochem. Photobiol., A* **2010**, *209* (2–3), 186–192.
46. Berg, S. M.; Whiting, Q. T.; Herrli, J. A.; Winkels, R.; Wammer, K. H.; Remucal, C. K. The role of dissolved organic matter composition in determining photochemical reactivity at the molecular level. *Environ. Sci. Technol.* **2019**, *53* (20), 11725–11734.
47. McConville, M. B.; Hubert, T. D.; Remucal, C. K. Direct photolysis rates and transformation pathways of the lampricides TFM and niclosamide in simulated sunlight. *Environ. Sci. Technol.* **2016**, *50* (18), 9998–10006.
48. White, A. M.; Nault, M. E.; McMahan, K. D.; Remucal, C. K. Synthesizing laboratory and field experiments to quantify dominant transformation mechanisms of 2,4-dichlorophenoxyacetic acid (2,4-D) in aquatic environments. *Environ. Sci. Technol.* **2022**, *56* (15), 10838–10848.
49. Gueymard, C. A. Interdisciplinary applications of a versatile spectral solar irradiance model: a review. *Energy* **2005**, *30* (9), 1551–1576.

50. Schwarzenbach, R. P.; Gschwend, P. M.; Imboden, D. M. *Environmental Organic Chemistry, 3rd edition*, Wiley-Interscience, New Jersey, **2017**.
51. Kellogg Soil Survey Laboratory Methods Manual <https://www.nrcs.usda.gov/sites/default/files/2023-01/SSIR42.pdf>, (accessed April 2023).
52. West, S. D.; Day, E. W.; Burger, R. O. Dissipation of the experimental aquatic herbicide fluridone from lakes and ponds. *J. Agric. Food Chem.* **1979**, *27* (5), 1067-1072.
53. Fluridone Human Health and Ecological Risk Assessment https://www.dec.ny.gov/docs/lands_forests_pdf/seraflurid.pdf (accessed April 2023).
54. Banks, P. A.; Ketchersid, M. L.; Merkle, M. G. The Persistence of Fluridone in Various Soils under Field and Controlled Conditions. *Weed Sci.* **1979**, *27*, 631-633.
55. Marquis, L. Y.; Comes, R. D.; Yang, C. P. Degradation of fluridone in submersed soils under controlled laboratory conditions. *Pestic. Biochem. Physiol.* **1982**, *17*, 68-75.
56. Rainey, D. P. *Lilly Research Laboratories*, Greenfield, IN, **1980**.
57. Mezzanotte, V.; Bertani, R.; Innocenti, F. D.; Tosin, M. Influence of inocula on the results of biodegradation tests. *Polym. Degrad. Stab.* **2005**, *87* (1), 51-56.
58. Ott, A.; Martin, T. J.; Snape, J. R.; Davenport, R. J. Increased cell numbers improve marine biodegradation tests for persistence assessment. *Sci. Total Environ.* **2020**, *706*, 135621.
59. Zhi, H.; Miannecki, A. L.; Kolpin, D. W.; Klaper, R. D.; Iwanowicz, L. R.; LeFevre, G. H. Tandem field and laboratory approaches to quantify attenuation mechanisms of pharmaceutical and pharmaceutical transformation products in a wastewater effluent-dominated stream. *Water Res.* **2021**, *203*, 117537.
60. Seller, C.; Honti, M.; Singer, H.; Fenner, K. Biotransformation of chemicals in water-sediment suspensions: Influencing factors and implications for persistence assessment. *Environ. Sci. Technol. Lett.* **2020**, *7* (11), 854-860.
61. Seller, C.; Özel Duygan, B. D.; Honti, M.; Fenner, K. Biotransformation of chemicals at the water-sediment interface—Toward a robust simulation study setup. *ACS Environ. Au* **2021**, *1* (1), 46-57.
62. Koseki, S.; Nonaka, J. Alternative approach to modeling bacterial lag time, using logistic regression as a function of time, temperature, pH, and sodium chloride concentration. *Appl. Environ. Microbiol.* **2012**, *78* (17), 6103-6112.
63. Tjørve, K. M. C.; Tjørve, E. The use of gompertz models in growth analyses, and new gompertz-model approach: An addition to the unified-richards family. *PLoS ONE* **2017**, *12*, e0178691.
64. Beste, C. E. *Herbicide handbook of the Weed Society of America*, Weed Society of America, Champaign, IL, 1983.
65. Vassios, J. D.; Nissen, S. J.; Koschnick, T. J.; Hielman, M. A. Fluridone, penoxsulam, and triclopyr absorption and translocation by Eurasian watermilfoil (*Myriophyllum spicatum*) and hydrilla (*Hydrilla verticillata*). *J. Aquat. Plant Manage.* **2017**, *55*, 58-64

Chapter 4. Conclusions

Aquatic herbicides can be used as tools to investigate the environmental fate and transformation of polar organic compounds in natural waters due to their ability to be studied under field conditions starting from introduction into the lake. The underlying goal of this thesis was to characterize how herbicide behavior in laboratory studies can translate to their behavior under environmentally relevant conditions with tandem field studies. Two herbicides were studied with varying required exposure times, effective concentrations, modes of actions, and physical-chemical properties, which allowed for a range of investigation into strategic herbicide application.

Susceptibility of the herbicides to photodegradation, biodegradation, hydrolysis, and sorption was analyzed through laboratory experiments under isolated and controlled conditions. Parallel field campaigns were then conducted to contextualize these conclusions through quantifying herbicide degradation and transformation product formation directly following treatment. These results were used to determine the dominant transformation mechanisms acting on each herbicide in the aquatic environment, as well as to draw broader conclusions about laboratory-based narratives on the environmental fate of organic compounds.

As detailed in the prologues of Chapters 2 and 3, the chapters of this thesis are draft manuscripts in preparation for submittal to academic journals for publication. These drafts will continue to be edited in the coming months by coauthors and reviewers.

FPB summary and future research needs. Florpyrauxifen-benzyl (FPB) is a newly developed herbicide that was registered with the Environmental Protection Agency (EPA) for aquatic use in 2017.^{1,2} It was developed to combat invasive plant species resistance to previous auxin mimic herbicides by targeting a different binding site.^{3,4} It was found through laboratory studies that FPB is extremely susceptible to photodegradation and modeled half-lives under field conditions predicted rapid loss in the epilimnion. However, field studies of FPB paint a different picture as photodegradation products were formed, but they only accounted for around 4-9% of total FPB loss.

The two dominant transformation products detected in the field were florpyrauxifen and hydroxy-florpyrauxifen. Based on laboratory experiments isolating hydrolysis reactions, FPB undergoes base-promoted hydrolysis to produce florpyrauxifen. Microcosm incubations of both FPB and florpyrauxifen show that hydroxy-florpyrauxifen is a biodegradation product that forms directly from florpyrauxifen. Sorption to sediments was also determined to be an important loss pathway for FPB through laboratory experiments, and field sediment samples demonstrated that around 12% of the total added FPB was sorbed to the sediments.

While FPB hydrolysis is a base-promoted reaction, florpyrauxifen formation in lakes was faster than any hydrolysis or microcosm experiment at the same pH. This was hypothesized to be due to plant-catalyzed hydrolysis in lake, which is described as part of the toxicity mechanism of FPB as well as its terrestrial predecessor halauxifen-methyl.^{3,5,6} This was corroborated by plant extractions conducted with plant biomass samples taken throughout treatment, with high concentrations of both FPB and florpyrauxifen recovered during the early

stages of treatment. Since hydrolysis is the dominant loss pathway of FPB, observed degradation rates in aquatic environments are likely most dependent on physical and chemical lake parameters such as plant density and pH.

Since flurpyrauxifen and hydroxy-flurpyrauxifen persisted in the water column for much longer than FPB, future research is needed to investigate their potential negative effects on non-target communities such as native aquatic plants and fish populations. FPB acts as a proherbicide, meaning that the parent compound must undergo a chemical conversion in order to become biologically active. Flurpyrauxifen acts as the herbicidal product for FPB by accumulating inside the plant tissue, indicating that it could retain biological effects in the water on its own.^{4,7} Previous work has demonstrated that transformation of one toxic chemical to a degradation product does not necessarily eliminate toxicity,⁸⁻¹² thus the persistence of flurpyrauxifen must be investigated further to understand the potential for inadvertent effects on aquatic ecosystems.

Fluridone summary and future research needs. Fluridone has a long history of use in aquatic systems, with its initial EPA registration occurring in 1986.¹³ It has a unique mode of action that inhibits the production of protective pigment by the plant which causes photobleaching.^{14,15} Laboratory studies found fluridone underwent degradation the fastest through photodegradation, with the shortest half-lives produced through modeling calculations in the epilimnion. This is consistent with many literature studies establishing the dominant loss pathway of fluridone to be photodegradation.¹⁶⁻¹⁹ Fluridone was also determined to be susceptible to biodegradation, with loss occurring only in the sediment microcosms which was

similar to FPB. However, the half-life of fluridone observed in the sediment microcosms was longer than photodegradation by about 40 days. Sorption was observed to be an important loss pathway through isotherms returning a K_{oc} value of $340 \pm 28 \text{ L kg}^{-1}$, and sediment samples returned $(15 \pm 5.1) \%$ of total fluridone added to the microcosms.

While laboratory studies demonstrated susceptibility of fluridone to several transformation pathways, little loss was observed through quantification in the field for 60 days post-treatment. The type of fluridone used during application was a pellet formulation designed for slow release into the water column, which is expected to reach maximum concentration by 1-3 weeks.²⁰⁻²² Despite this delay in fluridone accumulation, the half-lives calculated in the lab were not relevant under environmental conditions. These discrepancies highlight the importance of tandem field and laboratory studies when characterizing organic compound behavior in the environment. Future studies on fluridone need to be conducted from a holistic perspective, with a complete characterization of fluridone from initial application to below detection in order to truly understand its persistence in lakes. Based on our observations, physical lake parameters such as water depth, water clarity, and sediment-water surface area are most likely important factors in fluridone environmental fate given its potential for photodegradation, biodegradation, and sorption.

References

1. Wisconsin Department of Natural Resources. Florpyrauxifen-benzyl Chemical Fact Sheet
<https://dnr.wi.gov/water/wsSWIMSDocument.ashx?documentSeqNo=164039981>
(accessed April 2023).

2. SePRO. ProcellaCOR EC https://sepro.com/Documents/ProcellaCOR_EC--Label.pdf (accessed April 2023).
3. Epp, J. B.; Alexander, A. L.; Balko, T. W.; Buysse, A. M.; Brewster, W. K.; Bryan, K.; Daeuble, J. F.; Fields, S. C.; Gast, R. E.; Green, R. A.; Irvine, N. M.; Lo, W. C.; Lowe, C. T.; Renga, J. M.; Richburg, J. S.; Ruiz, J. M.; Satchivi, N. M.; Schmitzer, P. R.; Siddall, T. L.; Webster, J. D.; Weimer, M. R.; Whiteker, G. T.; Yerkes, C. N. The discovery of ArylexTM active and RinskorTM active: Two novel auxin herbicides. *Bioorg. Med. Chem.* **2016**, *24* (3), 362–371.
4. Netherland, M. D.; Richardson, R. J. Evaluating sensitivity of five aquatic plants to a novel arylpicolinate herbicide utilizing an organization for economic cooperation and development protocol. *Weed Sci.* **2016**, *64* (1), 181–190.
5. Miller, M. R.; Norsworthy, J. K. Influence of soil moisture on absorption, translocation, and metabolism of Florpyrauxifen-Benzyl. *Weed Sci.* **2018**, *66* (4), 418–423.
6. Deboer, G. J.; Satchivi, N. Comparison of translocation properties of insecticides versus herbicides that leads to efficacious control of pests as specifically illustrated by IsoclastTM active, a new insecticide, and ArylexTM active, a new herbicide. *ACS Symp. Ser.* **2014**, *4*, 75-93.
7. Beets, J.; Heilman, M.; Netherland, M. D. Large-scale mesocosm evaluation of florpyrauxifen-benzyl, a novel arylpicolinate herbicide, on Eurasian and hybrid watermilfoil and seven native submersed plants. *J. Aquat. Plant Manage.* **2019**, *57*, 49–55.
8. Tian, Z.; Zhao, H.; Peter, K. T.; Gonzalez, M.; Wetzal, J.; Wu, C.; Hu, X.; Prat, J.; Mudrock, E.; Hettinger, R.; Cortina, A. E.; Biswas, R. G.; Vinicius, F.; Kock, C.; Soong, R.; Jenne, A.; Du, B.; Hou, F.; He, H.; Lundeen, R.; Gilbreath, A.; Sutton, R.; Scholz, N. L.; Davis, J. W.; Dodd, M. C.; Simpson, A.; McIntyre, J. K.; Kolodziej, E. P. A ubiquitous tire rubber- 153 derived chemical induces acute mortality in coho salmon. *Science* **2021**, *371*, 185– 189.
9. Wiener, E. A.; Lefevre, G. H. White rot fungi produce novel tire wear compound metabolites and reveal underappreciated amino acid conjugation pathways. *Environ. Sci. Technol. Lett.* **2022**, *9* (5), 391-399.
10. Unice, K.; Bare, J.; Kreider, M.; Panko, J. Experimental methodology for assessing the environmental fate of organic chemicals in polymer matrices using column leaching studies and oecd 308 water/sediment systems: application to tire and road wear particles. *Sci. Total Environ.* **2015**, *533*, 476–487.
11. Sinclair, C. J.; Boxall, A. B. A. Assessing the ecotoxicity of pesticide transformation products. *Environ. Sci. Technol.* **2003**, *37* (20), 4617–4625.
12. Cwiertny, D. M.; Snyder, S. A.; Schlenk, D.; Kolodziej, E. P. Environmental designer drugs: When transformation may not eliminate risk. *Environ. Sci. Technol.* **2014**, *48* (20), 11737–11745.

13. Wisconsin Department of Natural Resources. Fluridone Chemical Fact Sheet <https://dnr.wi.gov/lakes/plants/factsheets/FluridoneFactsheet.pdf> (accessed April 2023).
14. Arnold, W. R. Fluridone: A new aquatic herbicide. *J. Aquat. Plant Manage.* **1979**, *17*, 30–33.
15. Bartels, P. G.; Watson, C. W. Inhibition of carotenoid synthesis by fluridone and norflurazon. *Weed Sci.* **1978**, *26* (2), 198–203.
16. Mossler, M. A.; Shilling, D. G.; Haller, W. T. Photolytic degradation of fluridone. *J. Aquat. Plant Manage.* **1989**, *27*, 69–73.
17. Saunders, D. G.; Mosier, J. W. Photolysis of the aquatic herbicide fluridone in aqueous solution. *J. Agric. Food Chem.* **1983**, *31* (2), 237–241.
18. Macdonald, G. E.; Haller, W. T.; Shilling, D. G. UV-B filtration to reduce photolysis of fluridone in experimental tanks. *J. Aquat. Plant Manage.* **1996**, *34* (2), 78–80.
19. West, S. D.; Day, E. W.; Burger, R. O. Dissipation of the experimental aquatic herbicide fluridone from lakes and ponds. *J. Agric. Food Chem.* **1979**, *27* (5), 1067–1072.
20. Koschnick, T. J.; Haller, W. T.; Vandiver, V. V.; Santra, U. Efficacy and residue comparisons between two slow-release formulations of fluridone. *J. Aquat. Plant Manage.* **2003**, *41*, 25–27.
21. Netherland, M. D.; Sisneros, D.; Fox, A. M.; Haller, W. T. Field Evaluation of Low-Dose Metering and Polymer Endothall Applications and Comparison of Fluridone Degradation from Liquid and Slow Release-Pellet Applications. <https://erdc-library.erd.dren.mil/jspui/bitstream/11681/6301/1/8745.pdf> (accessed April 2023).
22. Mossler, M. A.; Shilling, D. G.; Milgram, K. E.; Haller, W. T. Interaction of formulation and soil components on the aqueous concentration of fluridone. *J. Aquat. Plant Manage.* **1993**, *31*, 257–260.

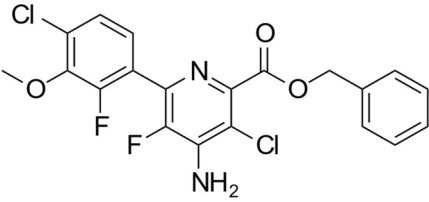
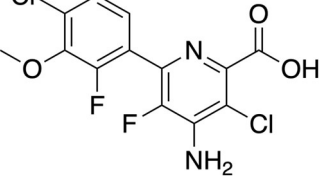
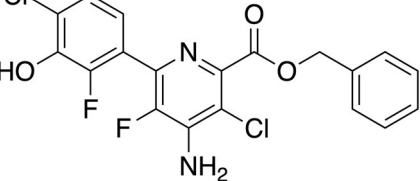
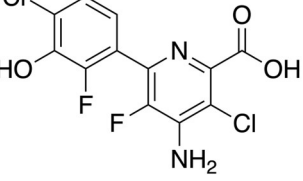
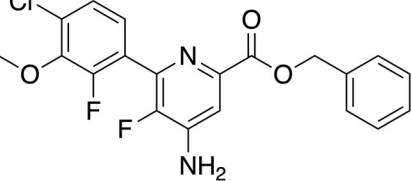
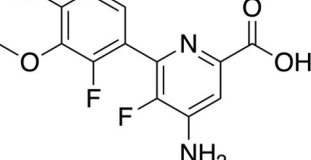
Appendix A. Supplementary Material for Chapter 2

Section A.1. Materials and chemical structures

Dibasic potassium phosphate (ACS, 98%) and monobasic potassium phosphate (ReagentPlus(R)) were purchased from Sigma Aldrich. Acetonitrile (HPLC grade) and formic acid (ACS, 88%) were purchased from Fisher Chemical. 2-Nitrobenzaldehyde (99%) was purchased from Acros Organics. Florpyrauxifen-benzyl (99.5%) was purchased from Chem Service, Inc. Florpyrauxifen (98.5%) was purchased from LGC Standards. Sodium borate was purchased from Amresco. Sodium acetate (ACS purity) was purchased from Alfa Aesar. Methanol (>99.8%) purchased from VWR. Standards for hydroxy-FPB, hydroxy-florpyrauxifen, dechloro-FPB, and dechloro-florpyrauxifen (**Table A.1**), as well as ¹³C-labeled florpyrauxifen-benzyl and florpyrauxifen, were not commercially available and were provided courtesy of Corteva Agrisciences. All chemicals were used as received.

Ultrapure water (18.2 MΩ cm) for all analyses and photochemical irradiations was obtained from Milli-Q water purification system. Calibration solutions for the pH meter were obtained from Aqua Solutions.

Table A.1. Chemical structures, formulas, and molecular weight of florpyrauxifen-benzyl and five degradation products.¹⁻³

Chemical Name and Formula	Structure
Florpyrauxifen-benzyl Molecular Formula: C ₂₀ H ₁₄ C ₁₂ F ₂ N ₂ O ₃ Molecular Weight: 439.24 CAS Number: 1390661-72-9	
Florpyrauxifen Molecular Formula: C ₂₀ H ₁₄ C ₁₂ F ₂ N ₂ O ₃ Molecular Weight: 439.24 CAS Number: 1390661-72-9	
Hydroxy-FPB Molecular Formula: C ₁₉ H ₁₂ C ₁₂ F ₂ N ₂ O ₃ Molecular Weight: 425.21	
Hydroxy-florpyrauxifen Molecular Formula: C ₁₂ H ₆ C ₁₂ F ₂ N ₂ O ₃ Molecular Weight: 335.09	
Dechloro-FPB Molecular Formula: C ₂₀ H ₁₅ ClF ₂ N ₂ O ₃ Molecular Weight: 404.79	
Dechloro-florpyrauxifen Molecular Formula: C ₁₃ H ₉ ClF ₂ N ₂ O ₃ Molecular Weight: 314.67	

Section A.2. Field sampling methods

Five FPB treatments were studied during the summers of 2021 and 2022 (**Figure A.1**). FPB was applied to areas of high-density Eurasian watermilfoil but had the potential to mix completely throughout the lake. Pretreatment surface water and sediment were collected from the epilimnion and nearshore area ≤ 2 hours prior to treatment and stored at 4°C until processing. Pretreatment samples used for bulk water chemistry measurements and photochemical irradiations were collected in 4 L combusted glass amber bottles, filtered through a 0.45 μM nylon filter, and preserved at 4°C until analysis. Water for microcosm incubations was collected with 10 L HDPE cubitainers and stored in the dark on ice until microcosm set up. Sediment for microcosm incubations was collected by Eckman dredge or hand-coring at a nearshore site of each and stored in the dark on ice until microcosms set up which occurred within 24 hours.

Water samples collected during and after FPB treatments were stored on ice and in the dark until processing, typically on site (i.e., within 1 hour of collection) but no more than 24 hours after collection, and preserved with methanol, formic acid, and a ^{13}C -labeled florpyrauxifen-benzyl internal standard (2.2 nM).

Water samples were collected at three sites on each lake, with at least one site in treatment area, one outside of treatment area (i.e., not intended to be treated) to monitor advective transport out of the treatment area, and one site at the deepest point of the lake. Samples were collected immediately after FPB application (<1 hour after application) and at 3- to-4-hour intervals for 12 hours after treatment, every 1 to 2 days after treatment for one

week after treatment, and then weekly thereafter. Additional depth discrete samples were collected with a Van Dorn sampler at 2 or 3 m intervals the deep hole of Muskellunge and Silver Lakes. At each sampling event, surface water was analyzed for all six target compounds (Table A.1).

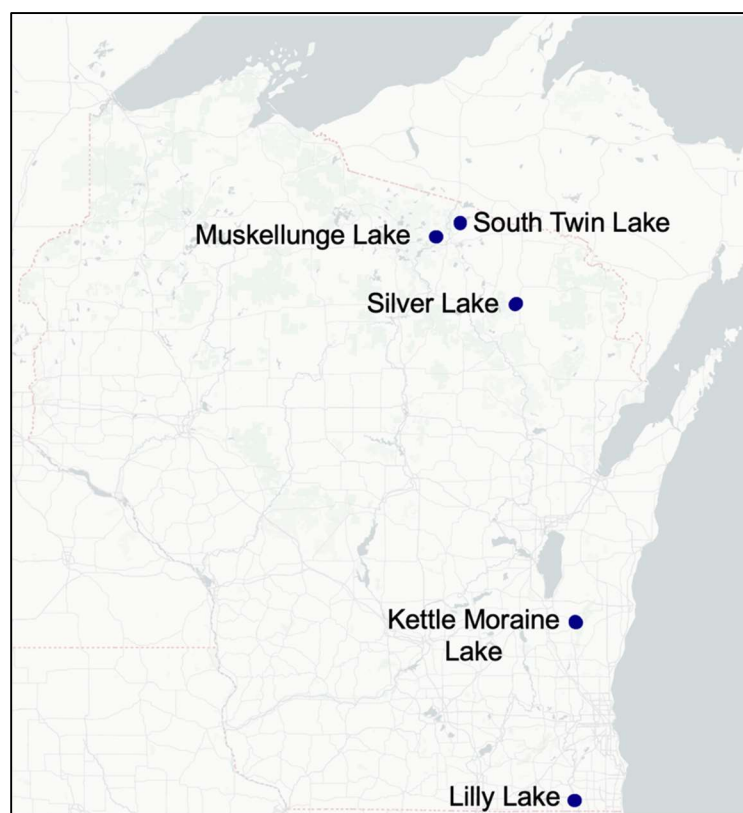


Figure A.1. Map of lakes sampled during 2021 and 2022 field campaigns. Map made using Leaflet package in RStudio.

Section A.3. Analytical methods

FPB, ^{13}C -FPB, ^{13}C -florpyrauxifen, florpyrauxifen, hydroxy-FPB, hydroxy-florpyrauxifen, dechloro-FPB, and dechloro-florpyrauxifen were quantified using an Agilent Triple Quad 6460 liquid chromatograph-tandem mass spectrometer (LC-MS/MS; **Table A.2**). Samples were analyzed using a gradient method (**Table A.3**) of aqueous buffer (A; 0.1% formic acid in ultra-pure water) and organic phase of 100% methanol (B) at 0.35 mL min^{-1} on an Agilent InfinityLab Poroshell 120 EC-C18 (3.0 x 50 mm) column and a column temperature control of 40°C .

LC-MS/MS running conditions and method details for FPB and degradation products:

Mode: Positive electrospray ionization

Scan type: MRM

Gas temp: 400°C

Speed: 13 L/min

Nebulizer pressure: 45 psi

Sheath gas temperature: 400°C

Sheath gas flow rate: 12 L/min

Capillary voltage: 4500 V

Dwell: 100 msec

Table A.2. Precursor and product ion information for FPB, internal standards, and degradation products.

Compound	Retention Time (min)	Precursor <i>m/z</i>	Product <i>m/z</i>	Fragmentor voltage	Collision energy	Cell accelerator voltage	LOD (nM)
FPB	5.1	439	91	95	98	4	0.07
			65	95	110	4	
¹³ C FPB	5.1	445	91	95	98	4	0.07
			65	95	110	4	
Florpyrauxifen	4.2	349	268	96	25	7	0.09
			303	96	20	7	
¹³ C Florpyrauxifen	4.2	355	274	96	25	7	0.09
			309	96	20	7	
Hydroxy-FPB	4.8	425	91	102	50	7	0.08
			65	102	100	7	
Dechloro-FPB	4.9	405	91	93	30	7	0.03
			65	93	100	6	
Hydroxy-florpyrauxifen	2.9	335	289	12	21	5	0.07
			254	102	34	5	
Dechloro-florpyrauxifen	3.7	315	234	98	30	4	0.13
			191	98	60	4	

Table A.3. Gradient chromatography details for LC-MS/MS analytical method of FPB, internal standard, and degradation products.

Time (minutes)	A%	B%
0.0	50	50
1.0	50	50
1.25	20	80
2.0	0	100
5.2	0	100
5.3	50	50
8.5	50	50

The actinometer 2-nitrobenzaldehyde was quantified using an Agilent 1260 high-performance liquid chromatograph (HPLC) equipped with a diode-array detector. Samples were analyzed using an isocratic method with acetonitrile as a mobile phase and an aqueous buffer of 90:10 ultrapure water: aqueous buffer of 10 % acetonitrile and 0.1% formic acid in

ultrapure water (**Table A.4**). An Agilent InfinityLab Poroshell 120 EC-C18 (3.0 x 50 mm) column was used with a column temperature control of 30°C.

Table A.4. Method information for quantification of 2-nitrobenzaldehyde via high pressure liquid chromatography.

Compound	% Aqueous Buffer	Flow (mL min⁻¹)	Detection wavelength (nm)	Retention Time (min)	Purpose	LOD (μM)
2-nitrobenzaldehyde	80	0.5	231	2.9	311 nm actinometer	0.5

Section A.4. Hydrolysis experiments

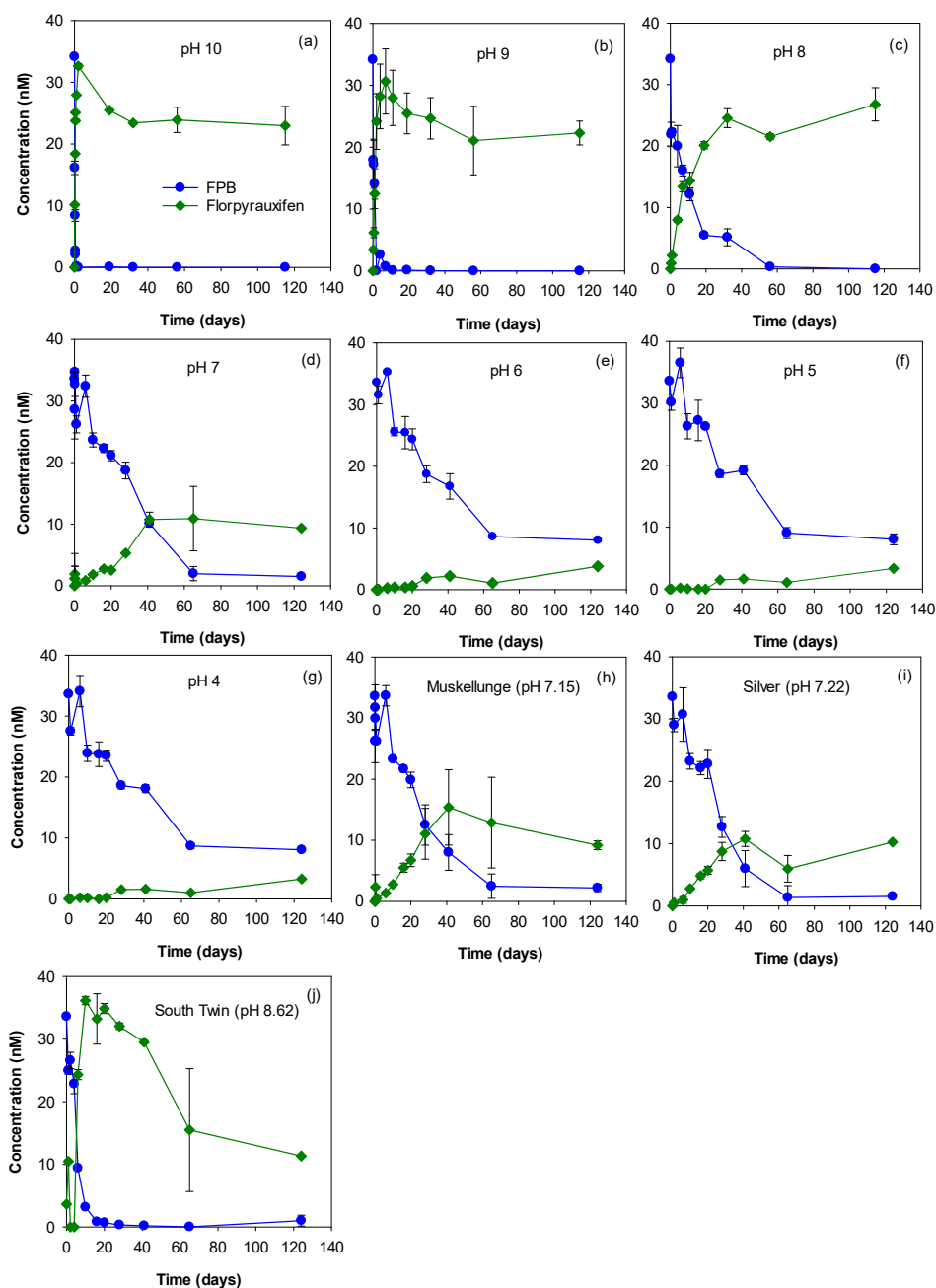


Figure A.2. FPB and florpyrauxifen concentrations in hydrolysis experiments in buffered ultrapure water at (a) pH 10, (b) pH 9, (c) pH 8, (d) pH 7, (e) pH 6, (f) pH 5, and (g) pH 4, as well as in unbuffered water from (h) Muskellunge (pH 7.15), (i) Silver (pH 7.22), and (j) South Twin (pH 8.62) lakes. Error bars represent the standard deviation of triplicate reactors.

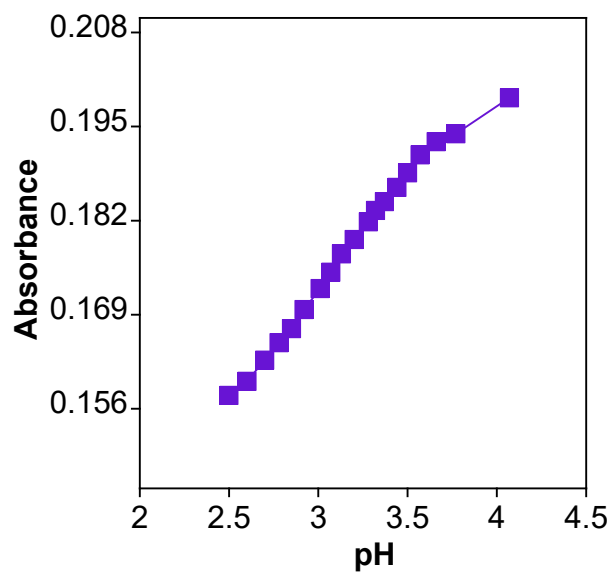


Figure A.3. Absorbance data for florpyrauxifen from pH 2.5-4 at 239 nm. An acid dissociation constant (pK_a) of 3.18 was determined by measuring pH at different wavelengths and using least squares regression.⁴

Section A.5. Sorption experiments

Sorption isotherms were calculated for FPB and florpyrauxifen with Kettle Moraine Lake and Lilly Lake sediments. The concentration remaining in the water at equilibrium (C_w) was quantified after 8 hours for FPB and after 24 hours for florpyrauxifen; timepoints were determined based on preliminary kinetics experiments (shown for FPB in **Figure A.4**). The concentration remaining in the sediment at equilibrium was calculated based on Equation S1:

$$C_s = \frac{V (C_0 - C_w)}{M} \quad \text{Eq. S1}$$

where V is the volume of the solution, C_0 is the initial spiked concentration of FPB or florpyrauxifen, and M is the mass of lake sediment used.⁵ The batch reactors were spiked with 4.6, 9.1, 14, 18, and 22 nM FPB and 5.7, 11, 17, 23, and 29 nM florpyrauxifen.

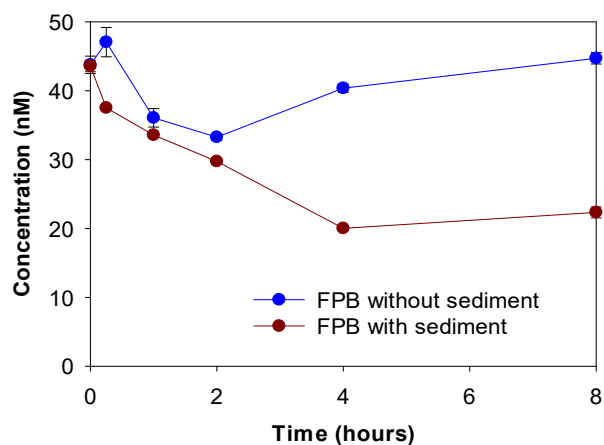


Figure A.4. Sorption kinetics of FPB interaction with lake sediment and control of FPB without sediment over time. FPB with sediment shows equilibrium is reached by 8 hours of sediment interaction. FPB control without sediment shows little to no loss occurs through volatilization, photodegradation, or sorption to the glass bottles.

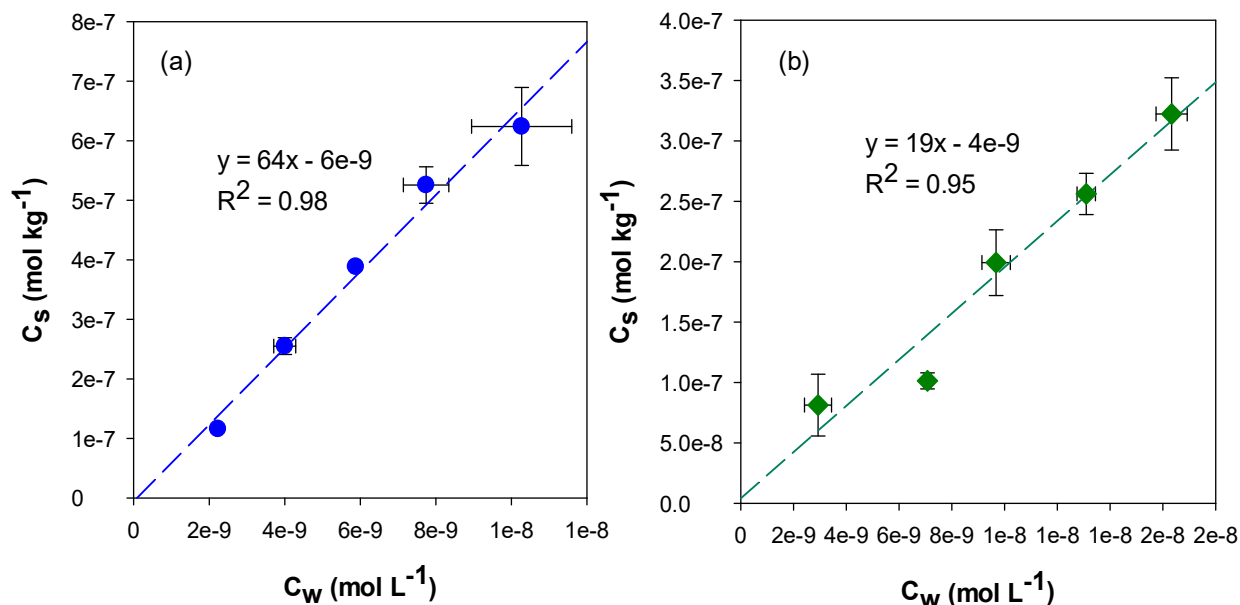


Figure A.5. Lilly Lake sediment sorption isotherms for (a) FPB and (b) florpyrauxifen. The slope of the isotherm is equivalent to the sediment sorption partitioning coefficient (K_d) in L kg⁻¹. Error bars represent the standard deviation of triplicate reactors.

The organic content was measured for Kettle Moraine and Lilly Lake sediments through a loss-on-ignition method by combusting the dried sediment at 550°C for 4 hours.⁶ The organic content was used to calculate the K_{oc} of FPB and florpyrauxifen using Equation S2:

$$K_{oc} = \frac{K_d}{f_{oc}} \quad \text{Eq. S2}$$

where K_d is the sediment-specific sorption partitioning coefficient and f_{oc} is the fraction of organic content (Table A.6).⁵

Table A.6. Sediment sorption parameters for FPB and florpyrauxifen. K_d is the sediment-specific partitioning coefficient in $L\ kg^{-1}$ and f_{oc} is the fraction of organic content in each sediment.

Lake sediment	f_{oc}	K_d – FPB ($L\ kg^{-1}$)	K_{oc} – FPB ($L\ kg^{-1}$)	K_d – Florpyrauxifen ($L\ kg^{-1}$)	K_{oc} – Florpyrauxifen ($L\ kg^{-1}$)
Kettle Moraine	5.7%	710 ± 69	12000 ± 1200	220 ± 8	3900 ± 150
Lilly	0.4%	64 ± 5	15000 ± 1400	19 ± 3	4600 ± 700

Section A.6. Microcosm incubations

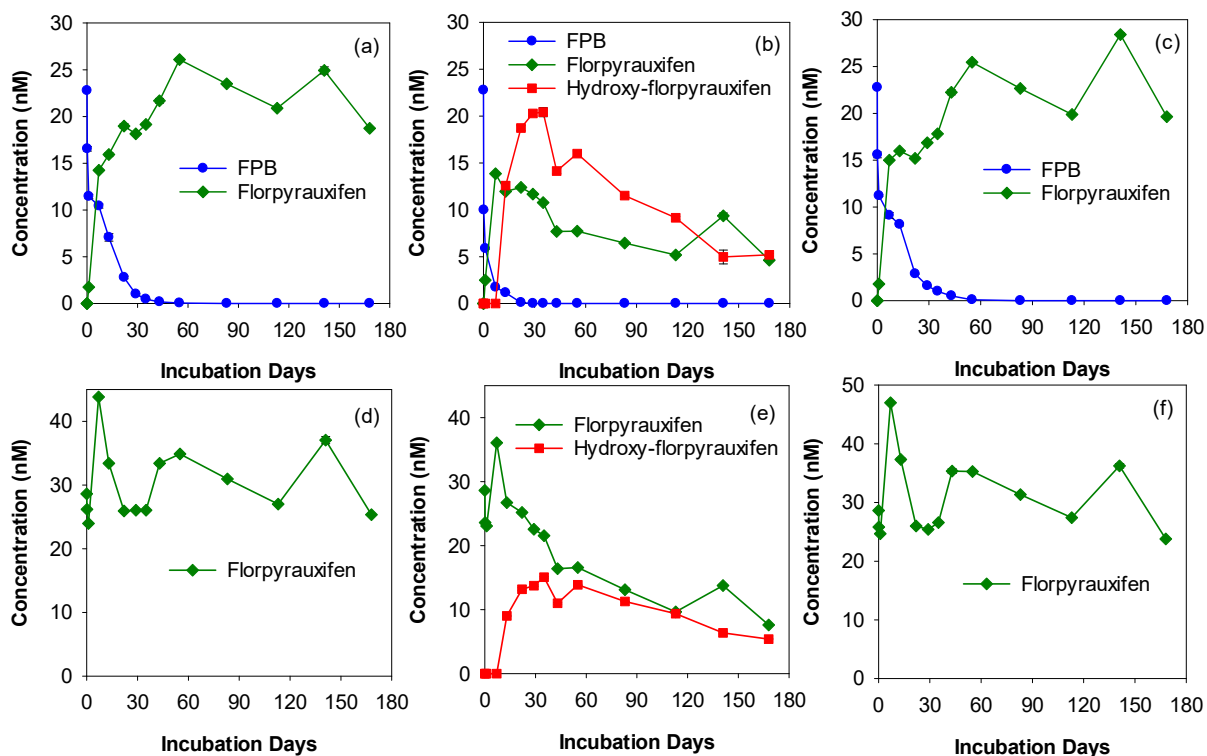


Figure A.6. Lilly Lake microcosms incubated with (a-c) FPB and (d-f) florpyrauxifen. Reactors contained (a, d) 0.2 μm filter sterilized water only (abiotic controls), (b, e) 0.2 μm filter sterilized water with sediment, and (c, f) unfiltered lake water only. Error bars represent the standard deviation of samples from triplicate microcosms. Error bars in each figure are smaller than the data point symbols.

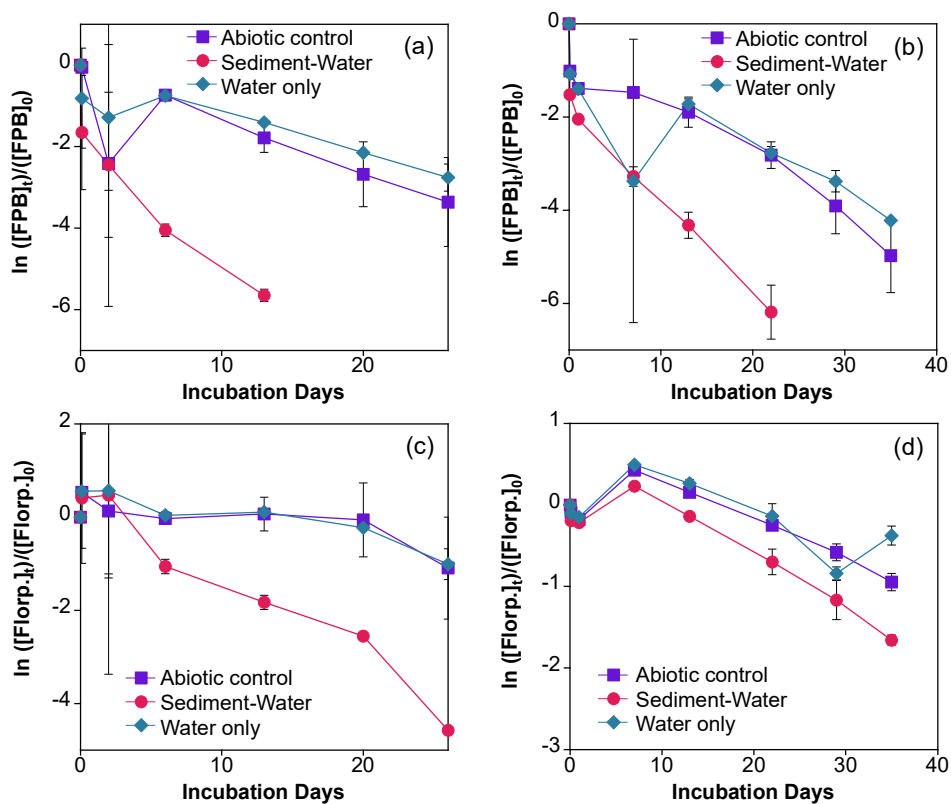


Figure A.7. Pseudo-first-order microcosm kinetics for FPB in (a) Kettle Moraine Lake and (b) Lilly Lake, as well as floryprauxifen incubations in (c) Kettle Moraine Lake and (d) Lilly Lake. “Abiotic control” is 0.2 μm filter sterilized water only, “sediment-water” is 0.2 μm filter sterilized water with sediment, and “water only” is unfiltered lake water. Error bars represent the standard deviation of triplicate reactors.

Section A.7. Photochemical irradiations and modeling

Irradiation experiments. Irradiation experiments were carried out using bulbs that emit light at 311 ± 22 nm (width at half-max) alongside a 2-nitrobenzaldehyde actinometer.⁷ Lake water used for indirect photodegradation analysis was diluted to 3 mg-C L^{-1} .

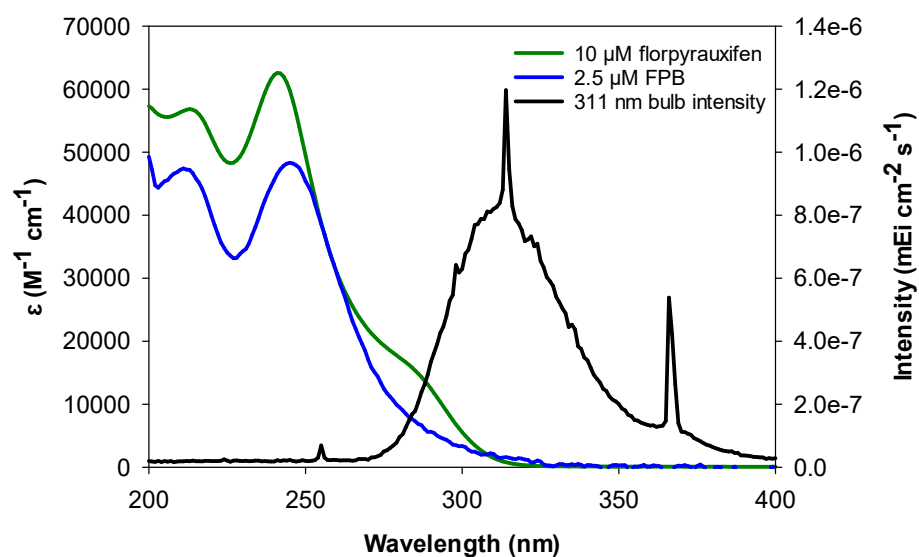


Figure A.8. Molar absorptivity (ϵ) of FPB and florpyrauxifen overlapping with 311 nm intensity of Rayonet bulbs used in photochemistry experiments.

Quantum yield calculations. Quantum yields were calculated for FPB and florpyrauxifen as described previously.^{4,8} Briefly, the observed photodegradation rate constants (k_{obs}) were corrected for light screening in all solutions using by calculating a screening factor at each wavelength (S_λ):

$$S_\lambda = \frac{1 - 10^{-\alpha_\lambda * l}}{2.303 * -\alpha_\lambda * l} \quad \text{Eq. A3}$$

where α_λ is the solution decadic absorbance measured using a UV-vis spectrophotometer and l is the pathlength of the cuvette (1 cm). An average weighted screening factor ($S_{weighted}$) was calculated from 250-455 nm and was used to correct the observed degradation rate constants for all lake waters and the direct control using the Equation A4:

$$k_{screened} = \frac{k_{obs}}{S_{weighted}} \quad \text{Eq. A4}$$

The light absorbance rate constant (k_{abs}) was calculated using Equation A5:

$$k_{abs} = \sum \frac{2.303 \times I_\lambda \times \alpha_\lambda \times S_\lambda}{[C] \times j} \quad \text{Eq. A5}$$

where I_λ is the intensity of light ($\text{mEi cm}^{-2} \text{s}^{-1}$), α_λ is the solution decadic absorbance, S_λ is the weighted screening factor, $[C]$ is FPB concentration (molar), and j is a conversion factor of 1 einstein-mol⁻¹.⁹

The quantum yield (Φ) was then calculated using Equation A6:^{4,8,10}

$$\Phi_{FPB} = \frac{k_{screened,direct,unk}}{k_{direct,act}} \times \frac{k_{abs,act}}{k_{abs,unk}} \times \Phi_{act} \quad \text{Eq. A6}$$

where $k_{screened,direct,unk}$ is the light screening corrected direct photodegradation rate constant for the direct control (s^{-1}), $k_{direct,act}$ is the photodegradation rate constant of the actinometer (s^{-1}), $k_{abs,act}$ (s^{-1}) is the rate of light absorbance of the actinometer, and $k_{abs,unk}$ (s^{-1}) is the rate of light absorption for the target compound. Φ_{act} is the quantum yield for 2-nitrobenzaldehyde (0.41).⁷

In-lake photodegradation modeling. The FPB calculated quantum yield was coupled with solar irradiance modeling using the Simple Model of Atmospheric Transfer of Sunshine (SMARTS)¹¹ to calculate FPB half-lives in the study lakes. A light absorbance rate constant,

$k_{abs,sun}$, was calculated for the horizontal global irradiance spectrum (**Figure A.9**) using Equation S5. ⁸ $k_{abs,sun}$ was then used to calculate direct photodegradation rates in lakes with site-specific solar intensity using Equation A7:

$$k_{photodegradatio} = k_{abs,sun} \times \Phi_{FPB} \quad \text{Eq. A7}$$

A depth integrated photodegradation rate was calculated by varying the pathlength (Eq. S3) to find a new $k_{photodegradation}$ at 1 cm intervals throughout a 1 m water column (i.e., 1 cm, 2 cm, ... 100 cm). The depth discrete rates were then averaged together to find a depth integrated photodegradation rate.

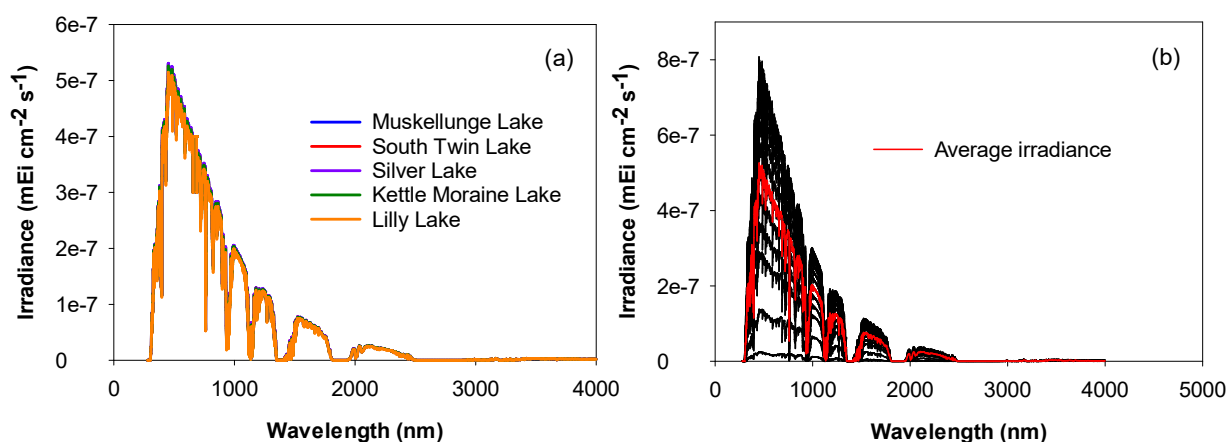


Figure A.9. (a) Irradiance data for the global horizontal irradiance spectra of each study lake generated using SMARTS. (b) Hourly irradiance at Kettle Moraine Lake during the day of treatment from 7 am to 7 pm.

Table A.7. SMARTS modeling input parameters for the in-lake photolysis degradation of FPB.

Card Number/ Description	Muskellunge	South Twin	Silver	Kettle Moraine	Lilly
1. Comment	'Muskellunge'	'South Twin'	'Silver'	'Kettle Moraine'	'Lilly'
1. Manually input pressure	1	1	1	1	1
2a. Pressure, surface altitude, and height	1013.25 0.495 0	1013.25 0.517 0	1013.25 0.476 0	1013.25 0.313 0	1013.25 0.228 0
3. Option to use default atmosphere	1	1	1	1	1
3a. Midlatitude Summer	'MLS'	'MLS'	'MLS'	'MLS'	'MLS'
4. Use default Water vapor	1	1	1	1	1
5. Use default ozone abundance	1	1	1	1	1
6. Use default gas abundance except CO ₂	1	1	1	1	1
7. Carbon dioxide from June 2021 and 2022	415.2	415.2	415.2	417.46	417.46
7a. Use default synthetic spectrum	0	0	0	0	0
8. Use continental aerosol model	'SRA_CONTL',	'SRA_CONTL',	'SRA_CONTL',	'SRA_CONTL',	'SRA_CONTL',
9. Use aerosol optical depth of 55 nm	5	5	5	5	5
9a.	0.084	0.084	0.084	0.084	0.084

10. Select “water” for albedo	2	2	2	2	2
10b. ITILT	1	1	1	1	1
ITILT is an option for tilted surface calculations. Leave box unchecked	51 37. 180.	51 37. 180.	51 37. 180.	51 37. 180.	51 37. 180.
11. Minimal spectral range, max spectral range, variability in irradiance, and default solar constant.	280 4000 1.0 1366.1	280 4000 1.0 1366.1	280 4000 1.0 1366.1	280 4000 1.0 1366.1	280 4000 1.0 1366.1
12. Option to generate results with spreadsheet	2	2	2	2	2
12a: Interval for printing results	280 4000 1	280 4000 1	280 4000 1	280 4000 1	280 4000 1
12b. Total number of outputs	5	5	5	5	5
12c. Outputs: (1) extraterrestrial spectrum, (2) direct normal irradiance, (3) diffuse horizontal irradiance, (4) global horizontal irradiance and (5) direct horizontal irradiance	1 2 3 4 5	1 2 3 4 5	1 2 3 4 5	1 2 3 4 5	1 2 3 4 5
13. Bypass circumsolar radiation	0	0	0	0	0

14. Bypass smoothing calculation	0	0	0	0	0
15. Illuminance using CIE photopic curve	1	1	1	1	1
16. No special UV calculations	0	0	0	0	0
17. Set inputs for card 17	3	3	3	3	3
17a. Year, month, day, hour, latitude, longitude, time zone.	2021 06 23 12.1 45.951384 -89.379651 -6	2021 06 09 12.1 46.031795 -89.171600 -6	2021 06 23 12.1 45.557370 -88.707779 -6	2022 06 03 12.1 43.653153 -88.209903 -6	2022 05 22 12.1 42.563358 -88.212591 -6

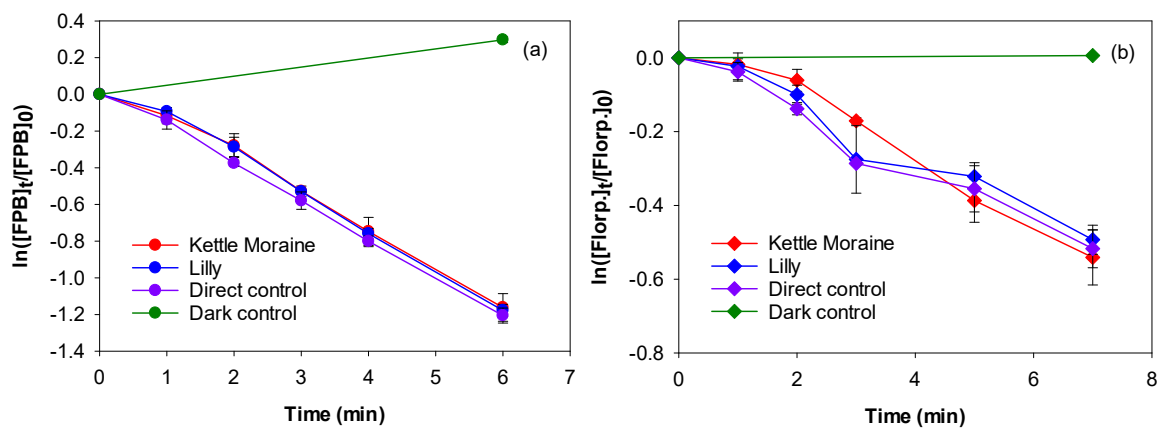


Figure A.10. First-order kinetics of photodegradation of (a) FPB and (b) florpyrauxifen at 311 nm in buffered ultrapure water (direct control) and filtered lake water (Kettle Moraine and Lilly) alongside dark controls. Error bars represent the standard deviation of triplicate reactors.

Section A.8. Sediment and plant extractions

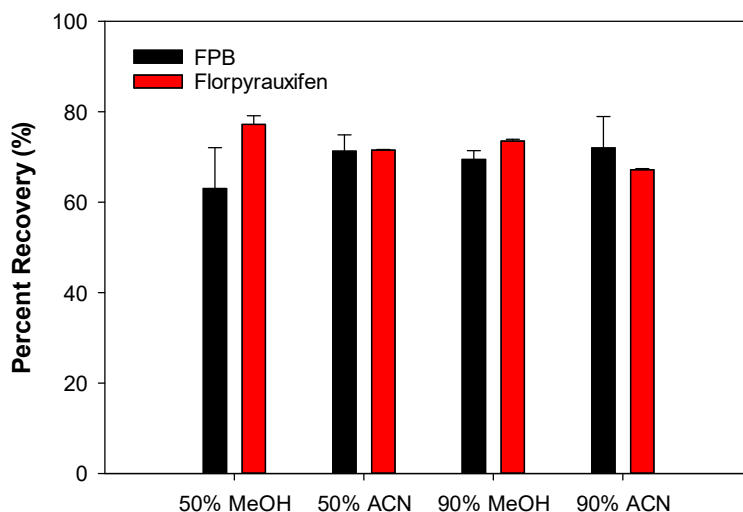


Figure A.11. Solution determination for sediment and plant extractions. All solution recoveries were comparable; therefore 90% ACN was chosen due to being a previously established method.^{3,12}

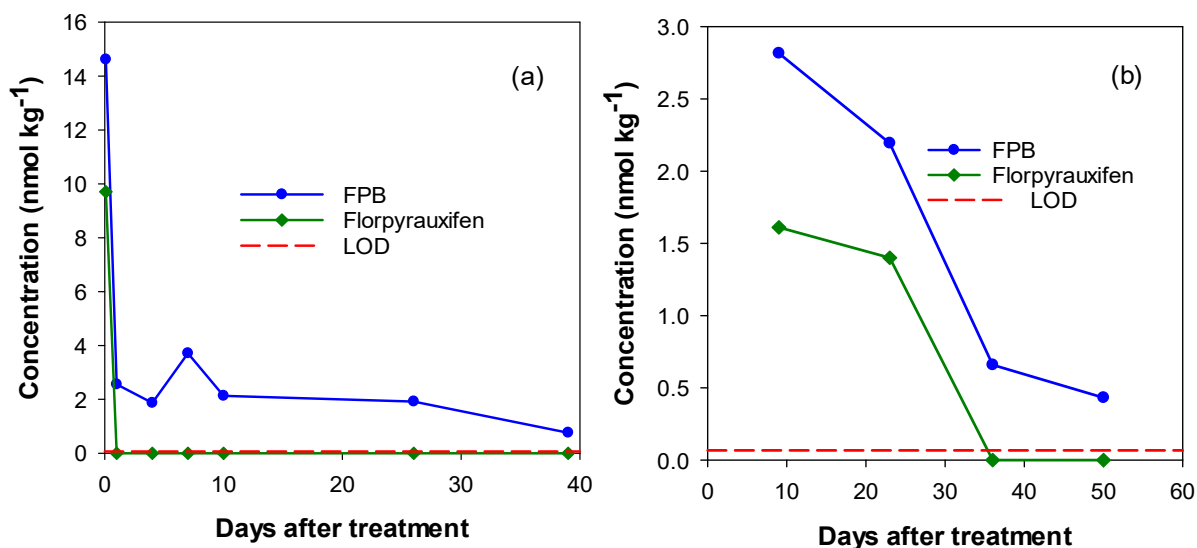


Figure A.12. FPB and florpyrauxifen concentrations in nearshore sediment from (a) Kettle Moraine Lake and (b) Lilly Lake. Concentration represents nmol per kg of dried sediment. ¹³C-FPB and ¹³C-florpyrauxifen concentrations were used to correct for extraction efficiency.

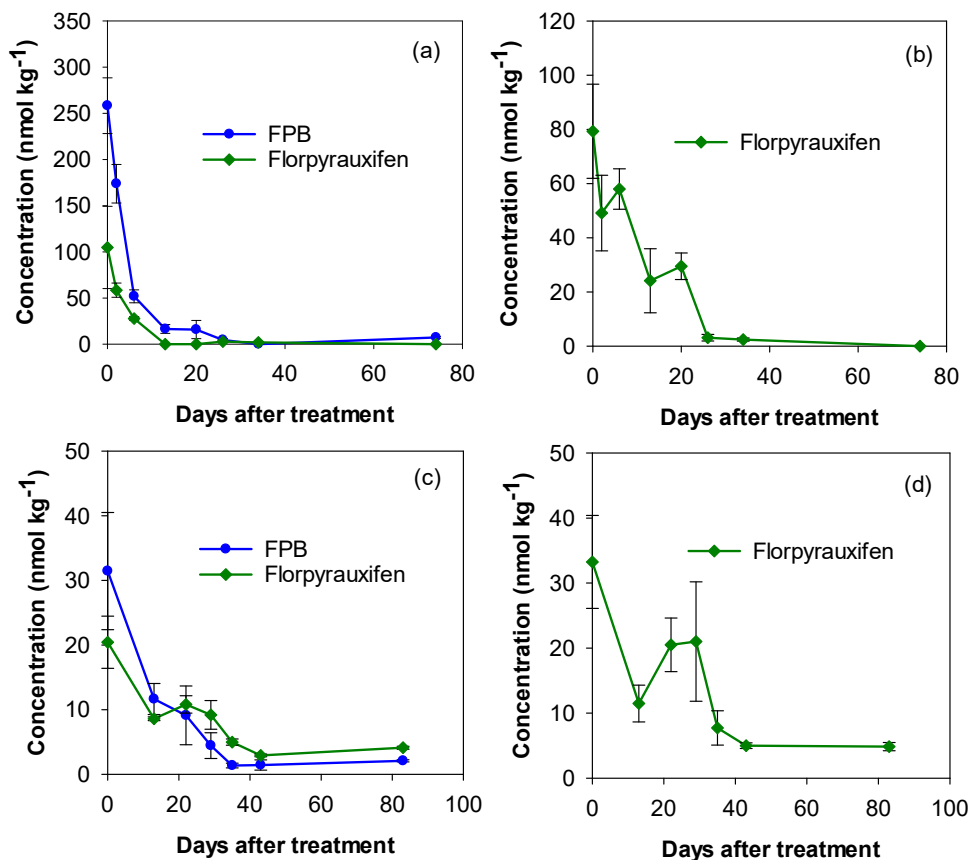


Figure A.13. Sediment extraction data from Kettle Moraine Lake microcosms incubated with (a) FPB and (b) florpyrauxifen and Lilly Lake microcosms incubated with (c) FPB and (d) florpyrauxifen. Concentration represents nmol per kg of dried sediment. ¹³C-FPB and ¹³C-florpyrauxifen concentrations were used to correct for extraction efficiency.

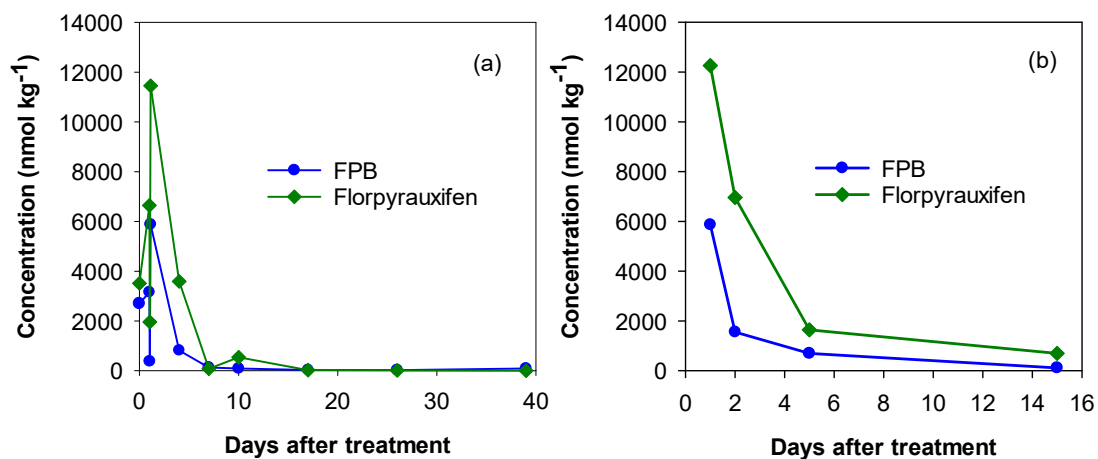


Figure A.14. Plant extraction data from (a) Kettle Moraine Lake and (b) Lilly Lake. Concentration represents nmol per kg of dried plant material. ¹³C-FPB and ¹³C-florpyrauxifen concentrations were used to correct for extraction efficiency.

Section A.9. Treatment data

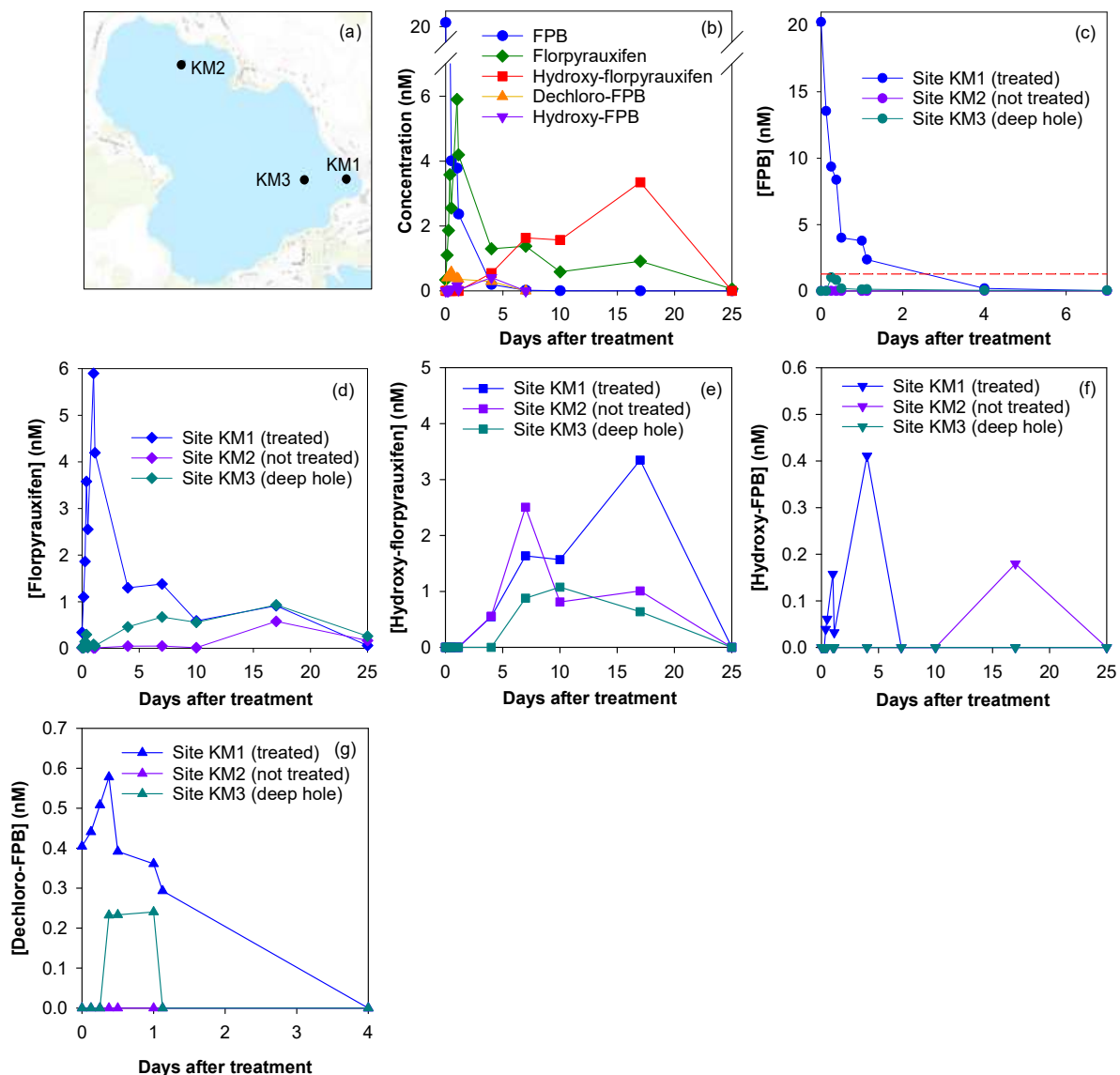


Figure A.15. (a) All sites on Kettle Moraine Lake. Concentrations of (b) FPB, florpyrauxifen, hydroxy-florpyrauxifen, hydroxy-FPB, and dechloro-FPB in site KM1. Concentrations of (c) FPB, (d) florpyrauxifen, (e) hydroxy-florpyrauxifen, (f) hydroxy-FPB, and (g) dechloro-FPB in all sites. Dashed line in panel (c) is the potential lake-wide FPB concentration of 1.28 nM.

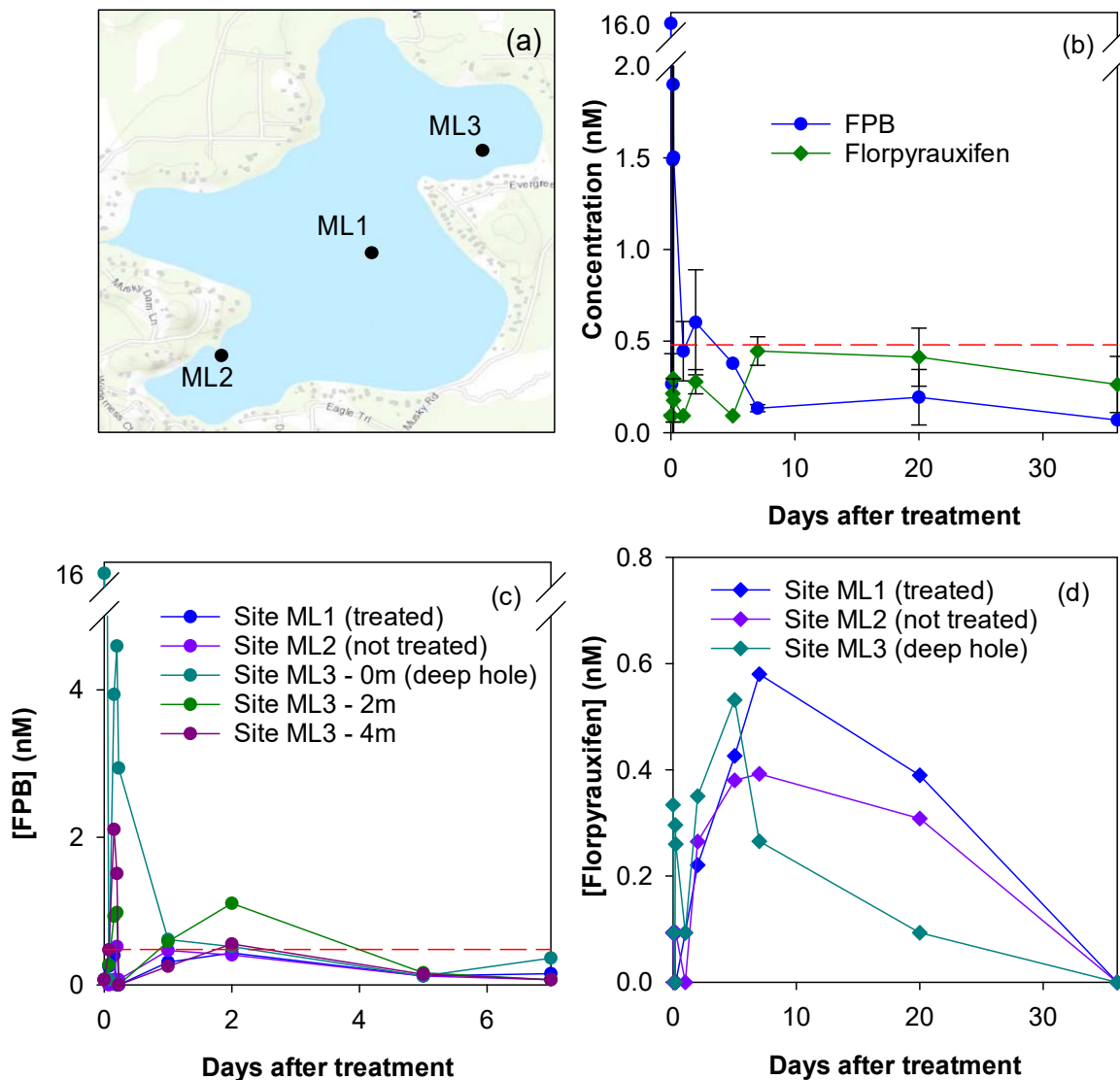


Figure A.16. (a) All sites on Muskellunge Lake. (b) Lake-wide average concentrations of FPB and florpyrauxifen. Concentrations of (c) FPB and (d) florpyrauxifen in all sites. Dashed line in panel (b) is potential lake-wide FPB concentration of 0.48 nM. Error bars in (b) represent standard deviation of three samples (one from each site) at each time point.

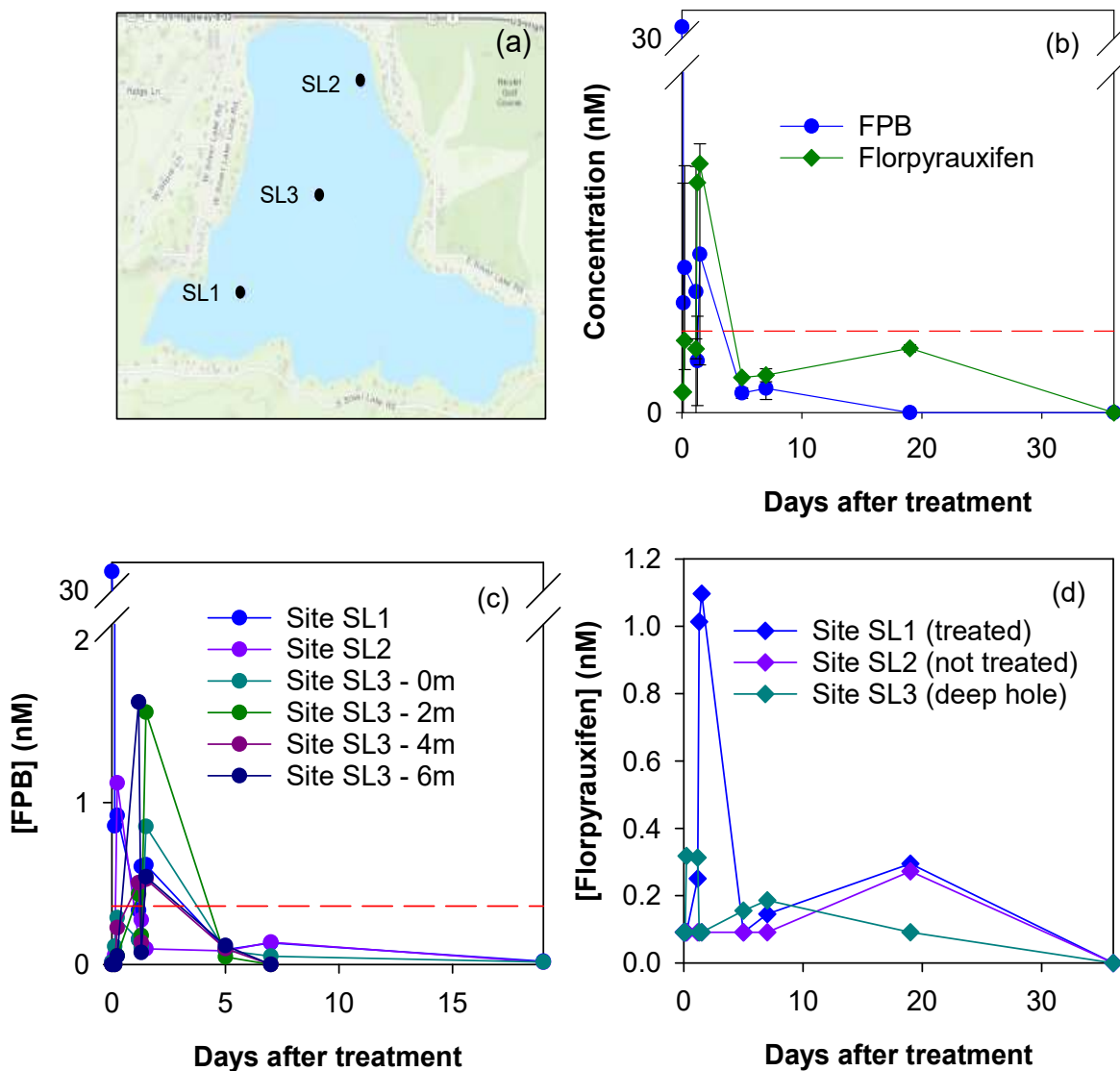


Figure A.17. (a) All sites on Silver Lake. (b) Lake-wide average concentrations of FPB and florpyrauxifen. Concentrations of (c) FPB and (d) florpyrauxifen in all sites. Dashed line panels (b) and (c) is potential lake wide concentration of 0.36 nM. Error bars in (b) represent standard deviation of three samples (one from each site) at each time point.

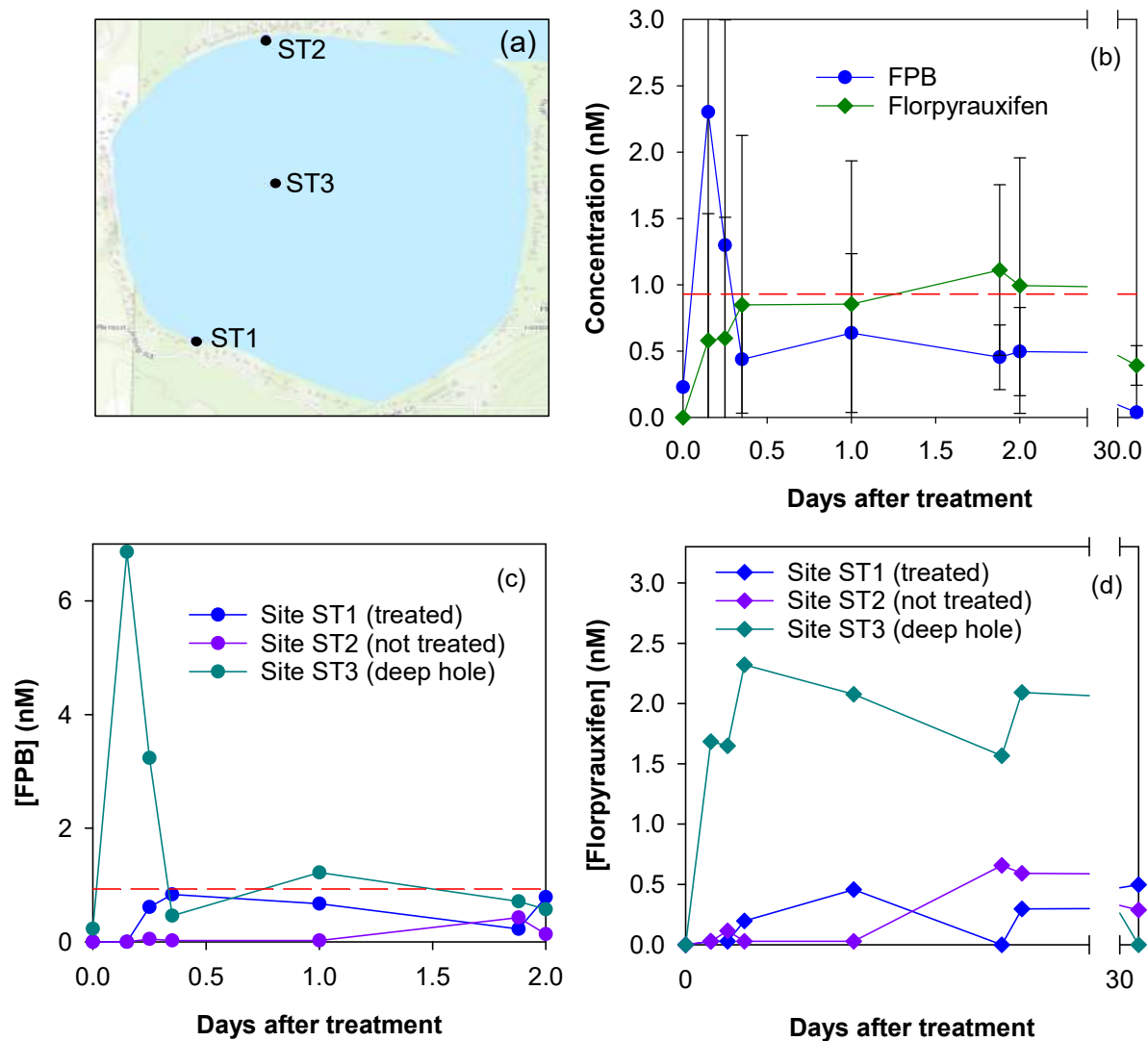


Figure A.18. (a) All sites on South Twin Lake. (b) Lake-wide average concentrations of FPB and florpyrauxifen. Concentrations of (c) FPB and (d) florpyrauxifen in all sites. Dashed line in panels (b) and (c) is potential lake wide concentration of 0.93 nM. Error bars in (b) represent standard deviation of three samples (one from each site) at each time point.

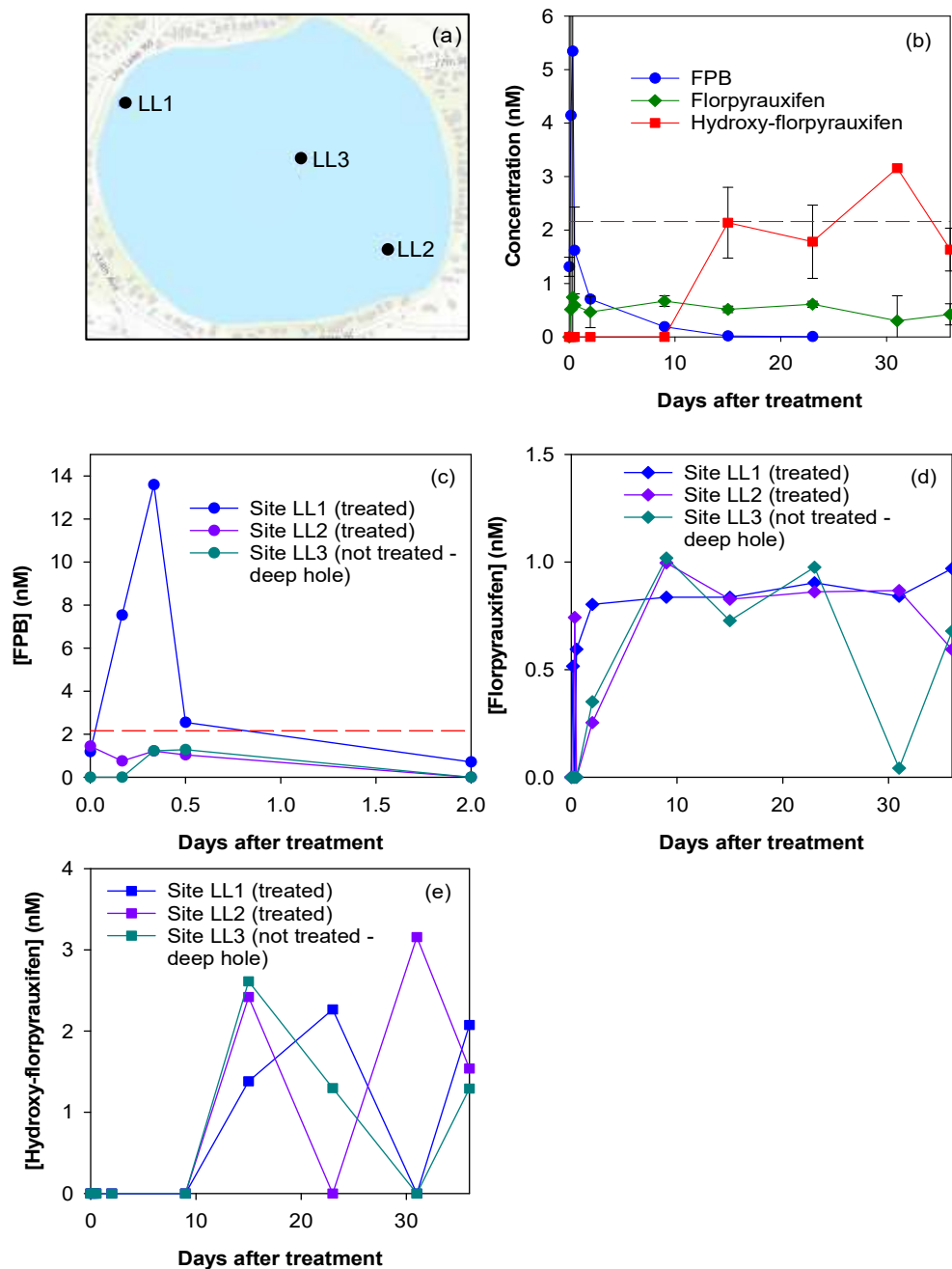


Figure A.19. (a) All sites on Lilly Lake. (b) Lake-wide average concentrations of FPB, florpyrauxifen, and hydroxy-florpyrauxifen. Concentrations of (c) FPB, (d) florpyrauxifen, and (e) hydroxy-florpyrauxifen in all sites. Dashed line in panels (b) and (c) is potential lake wide concentration of 2.16 nM. Error bars in (b) represent standard deviation of three samples (one from each site) at each time point.

Section A.10. Material balance calculations

FPB recovery in lakes. Calculations were carried out to calculate the recovery of FPB and its primary degradation product florpyrauxifen in all the lake treatments (i.e., to assess whether florpyrauxifen accounted for all observed loss of FPB; **Table A.8**). An estimate of time of lake mixing, specifically when lake-wide concentrations began to stabilize, was made within the first 12-48 hours based on FPB concentrations at all three sampling sites in a lake (**Figures A.15-A.19**). Percent recovery was calculated using Equation A8:

$$\% \text{FPB}_{\text{lake}} \text{ recovery} = \frac{[\text{FPB}]_{\text{mixed}} + [\text{florpyrauxifen}]_{\text{mixed}}}{\text{Expected lake wide } [\text{FPB}]}$$
 Eq. A8

where $[\text{FPB}]_{\text{mixed}}$ is the average of $[\text{FPB}]$ at all sampling stations and $[\text{florpyrauxifen}]_{\text{mixed}}$ is the average $[\text{florpyrauxifen}]$ at all three sites found in the lake at the time of mixing. The expected lake wide $[\text{FPB}]$ is found on the herbicide treatment plan or calculated using lake volume¹³ and mass of FPB applied from treatment record.

Table A.8. Half-lives of FPB in field study and laboratory experiments.

Lake	In-lake recovery of FPB	Lake half-life (days)	Photodeg. half-life in top 1 cm (days)	Microcosm half-life (days)			Hydrolysis half-life (days)
				Abiotic	Water only	Water-Sediment	
South Twin Lake	160%	1	0.16	-	-	-	5.5
Muskellunge Lake	112%	2	0.15	-	-	-	14
Silver Lake	126%	3	0.16	-	-	-	18
Lilly Lake	103%	0.2	0.16	6.6	7.3	2.5	6.6
Kettle Moraine Lake	103%	1	0.16	6.5	8.5	1.8	6.1

Material balance using product yields from field data. To calculate a percent contribution for each transformation pathway using the field data, the concentration of products associated with a specific pathway were divided by the sum of all products measured in the lake at the time of mixing (24 hours after treatment) assuming a 1:1 molar ratio of FPB loss to product formation as described by Equation A9.

$$\% \text{ contribution of } X \text{ pathway} = \frac{[\text{products of } X \text{ pathway}]_{24 \text{ hr}}}{[\text{sum of all products}]_{24 \text{ hr}}} \quad \text{Eq. A9}$$

We assumed that dechloro-FPB was produced through photodegradation, hydroxy-florpyrauxifen and hydroxy-FPB were produced through biodegradation, and florpyrauxifen was produced through hydrolysis based on laboratory experiments.

To calculate the percent contribution of sorption, the concentration of FPB estimated to be remaining in the sediment at equilibrium (C_s), which was calculated through Equation A10, was divided by the initial FPB concentration detected in the lake.

$$C_s = \frac{[FPB] * K_d * m}{V} \quad \text{Eq. A10}$$

The value of K_d was obtained from the sorption experiment with Kettle Moraine Lake sediment (**Table A.6**). The volume of the lake was estimated by multiplying the area of the lake by the mean depth.¹³ The mass of sediment was estimated by assuming FPB interacts with the top 2.5-cm layer of sediment with the same surface area as the lake and the sediment bulk density is 1.2 g/cm³.¹⁴

Material balance based on measured kinetics under laboratory conditions. A second material balance was conducted for Kettle Moraine Lake using first-order rate loss calculations from hydrolysis, photodegradation, and biodegradation in the following equation:

$$C_t = C_0 \times e^{-(k_{hydrolysis} + k_{biodegradation} + k_{photodegradation}) t} \quad \text{Eq. A11}$$

where C_t is [FPB] at time t , C_0 is initial [FPB] measured, $k_{hydrolysis}$ is the hydrolysis rate calculated from hydrolysis experiments at pH 8, $k_{photodegradation}$ is the modeled direct photodegradation rate in sunlight averaged over the top 1 m of the lake, and $k_{biodegradation}$ is the biodegradation rate calculated using microcosm incubations.

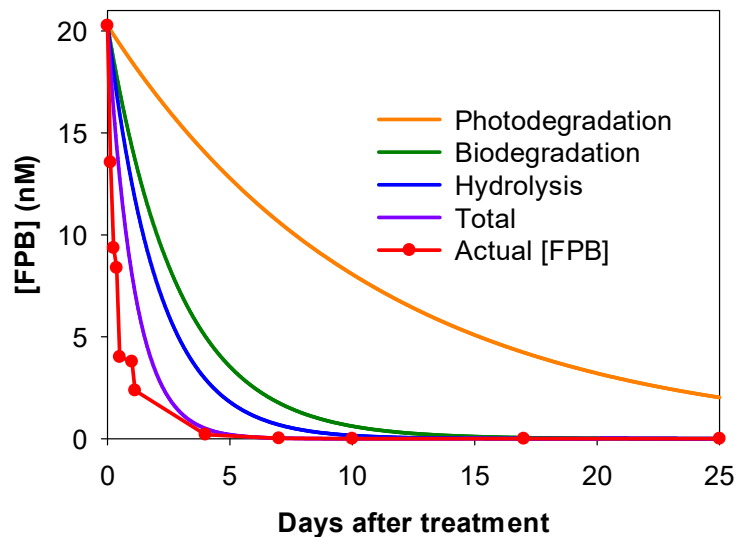


Figure A.20. Modeling results of first-order kinetics compared with measured epilimnion concentrations of FPB in Kettle Moraine Lake.

To calculate the percent contribution of each transformation pathway, each rate constant was divided by the pseudo-first-order rate constant for FPB loss observed in the field. The actual rate of FPB loss observed in Kettle Moraine, however, was still faster than the total material balance rate calculated. This could be due to sediment sorption, which could not be included in the first-order rate model, physical transport, or other processes. Specifically, a process called “phloem-trapping”, which is the uptake of FPB by targeted plants and release of florpyrauxifen, could have contributed to the loss in the water column.^{15,16}

References

1. Arena, M.; Auteri, D.; Barmaz, S.; Brancato, A.; Brocca, D.; Bura, L.; Carrasco Cabrera, L.; Chaideftou, E.; Chiusolo, A.; Civitella, C.; Court Marques, D.; Crivellente, F.; Ctverackova, L.; de Lentdecker, C.; Egsmose, M.; Erdos, Z.; Fait, G.; Ferreira, L.; Goumenou, M.; Greco, L.; Ippolito, A.; Istace, F.; Jarrah, S.; Kardassi, D.; Leuschner, R.; Lostia, A.; Lythgo, C.; Magrans, J. O.; Medina, P.; Mineo, D.; Miron, I.; Molnar, T.; Padovani, L.; Parra Morte, J. M.; Pedersen, R.; Reich, H.; Sacchi, A.; Santos, M.;

- Serafimova, R.; Sharp, R.; Stanek, A.; Streissl, F.; Sturma, J.; Szentes, C.; Tarazona, J.; Terron, A.; Theobald, A.; Vagenende, B.; van Dijk, J.; Villamar-Bouza, L. Peer review of the pesticide risk assessment of the active substance florpyrauxifen (variant assessed florpyrauxifen-benzyl). *EFSA J.* **2018**, *16* (8), 5378.
2. U.S. EPA. Independent Laboratory Validation of a Dow AgroSciences Method for the Determination of XDE-848 Benzyl Ester and Five Metabolites (X11438848, X12300837, X11966341, X12131932 and X12393505) in Water https://www.epa.gov/sites/production/files/2017-09/documents/ilv_-_florpyrauxifen-benzyl_degradates_in_water_-_mrid_49677802.pdf (accessed April 2023).
 3. U.S. EPA. Independent Laboratory Validation of a Dow AgroSciences Method for the Determination of XDE-848 Benzyl Ester and Three Metabolites (X11438848, X12300837 and X11966341) in Soil https://www.epa.gov/sites/default/files/2017-09/documents/ilv_-_florpyrauxifen-benzyl_degradates_in_soil_-_mrid_49677776.pdf (accessed April 2023)
 4. McConville, M. B.; Hubert, T. D.; Remucal, C. K. Direct photolysis rates and transformation pathways of the lampricides TFM and niclosamide in simulated sunlight. *Environ. Sci. Technol.* **2016**, *50* (18), 9998–10006.
 5. Schwarzenbach, R. P.; Gschwend, P. M.; Imboden, D. M. *Environmental Organic Chemistry, 3rd edition*, Wiley-Interscience, New Jersey, 2017.
 6. USDA. Kellogg Soil Survey Laboratory Methods Manual <https://www.nrcs.usda.gov/sites/default/files/2023-01/SSIR42.pdf> (accessed April 2023).
 7. Galbavy, E. S.; Ram, K.; Anastasio, C. 2-Nitrobenzaldehyde as a chemical actinometer for solution and ice photochemistry. *J. Photochem. Photobiol., A* **2010**, *209* (2–3), 186–192.
 8. White, A. M.; Nault, M. E.; McMahon, K. D.; Remucal, C. K. Synthesizing laboratory and field experiments to quantify dominant transformation mechanisms of 2,4-dichlorophenoxyacetic acid (2,4-D) in aquatic environments. *Environ. Sci. Technol.* **2022**, *56* (15), 10838–10848.
 9. Leifer, A. *The Kinetics of Environmental Aquatic Photochemistry: Theory and Practice*, American Chemical Society, Washington, DC, 1988.
 10. Remucal, C. K.; McNeill, K. Photosensitized amino acid degradation in the presence of riboflavin and its derivatives. *Environ. Sci. Technol.* **2011**, *45* (12), 5230–5237.
 11. Gueymard, C. A. Interdisciplinary applications of a versatile spectral solar irradiance model: A review. *Energy* **2005**, *30* (9), 1551–1576.
 12. Miller, M. R.; Norsworthy, J. K. Influence of soil moisture on absorption, translocation, and metabolism of Florpyrauxifen-Benzyl. *Weed Sci.* **2018**, *66* (4), 418–423.
 13. Wisconsin DNR. Wisconsin Lake Finder <https://dnr.wi.gov/lakes/findalake/> (accessed April 2023)

14. Schueler, T. The Compaction of Urban Soils. *Watershed Protect. Techniq.* **2000**, *3* (2), 661–665.
15. Epp, J. B.; Alexander, A. L.; Balko, T. W.; Buysse, A. M.; Brewster, W. K.; Bryan, K.; Daeuble, J. F.; Fields, S. C.; Gast, R. E.; Green, R. A.; Irvine, N. M.; Lo, W. C.; Lowe, C. T.; Renga, J. M.; Richburg, J. S.; Ruiz, J. M.; Satchivi, N. M.; Schmitzer, P. R.; Siddall, T. L.; Webster, J. D.; Weimer, M. R.; Whiteker, G. T.; Yerkes, C. N. The discovery of arylexTM active and rinskorTM active: two novel auxin herbicides. *Bioorg. Med. Chem.* **2016**, *24* (3), 362–371.
16. Deboer, G. J.; Satchivi, N. Comparison of translocation properties of insecticides versus herbicides that leads to efficacious control of pests as specifically illustrated by IsoclastTM active, a new insecticide, and ArylexTM active, a new herbicide. *ACS Symp. Ser.* **2014**, *4*, 75-93.

Appendix B. Supplementary Material for Chapter 3

Section B.1. Summary of previous fluridone studies

Table B.1. Summary of literature reports of field, photodegradation, biodegradation, and sorption studies of fluridone.

Half-life	Study type	Ref. #
Field Studies		
2-11 days	Three ponds and one lake in MI, NY, FL, & Panama Canal	1
4 – 7 days	Small ponds in Manitoba, Canada	2
5-60 days	Ponds in TX, WV, MO, CA, IN, and FL	3
30-50 days	Small- medium ponds in Greenfield, Indiana	4
17 weeks	Small artificial ponds in Manitoba, Canada	5
8 months	Lake, Silver Lake, Wisconsin	6
Photodegradation Studies		
15-36 hours	Ultrapure water, natural light, filtered > 297 nm	7
23 hours	Ultrapure water, simulated sunlight 280-365 nm	1
28-55 hours	Ultrapure water, simulated sunlight 280-365 nm	8
35 hours	Ultrapure water, natural sunlight, 325-355 nm	7
8.8 days	Ultrapure water, simulated sunlight, 310-380 nm	7
7 days	Well water, natural sunlight	9
12 days	Ultrapure & lake water, natural sunlight	8
33 days	Well water, natural sunlight, 290 - 320 nm light filtered out	9
Biodegradation Studies		
50 days	Microcosms with silty and sandy soil, saturated with tap water	10
>150 days	Microcosm with lake sediment	11
>150 days	Cultures enriched from lake sediments	11
12 months	Culture flasks with three sediment types	5
Sorption Studies		
10% sorbed in 30 days	Silty and sandy soil, saturated with tap water	10
16-27% sorbed in 28 days	Pond application in New York and Florida	1
14-52% sorbed in over 150 days	Pond sediments in Manitoba, Canada	5
K_{oc} : 883- 2462 L kg ⁻¹	Pond sediments in Manitoba, Canada	2

Section B.2. Field sampling methods

Lake water was collected from six lakes for bulk water chemistry measurements and photochemical irradiations. Surface water was collected from the epilimnion and nearshore area in 4 L combusted glass amber bottles, filtered through a 0.45 μm nylon filter, and preserved at 4°C until analysis.

Table B.2. Location, pH, dissolved organic carbon, E₂:E₃ (absorbance at 250 nm divided by absorbance at 365 nm),¹² and SUVA₂₅₄ (specific UV absorbance at 254 nm)¹³ for all lakes visited during field sampling.

Lake	Coordinates	pH	DOC (mg/L)	SUVA ₂₅₄	E ₂ :E ₃
Silver	45.92°N, 89.24°W	7.95	6.54	1.55	7.17
Pike	43.31°N, 88.33°W	8.21	7.18	1.83	9.24
Tomahawk	46.37°N, 91.52°W	8.02	4.52	1.06	10.06
Pleasant	42.79°N, 88.55°W	8.04	6.16	0.86	9.61
Hooker	44.56°N, 88.10°W	8.01	7.60	2.21	8.35

Pretreatment water used for microcosm incubations was collected with 10 L HDPE cubitainers and stored in the dark on ice until microcosm set up. Sediment for microcosm incubations and sorption experiments was collected by Eckman dredge or hand-coring at a nearshore site of each and stored in the dark on ice until microcosms set up which occurred within 24 hours.

Water samples collected during the fluridone treatment of Hooker Lake were stored on ice and in the dark until processing which occurred no longer than 24 hours after collection. Processing involved filtration through a 0.45 μm nylon filter and preserved at 4°C until analysis. Water samples were collected at three sites on Hooker Lake, with two being opposite nearshore sites and one location being in the center to characterize behavior throughout the lake. Samples were collected every 1-2 weeks until 60 days post-treatment.

Section B.3. Photochemical irradiations

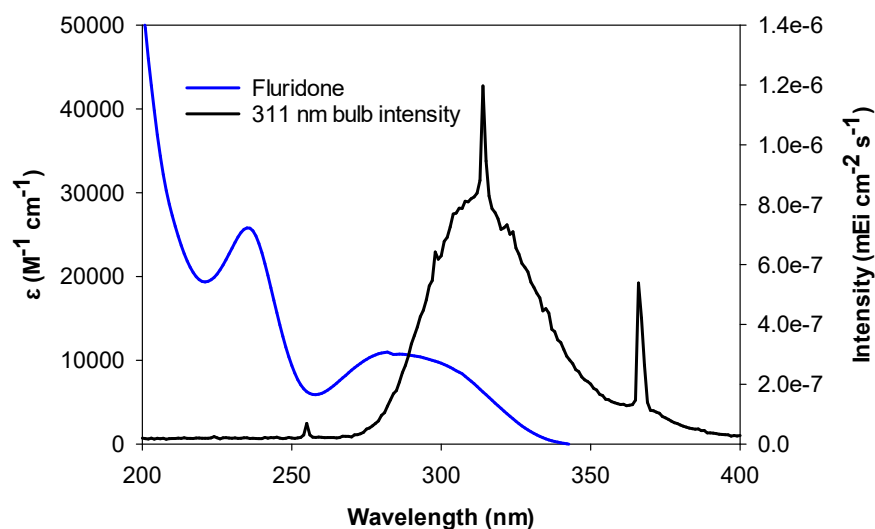


Figure B.1. Molar absorptivity (ϵ) fluridone and the irradiance of the 311 nm bulbs used in photochemistry experiments (second y-axis).

The observed photodegradation rate constants (k_{obs}) were corrected for light screening in all solutions using by calculating a screening factor at each wavelength (S_{λ}):

$$S_{\lambda} = \frac{1 - 10^{-\alpha_{\lambda} * l}}{2.303 * -\alpha_{\lambda} * l} \quad \text{Eq. B3}$$

where α_{λ} is the solution decadic absorbance measured using a UV-vis spectrophotometer and l is the pathlength of the cuvette (1 cm). An average weighted screening factor ($S_{weighted}$) was calculated from 250-455 nm and was used to correct the observed degradation rate constants for all lake waters and the direct control using the Equation B4:

$$k_{screened} = \frac{k_{obs}}{S_{weighted}} \quad \text{Eq. B4}$$

The light absorbance rate constant (k_{abs}) was calculated using Equation B5:

$$k_{abs} = \sum \frac{2.303 \times I_{\lambda} \times \alpha_{\lambda} \times S_{\lambda}}{[C] \times j} \quad \text{Eq. B5}$$

where I_{λ} is the intensity of light ($\text{mEi cm}^{-2} \text{s}^{-1}$), α_{λ} is the solution decadic absorbance, S_{λ} is the weighted screening factor, $[C]$ is fluridone concentration (molar), and j is a conversion factor of 1 einstein-mol⁻¹.¹⁴

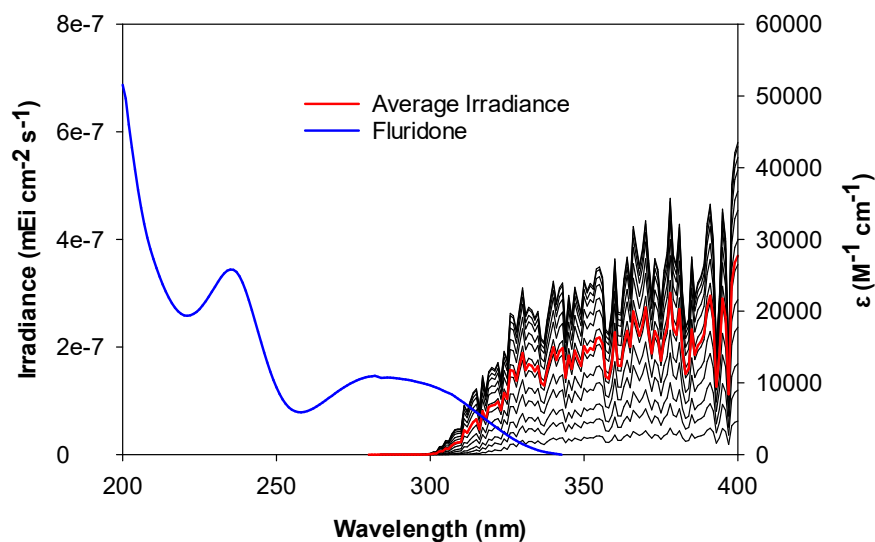


Figure B.2. Average of the hourly irradiance at Hooker Lake during the day of treatment from 6 am to 6 pm. Global horizontal irradiance spectra at each time was generated using SMARTS.¹⁵

Table B.3. SMARTS modeling input parameters for the in-lake photolysis degradation of fluridone in Hooker Lake on the day of treatment.

Card Number/ Description	Hooker Lake Parameters
1. Comment	'Hooker'
1. Manually input pressure	1
2a. Pressure, surface altitude, and height	1013.25 0.229 0
3. Option to use default atmosphere	1
3a. Midlatitude Summer	'MLS'
4. Use default Water vapor	1
5. Use default ozone abundance	1
6. Use default gas abundance except CO ₂	1
7. Carbon dioxide from June 2021 and 2022	417.46
7a. Use default synthetic spectrum	0
8. Use continental aerosol model	'SRA_CONTL'
9. Use aerosol optical depth of 55 nm	5
9a.	0.084
10. Select "water" for albedo	2
10b. ITILT	1
ITILT is an option for tilted surface calculations. Leave box unchecked	51 37. 180.
11. Minimal spectral range, max spectral range, variability in irradiance, and default solar constant.	280 4000 1.0 1366.1
12. Option to generate results with spreadsheet	2
12a: Interval for printing results	280 4000 1
12b. Total number of outputs	5
12c. Outputs: (1) extraterrestrial spectrum, (2) direct normal irradiance, (3) diffuse horizontal irradiance, (4) global horizontal irradiance and (5) direct horizontal irradiance	1 2 3 4 5
13. Bypass circumsolar radiation	0
14. Bypass smoothing calculation	0
15. Illuminance using CIE photopic curve	1
16. No special UV calculations	0
17. Set inputs for card 17	3
17a. Year, month, day hour, latitude, longitude, time zone.	2022 05 12 12.1 42.558952 -88.100541 -6

Section B.4. Sorption experiments

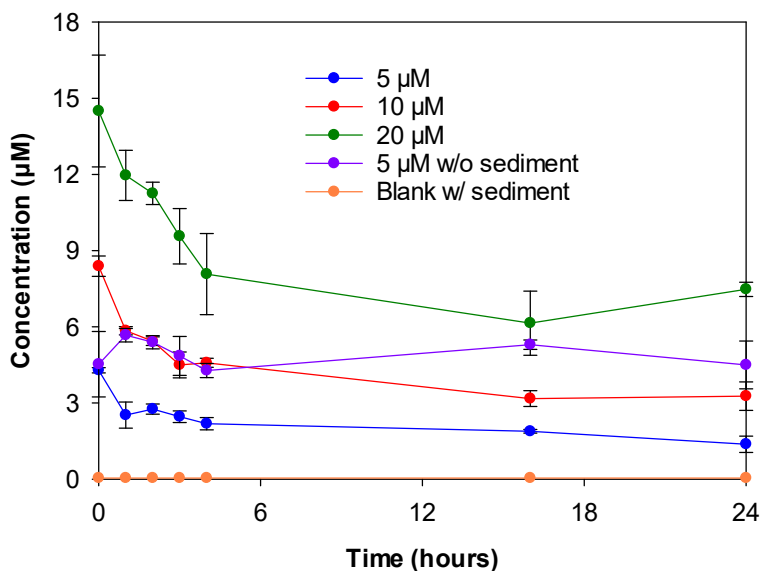


Figure B.3. Sorption kinetics of fluridone interaction with lake sediment along with controls of fluridone without sediment and the lake sediment with no fluridone. Fluridone with sediment shows equilibrium is reached by 6 hours of sediment interaction. Fluridone control without sediment shows little to no loss occurs through volatilization, photodegradation, or sorption to the glass bottles. The sediment control shows no signs of preexisting fluridone that would skew the measured concentrations. Error bars represent the standard deviation of triplicate reactors.

Section B.5. Microcosm incubations

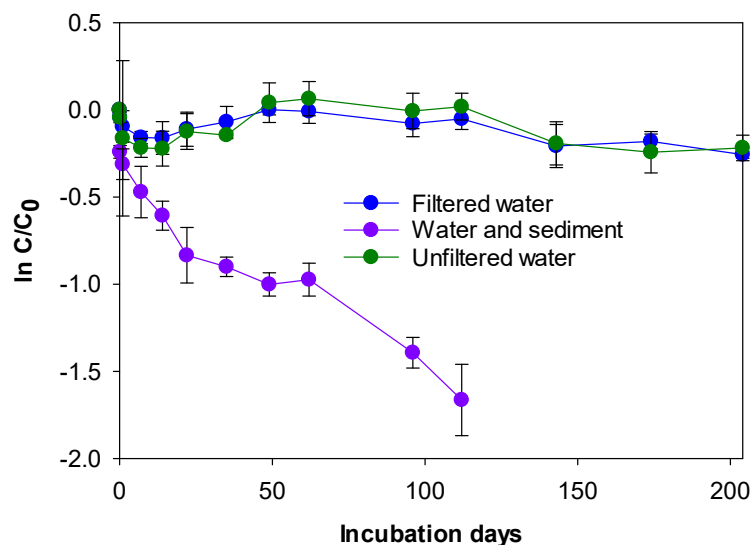


Figure B.4. Pseudo-first-order microcosm kinetics for fluridone. Error bars represent the standard deviation of triplicate reactors.

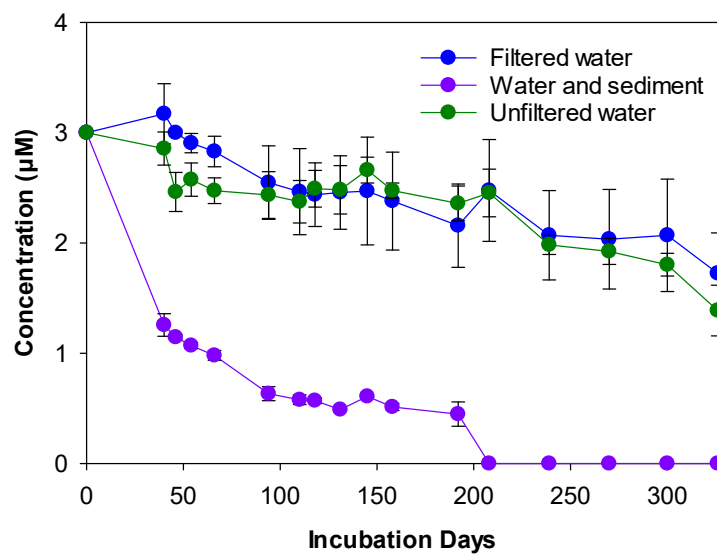


Figure B.5. [Fluridone] in original microcosms incubated with relevant environmental inocula from Hooker Lake at 3 μM .

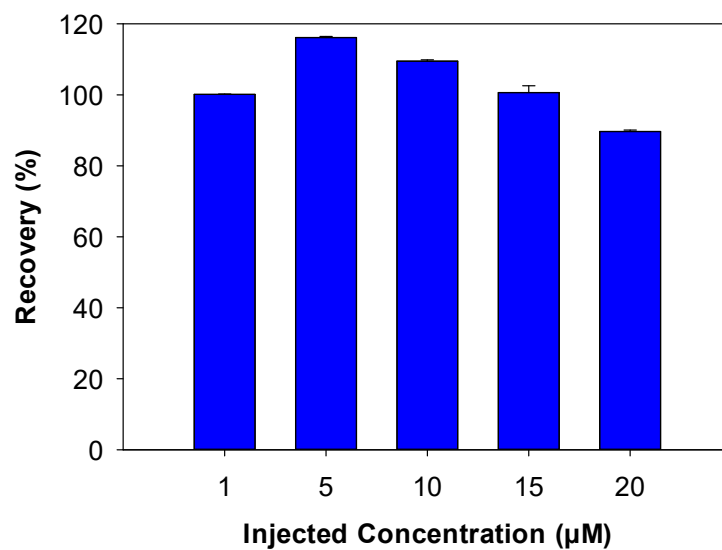
Section B.6. Sediment extractions

Figure B.6. Percent recovery of fluridone from sediment samples using a 50:50 methanol:water extraction solution. Error bars represent the standard deviation of triplicate reactors.

Section B.7. Analytical methods

Fluridone from laboratory experiments, 3-trifluoromethyl benzoic acid, and 2-nitrobenzaldehyde were analyzed via high performance liquid chromatography (HPLC). All methods used an Agilent Technologies 1260 Infinity instrument equipped with a diode array detector, an Agilent InfinityLab C-18 Poroshell 120 column, and an aqueous buffer composed of 10% acetonitrile and 0.1% formic acid in ultrapure water for the aqueous phase (A) and 100% acetonitrile for the mobile phase (B). Fluridone and 3-trifluoromethyl benzoic acid were analyzed using a gradient method (**Table B.4**)³¹ and 2-nitrobenzaldehyde was analyzed using an isocratic method (**Table B.5**). Fluridone analyzed through HPLC had a limit of detection (LOD) of 0.6 μM .

Table B.4. Time segments for gradient method used to analyze fluridone and 3-trifluoromethyl benzoic acid on HPLC.

Time (minutes)	A%	B%
0	60	40
0.8	0	100
1.25	0	100
1.30	60	40
3.5	60	40

Table B.5. Instrument parameters for detection of fluridone, 3-trifluoromethyl benzoic acid, and 2-nitrobenzaldehyde in water.

Compound	% Aqueous Buffer	Flow (mL min ⁻¹)	Detection wavelength (nm)	Retention Time (min)	Purpose	LOD (μM)
2-nitrobenzaldehyde	80	0.5	231	2.9	311 nm actinometer	0.5
fluridone	See Table B.4	0.8	313	1.8	herbicide	0.6
3-trifluoromethyl benzoic acid	See Table B.4	0.8	222	1.1	degradation product	0.01

Fluridone in the field samples was quantified using an Agilent Triple Quad 6460 liquid chromatograph-tandem mass spectrometer (LC-MS/MS) using positive mode electrospray ionization which had an LOD of 2.6 nM. Samples were analyzed using a gradient method (**Table B.6**) of aqueous buffer (A: 10% acetonitrile and 0.1% formic acid in ultra-pure water) and organic phase of 100% acetonitrile (B) at 0.4 mL min⁻¹ on an Agilent InfinityLab C-18 Poroshell 120 column with a column temperature control of 40°C.

LC-MS/MS running conditions and method details for fluridone:

Mode: Positive electrospray ionization	Retention time: 2.8 min
Scan type: MRM	Precursor <i>m/z</i> : 330
Gas temp: 300°C	Product <i>m/z</i> : 309, 259
Nebulizer pressure: 45 psi	Fragmentor voltage: 312
Sheath gas temperature: 250°C	Collision energy: 41, 56
Sheath gas flow rate: 11 L/min	Cell accelerator voltage: 4
Capillary voltage: 3500 V	LOD: 2.6 nM
Dwell: 80 msec	

Table B.6. Time segments for gradient method used to analyze fluridone on LC-MS/MS.

Time (minutes)	A%	B%
0	40	60
0.75	40	60
0.80	0	100
1.15	0	100
1.25	40	60
3.00	40	60

Dissolved organic carbon (DOC) was measured using a GE Sievers M5310 TOC analyzer. Calibration check solutions were made from analytical grade potassium hydrogen phthalate ranging from 0 - 10 mg-C L⁻¹. Ultraviolet-visible light spectra for each lake were collected using a Shimadzu 2401PC recording spectrophotometer in 1 nm increments from 200-800 nm.

References

1. West, S. D.; Day, E. W.; Burger, R. O. Dissipation of the experimental aquatic herbicide fluridone from lakes and ponds. *J. Agric. Food Chem.* **1979**, *27* (5), 1067-1072.
2. Muir, D.; Grift, N. P.; Blouw, A. P.; Lockhart, W. L. Persistence of fluridone in small ponds. *J. Environ. Qual.* **1980**, *9* (1), 151-156.
3. West, S. D.; Burger, R. O.; Poole, G. M.; Mowrey, D. H. Bioconcentration and field dissipation of the aquatic herbicide fluridone and its degradation products in aquatic environments. *J. Agric. Food Chem.* **1983**, *31* (3), 579-585.
4. Arnold, W. R. Fluridone: A new aquatic herbicide. *J. Aquat. Plant Manage.* **1979**, *17*, 30-33.
5. Muir, D. C. G.; Grift, N. P. Fate of fluridone in sediment and water in laboratory and field experiments. *J. Agric. Food Chem.* **1982**, *30* (2), 238-244.
6. Onterra. Silver Lake Management Plan https://www.townshipofmarion.com/wp-content/uploads/2018/01/SilverWaushara_HWMmonitorReport2017_v1-1.pdf (accessed April 2023).

7. Mossler, M. A.; Shilling, D. G.; Haller, W. T. Photolytic degradation of fluridone. *J. Aquat. Plant Manage.* **1989**, *27*, 69–73.
8. Saunders, D. G.; Mosier, J. W. Photolysis of the aquatic herbicide fluridone in aqueous solution. *J. Agric. Food Chem.* **1983**, *31* (2), 237–241.
9. Macdonald, G. E.; Haller, W. T.; Shilling, D. G. UV-B filtration to reduce photolysis of fluridone in experimental tanks. *J. Aquat. Plant Manage.* **1996**, *34* (2), 78–80.
10. Marquis, L. Y.; Comes, R. D.; Yang, C. P. Degradation of fluridone in submersed soils under controlled laboratory conditions. *Pestic. Biochem. Physiol.* **1982**, *17*, 68–75.
11. Mossler, M. A.; Shilling, D. G.; Albrecht, S. L.; Haller, W. T. Microbial degradation of fluridone. *J. Aquat. Plant Manage.* **1991**, *29*, 77–80.
12. Helms, J. R.; Stubbins, A.; Ritchie, J. D.; Minor, E. C.; Kieber, D. J.; Mopper, K. Absorption spectral slopes and slope ratios as indicators of molecular weight, source, and photobleaching of chromophoric dissolved organic matter. *Limnol. Oceanogr.* **2009**, *53*, 955–969.
13. Weishaar, J. L.; Aiken, G. R.; Bergamaschi, B. A.; Fram, M. S.; Fujii, R.; Mopper, K. Evaluation of specific ultraviolet absorbance as an indicator of the chemical composition and reactivity of dissolved organic carbon. *Environ. Sci. Technol.* **2003**, *37* (20), 4702–4708.
14. A. Leifer, *The Kinetics of Environmental Aquatic Photochemistry: Theory and Practice*, American Chemical Society, Washington, DC, 1988.
15. Gueymard, C. A. Interdisciplinary applications of a versatile spectral solar irradiance model: a review. *Energy* **2005**, *30* (9), 1551–1576.